JULY, 2023

AN EXPERIMENTAL INVESTIGATION ON SCALING

IN GASKETED PLATE HEAT EXCHANGERS

MSc Thesis
Rahul Nanda

Delft University of Technology

Master Thesis

ME55035

Experimental Investigation on Scaling in Gasketed Plate Heat Exchangers

Author:
Rahul Nanda (5475651)

Supervisor - TU Delft:
Kamel Hooman
3ME - Process and Energy Department

Supervisor - Alfa Laval:
Ron Faber
Process Heat Exchangers - Energy Division

Publicly Defended on July 28, 2023

Acknowledgements

This thesis project would not have been possible without the help and support of a number of generous people, only some of whom are mentioned here.

Firstly, I would like to thank my supervisor Professor Kamel Hooman for giving me the opportunity to work on such an exciting project under his mentorship. Your expertise and constructive criticism were invaluable in the successful completion of this project. I will be forever grateful for the freedom you extended towards me in steering this project in a direction of my choice and your constant support through all the difficulties I faced.

I would also like to thank Alfa Laval for commissioning this project and giving me this challenge. Thank you to my company supervisor, Ron Faber, for placing your trust in me and providing me with the required equipment for making this project possible. Without your guidance and constant words of encouragement, this project would not have been successful. It was a privilege for me to have worked alongside you for the past 8 months. I would also like to thank Maaike Leichsenring for bringing this project to TU Delft and selecting me to be a part of it. Thank you to Erik Engstrom and Olga Santos for your advice along every step of the way.

Thank you to Bart Hoek, without whom my experimental setup would have never come to life. Your experience and knowledge played a crucial role in designing the setup. Despite my complete lack of experience in practical matters, you patiently helped me build my test setup and were ever willing to help me through all my troubles. Thank you for sharing your practical knowledge with me and always lending me a helping hand.

I was blessed to have my family and friends beside me throughout my thesis journey. Thank you to my parents for giving me the opportunity to pursue my dreams and explore my passion for science and engineering. Without their unconditional love and support, I would not be where I am today. Thank you to Aditi for being by my side throughout my 2 years at TU Delft. You made my life in The Netherlands the most wonderful experience of my life. Thank you to Dimitris for the great friendship we shared and the countless assignments we completed together. Thank you to Suenley and Hamza for being the support system I needed during my thesis. Thank you to Marko for answering all my silly questions and always giving me a second opinion when I needed one. Working with all of you is something I will cherish for a lifetime.

Abstract

Gasketed Plate Heat Exchangers (GPHEs) are a sub-class of heat exchangers that enable heat transfer between 2 fluids via metal plates. A common problem encountered in all heat exchangers is fouling. Fouling can be described as the deposition and accumulation of unwanted materials such as scale, algae, suspended solids and insoluble salts on a heat transfer surface. Despite the widespread use of GPHEs and the common occurrence of fouling in heat exchangers, fouling is not clearly understood in GPHEs. Scale, one of the several types of fouling, has the most harmful effect on heat exchangers out of all fouling mechanisms and is the most common problem encountered in cooling water systems. When formed on heat exchanging surfaces, scale retards heat exchange, accelerates fouling, promotes certain types of corrosion and microbial growth, and increases pumping back pressure. These, in turn, result in decreased plant efficiency, reduced productivity, schedule delays, more downtime for maintenance, and increased costs for equipment repair and replacement. Since Alfa Laval is an active part of this project, and a large portion of the GPHEs they sell are used in cooling water applications, the focus of this project is to understand the effect of flowrate, inlet temperature and GPHE duty on scaling in GPHEs. The most common scale deposited on heat exchangers is calcium carbonate ($CaCO_3$), and therefore this study will only focus on $CaCO_3$ scaling.

In order to quantify the effect of changes in a parameter on scaling tendency and GPHE performance, an experimental setup is built. The experimental design ensures that when altering one parameter, all other operating conditions of the GPHE remain constant, thereby attributing any changes in scaling tendency solely to the test parameter. Throughout each experiment, media temperatures are monitored, and the overall heat transfer coefficient and fouling resistance are plotted against time to observe changes in GPHE performance. Additionally, since the deposited scale initially increases the performance of the GPHE, a time for 'onset of scale' is also determined for each experiment, where 'onset of scale' is defined as the moment when the deposited scale is detrimental to GPHE performance. Moreover, following each experiment, the GPHE is disassembled, and the scaled plates are weighed to determine the quantity of scale deposited on the plates. Finally, images of the scaled plates are compared with those of a clean plate to observe the distribution of scale on the plate surface.

After performing and analysing the results from all experiments, it can be concluded that all 3 parameters have a significant influence on GPHE performance. It was observed that higher flowrates led to a smaller amount of scale deposits on the plate and result in a greater duration to achieve the onset of scale condition. Conversely, higher inlet temperatures and GPHE duty led to a greater amount of scale deposits and result in a shorter time to achieve the onset of scale condition. The results also indicated that a change in GPHE duty has the greatest influence on scaling from all 3 parameters, provided the flowrate is greater than 250 kg/hr. However, for flowrates below 250 kg/hr, the flowrate of the test solution has the biggest impact on scaling tendency and GPHE performance. Additionally, an optimal performance region which would result in minimal scale deposition on the plates is determined for the current system. Finally, to predict the amount of scale deposited on the plates as a function of the test parameters, regression analysis is performed on the data and a 5th-degree polynomial function is established.

Contents

List of Figures

List of Tables

1 Introduction

1.1 Heat Exchangers

A heat exchanger is a device used to transfer heat between two fluids [1]. The fluids are usually separated by a solid wall to prevent mixing [2]. Since they allow for heat to be delivered or extracted from the working fluid, heat exchangers are used in a wide variety of heating and cooling applications such as space heating, refrigeration, power stations, air conditioning, etc. If heat is being delivered to water or if cooling water is accepting heat in a heat exchanger, a common problem encountered is the formation of a scale - a type of fouling which decreases the performance of the heat exchanger. The degree to which a heat exchanger is prone to fouling and how it impacts the performance of the heat exchanger can significantly vary among different heat exchangers. [3]. Hence, in order to better understand fouling of heat exchanging surfaces, each heat exchanger must be studied individually.

Alfa Laval are an active part of this project, and a majority of their business comes from the sale of gasketed plate heat exchangers (GPHEs), hence, this study will focus on GPHEs. Like any other heat exchangers in which water is accepting heat, these GPHEs scale. Alfa Laval and their customers want to know under what process conditions is the scale formation faster. This information can help customers better design the process conditions for their GPHEs. Alfa Laval would also be able to provide greater value to their customers by suggesting process conditions that increases the time before which the GPHE needs to be cleaned. Currently, Alfa Laval is able to provide only general guidelines of how the scaling process can be slowed down. However, they are keen to understand scaling on a deeper level so as to provide better suggestions to their customers. Hence, to understand the effect of various parameters on the scaling tendency and subsequent GPHE performance, this project was commissioned.

1.2 Gasketed Plate Heat Exchnagers

Gasketed Plate Heat Exchangers (GPHEs) are a subclass of heat exchangers that facilitate heat transfer between two fluids via metal plates. The plates are compressed together in a rigid frame and separated by gaskets, as seen in figure 1a. This forms an arrangement of parallel flow channels with alternating hot and cold fluids, as seen in figure 1b. The primary reason for their popularity and preference over other classes of heat exchangers is their ability to provide a large heat transfer surface area with a relatively small heat exchanger size. Additionally, the plates are often corrugated which not only increases the heat transfer surface area but also induces turbulence which increases the rate of heat transfer. Hence, even with low flow rates, these heat exchangers can maintain a high degree of turbulence and achieve high heat transfer coefficients [4]. These attributes coupled with GPHEs allowing approach temperatures as close as 1 °C makes them up to five times more efficient than shell-and-tube heat exchangers [5]. Additionally, the capacity of GPHEs can be easily changed by simply adding or removing plates, which serves as a major advantage as compared to other heat exchangers. The versatility of GPHES allows them to be designed and configured for a wide range of low and high duty applications and hence, they are used in heating, cooling, heat recovery, condensation and evaporation applications. As a result they are present in almost every industry ranging from HVAC and refrigeration to oil production and power generation [6].

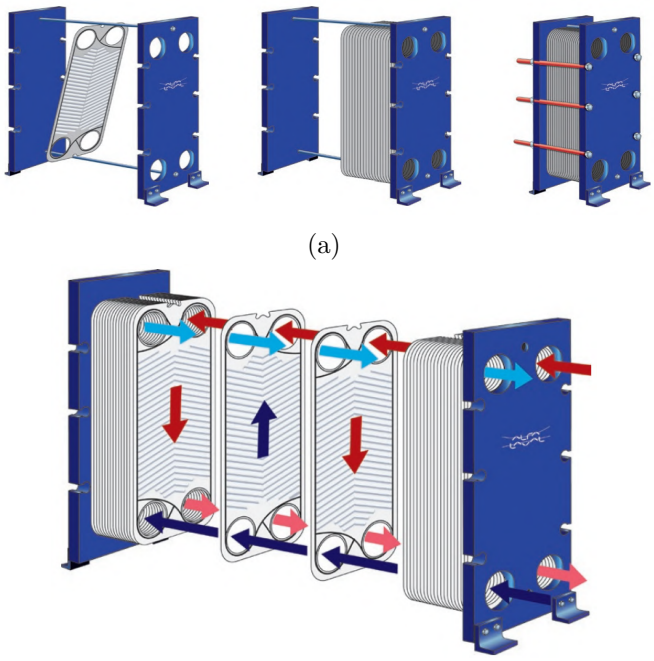

(a)

(b)

Figure 1: (a) A gasketed plate heat exchanger consists of a number of heat transfer plates which are held in place to form a complete unit. (b) The arrangement of the gaskets on each plate provides two separate channel systems in counter-current flow.

In spite of widespread use of plate heat exchangers, fouling in them is not clearly understood. As a result, fouling factors [1] to design PHEs are not readily available, like there are for shell-and-tube heat exchangers. If shell-and-tube heat exchanger fouling factors are used to design a PHE, it would result in severely oversizing it since the fouling factors of PHEs are far lower than that of shell-and-tube heat exchangers. Figure 2 shows the fouling resistances for cooling water inside a PHE in comparison with the tube-side of a shell-and-tube heat exchanger. Fouling resistance can be defined as the increase in the resistance to the flow of heat (m^2K/W) due to fouling, and in this figure a dramatic difference in the fouling resistances of PHEs and shell-and-tube heat exchangers is visible. Therefore, in order to efficiently design PHEs, it is essential to clearly understand fouling formation in them and further facilitate the development and use of fouling factors specially designed for PHEs.

[1] The fouling factor represents the theoretical resistance to heat flow due to the build-up of a fouling layer on the surfaces of the heat exchanger.

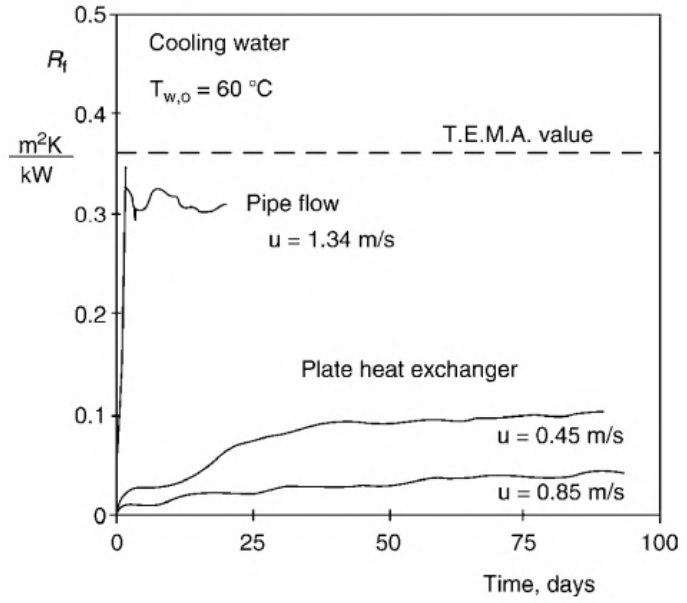

Figure 2: Comparison of fouling in plate and frame, and in shell-and-tube heat exchangers [7]

1.3 Fouling

Fouling can be described as the deposition and accumulation of unwanted materials such as scale, algae, suspended solids and insoluble salts on the heat transfer surface [8]. Fouling on process equipment surfaces can have a significant, negative impact on the operational efficiency of the unit. It not only reduces the amount of heat transferred through the heat exchanger due to its low thermal conductivity but also increases pumping back pressure due to increased friction and partial blockage of the channels [9]. This results in decreased plant efficiency, more downtime for maintenance, and increased costs for equipment repair and replacement.

1.4 Costs of Fouling

Despite the significant financial consequences of heat-exchanger fouling, very little research has been done to precisely calculate these costs and attribute them to the various elements of heat exchanger design and operation [10]. The total fouling-related costs consist of the following:

- **Capital expenditures:** Extra surface area, the price of stronger foundations, extra space requirements, and higher shipping and installation costs are examples of capital expenditures. Additionally, anti-fouling equipment has further capital expenses, such as setting up in-line cleaning devices, pretreatment facilities, and cleaning in-place equipment.
- **Fuel costs:** The deposition of the foulant on the heat exchnager surfaces reduces the amount of heat transferred. Hence, to maintain the required temperatures without cleaning the heat exchanger, extra fuel needs to be burnt in furnaces or more secondary energy such as electricity or process steam is needed. These costs can get very high if the heat exchnager is not cleaned frequently and effectively.
- **Maintenance costs:** Maintenance costs are costs for removing fouling deposits, costs for chemicals, or other operating costs of anti-fouling devices. According to Pritchard [11], heat exchangers and boilers account for 15% of a process plant's maintenance expenditures, and 50% of that is most likely caused by fouling.
- **Costs Due to Production Loss:** Large production losses are inevitable as a result of planned or unplanned plant shutdowns brought on by heat exchanger fouling. These

losses, which are very difficult to assess, are frequently thought of as the principal expense associated with fouling.

Ibrahim [3] reported that fouling is responsible for the emission of many millions of tonnes of carbon dioxide as well as the use and disposal of hazardous cleaning chemicals which can have a negative effect on health, safety, property or the environment. Pritchard [11] found that the total fouling costs for highly industrialized countries such as the United States and the United Kingdom are about 0.25% of the countries' gross national product (GNP). Therefore, the price we pay for heat exchanger fouling is very expensive from a financial as well as an environmental perspective.

1.5 Types of Fouling

Based on the foulant deposited on the heat exchnager surface, fouling can be divided into five major categories [12] [13] :

- **Crystallization Fouling (Scaling)**: Scaling is defined as the crystallization of solid salts, oxides, and hydroxides from solutions onto the heat transfer surface. This phenomenon occurs most often in water solutions when the concentration of the salts exceeds the saturation point. It is especially common in boilers and heat exchangers operating with hard water. The most common example is the formation of limescale due to the precipitation of calcium carbonate ($CaCO_3$) on the heating element of water heaters [14].
- **Particulate Fouling**: Deposition of tiny suspended particles like clay, silt, or iron oxide on heat transfer surfaces results in particulate fouling. This procedure is typically crucial for colloidal particles, which are particles smaller than 1 μm in at least one dimension (but which are much larger than atomic dimensions).
- **Corrosion Fouling**: The fouling due to products formed on the heat transfer surface as a result of in-situ corrosion of the substrate is termed as corrosion fouling. The thermal resistance of corrosion layers is usually low, however, the increased surface roughness may promote fouling due to other fouling mechanisms. Formation of an iron oxide or oxyhydroxide deposit from corrosion of the underlying carbon steel is an example of corrosion fouling.
- **Chemical Reaction Fouling**: When chemical species in the process fluid come into contact with heat transfer surfaces, chemical reactions may occur that result in the formation of a deposit. These deposits cause chemical reaction fouling. In these situations, the metallic surface occasionally serves as a catalyst. For example, milk processing in the food industry often suffers with chemical reaction fouling.
- **Biological Fouling**: Deposition of organic films consisting of microorganisms and their products such as bacteria and the attachment and growth of macro organisms such as mussels, algae etc. on the heat transfer surfaces result in biological fouling.

Due to the vast differences in the above mentioned fouling types, it is not feasible to study the effect of each one on PHE performance. Since a large part of the GPHEs manufactured by Alfa Laval are used for cooling water applications [15], i.e. applications which involve cooling with water, crystallization fouling or scaling was chosen as the fouling process to be studied. Additionally, Berce et. al. [16] reports that crystallization fouling/scaling has the most harmful effect of all types of fouling on heat exchangers. Hence, the focus of this project will be on scaling.

1.6 Crystallization Fouling or Scaling

Scaling can be defined as the precipitation and further deposition of dissolved salts from the solution onto the heat exchanging surface. The salts deposited on the heat exchanging surface, termed as scale, reduce the heat transferred by the heat exchanger due to their low thermal conductivity. If deposited in a channel, scale may also result in an increase in pressure drop due to partially blocking the flow. Scaling occurs when the solution becomes supersaturated [9]. This usually occurs at the heat transfer surface, but may also occur in the fluid bulk, leading to crystals forming in the fluid, i.e., bulk crystallization. Both bulk and surface crystallization can also be present simultaneously [16]. Supersaturation can occur as a result of any of the following reasons [16]:

- Evaporation of the solvent.
- Cooling a solution of normal solubility salts (NaCl, $CaCl_2$) below the solubility temperature.
- Heating a solution of inverse solubility salts ($CaSO_4$, $CaCO_3$, Na_2SO_4. $MgSiO_3$) above the solubility temperature.
- Mixing of solutions with different compositions.
- Variation of pH, which can affect solubility.

Berce et. al. [16] reported that it is usually inverse soluble salts that cause problems of scaling in aqueous systems. The solubility of an inverse soluble salt decreases as the temperature of the solution increases. As can be seen in figure 3, at A the solution of an inverse solubility salt is under-saturated. Upon heating it reaches the solubility limit point B at temperature T_1. If heated further, the solution becomes supersaturated reaching point C at temperature T_2. This is a meta-stable point and is where precipitation occurs. Further heating continues to remove material from solution and the concentration/temperature equilibrium moves towards point D [9].

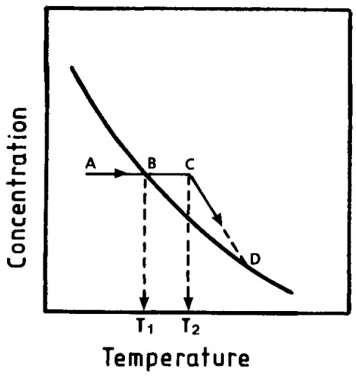

Figure 3: The heating of an inverse solubility salt solution [9].

1.6.1 Formation and Propagation of Scale

According to VDI [12], fouling generally occurs in five consecutive steps, which are illustrated in figure 4. These steps are further explained in the context of scaling:

1. **Initiation Period or Delay Period**: The initially high heat transfer coefficients of a new or cleaned heat exchanger may remain unchanged for a certain time. As reported by Zhao and Chen [17], supersaturation by itself cannot be a sufficient trigger for a system to begin crystallizing. Before crystals may form, the solution must contain a number of tiny solid

particles that serve as crystallization centers, such as embryos, nuclei, or seeds. If there is enough contact time, stable nuclei particles formed in a supersaturated solution, that are larger than the critical size, start to develop into visible deposits.

2. **Mass Transport**: In the case of bulk crystallization, the foulant is transferred from the fluid bulk to the heat transfer surface to produce a deposit. This usually occurs by diffusion. In the case of surface crystallization, no mass transport takes place since the foulant precipitated on the surface itself.

3. **Formation of Deposit**: The foulant (e.g. $CaCO_3$) must adhere to the heat transfer surface after precipitation.

4. **Removal or Auto-Retardation**: After the first deposit is laid down, removal of the foulant can occur right away, depending on the deposit's strength. If the foulant deposition exceeds the removal rate, the deposit on the heat transfer surface grows. According to Zhao and Chen [17], the removal rate (Eq. 1) is directly proportional to the wall shear stress of the bulk flow ζ, and the deposit thickness δ, and is inversely proportional to the shear strength exerted by the fluid flow on the deposit layer, σ_f. k_{rem} is a proportional constant.

$$\left(\frac{\mathrm{d}m}{\mathrm{d}t}\right)_{rem} = k_{rem}\frac{\zeta}{\sigma_f}\delta \tag{1}$$

The formation of deposit lowers the driving temperature difference between the heat transfer surface and fluid for the thermal boundary condition of constant temperature difference between heated and cooled fluid. This leads to auto-retardation of the process.

5. **Aging**: All deposits undergo aging. Through polymerization, re-crystallization, dehydration, and other processes, aging may make the deposit stronger. Some particles may bake onto the surface and get more challenging to remove with time.

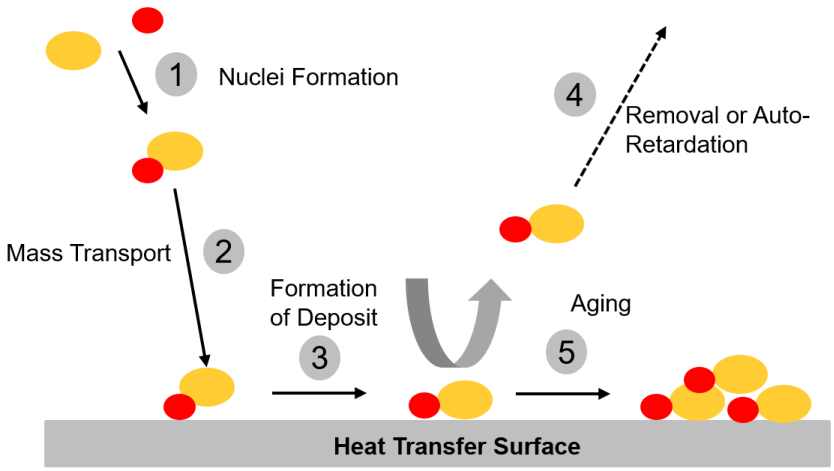

Figure 4: The five consecutive steps for fouling formation [18].

Berce et al. [16] reported that the initially high heat transfer coefficients will typically remain unchanged for a certain amount of time, which was named the initiation or delay phase. Once the nuclei are present, the formation of deposits begins through the process of mass transport. This transport occurs as the concentration gradient drives the foulant from the bulk fluid towards the surface of the material. Diffusion is the most common mechanism through which this transport

takes place, enabling the foulant to migrate and initiate the deposition process. This can simultaneously cause a decrease of the overall heat transfer coefficient due to the thermal resistance of the fouling layer and an increase of said coefficient because of turbulence enhancement near the fouled surface. As the deposition process has just started at this point, the scale thickness (and consequent flow constriction) is small to negligible, and the effect of roughness-induced turbulence is dominant. As a result, the heat transfer coefficient can temporarily increase, which is observed as negative fouling resistance (roughness control phase).

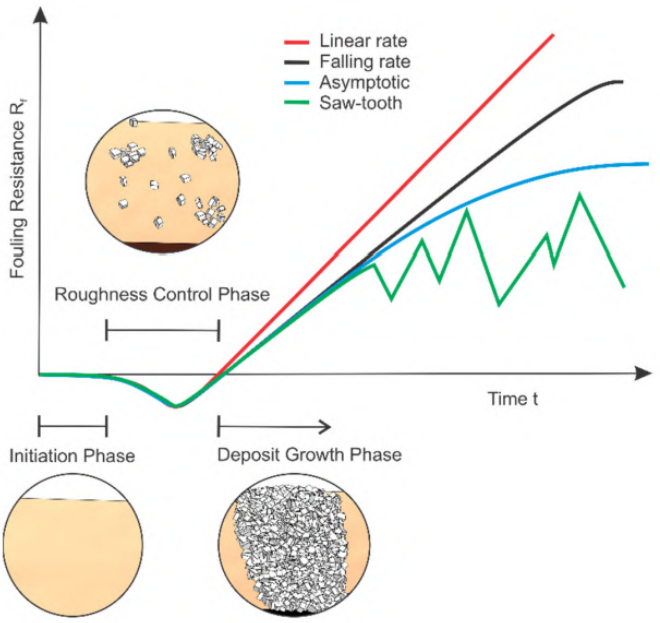

Figure 5: Possible fouling resistance versus time curves [16].

Depending on the heat transfer process and the accompanying fouling mechanisms, the observed fouling resistance can behave differently over time, as shown in figure 5. As mentioned previously, fouling resistance is defined as the increase in the resistance to the flow of heat (m^2K/W) due to fouling. Its behaviour depends greatly on the strength of the formed deposit, i.e. weaker deposits generally exhibit an asymptotic fouling resistance, while hard and resilient ones have a linear or falling rate tendency. The first three curves in figure 5 show idealized conditions, while the saw-tooth represents the oscillations, due to aging induced deposit break-off, that can be found in some experimental and industrial data [16]. For the saw-tooth fouling curve, due to the break-off, the fouling resistance is reduced. However, this means that the fouled surface becomes rougher. Increase in roughness means that the fouling resistance will increase again and the cycle repeats itself. Bansal, Chen, and Müller-Steinhagen [19] stated that, when it comes to crystallisation fouling, linear fouling curves have been reported by many authors. The fouling rate (net effect of deposition and removal rates) however, may not always remain linear for a longer period of time.

1.6.2 Importance of studying scaling

When formed on heat exchanger surfaces, scale reduces the operational efficiency of the heat exchanger. The amount of heat that the heat exchanger can transfer reduces because the deposited scale has a lower thermal conductivity than the metal heat exchanging surface. Additionally, due to increased friction and blockage of channels, scale increases the pressure drop across the heat exchanger [9]. This results in decreased plant efficiency, reduced productivity, schedule delays, more downtime for maintenance, and increased costs for equipment repair and replacement. All of which directly lead to higher operating costs and decreased profitability. It would

therefore be very beneficial to industries worldwide if scale formation could be prevented altogether. However, to ensure that no scale is formed under any process conditions, water with 0 hardness levels must be used for all cooling water applications. Since the total water hardness is the sum of the molar concentrations of Ca^{+2} and Mg^{+2} ions [20], the water must be devoid of all Ca^{+2} and Mg^{+2} ions to achieve this condition. All EU Member states have guidelines and regulations in place to control the hardness of tap water, but none of them employ a 0 hardness level supply [21]. Since water companies need to use chemicals and energy to soften water [22], hardness of water is brought down only to the prescribed limit. Hence, the water made available to industries always has a certain degree of hardness, which makes the formation of scale a possibility in some process conditions. Therefore, it is is important to know which parameters and under what process conditions is the rate of scale formation in heat exchangers high, so that industries can optimise their processes for maximum efficiency.

The most common type of scale found in cooling water systems are calcium carbonate and calcium sulphate [23]. However, since calcium carbonate is 100 times more insoluble than calcium sulphate at cooling water temperatures, it more frequently appears in the form of scale [23] [24]. Song et. al. [25], who studied composite fouling characteristics of $CaCO_3$ and $CaSO_4$, reported that $CaCO_3$ had a greater influence on fouling resistance due to its strong adhesive nature. Additionally, Müller-Steinhagen [26], Berce et al. [16] & Nalco Company [24] reported that calcium carbonate scaling is one of the most common problems encountered in cooling water systems, and has the most harmful effect on heat exchangers out of all fouling mechanisms. Hence for these reasons, the focus in this study will be on $CaCO_3$ scale formation in GPHE in cooling water systems.

2 Factors that affect Scaling Formation

Crystallization Fouling or Scaling has been extensively studied in literature. A majority of the work is focused on the precipitation of Calcium Carbonate ($CaCO_3$) and Calcium Sulphate ($CaSO_4$) on heat transfer surfaces, since they are one of the most common scale forming salts [9] [27]. Additionally, for heat transfer in aqueous systems, most fouling problems are related to scale formation of inverse solubility salts, due to occurrence of high temperatures [16]. Since $CaCO_3$ and $CaSO_4$ are both inverse soluble, previous work in this field is focused on the effect of various parameters on their precipitation. The rate of crystallization for both these salts follows a parabolic relationship with supersaturation, with an effective order of reaction of two [9]. Since a prerequisite for scaling is supersaturation, the parameters whose effect on scaling is being studied, remain largely the same, whether it be the study of $CaCO_3$ or $CaSO_4$ scaling on any heat transfer surface. Additionally, it is also clear from literature that when a certain parameter is changed, the precipitation of $CaSO_4$ is affected in the same way as the precipitation of $CaCO_3$ on any heat transfer surface [28–35] . Hence, even though the focus of this study is on $CaCO_3$ scaling in PHEs, a thorough examination of literature pertaining to $CaCO_3$ and $CaSO_4$ scaling on any heat transfer surface must be conducted in order to decide which parameters will be the focus of the experimental study.

2.1 Foulant concentration or Water Hardness Level

One of the most important factors that affects scale formation is the foulant concentration or the water hardness level. (High Ca^{+2} concentration is synonymous with hard water). Water hardness is often expressed in German degrees (°dH) or parts per million (ppm or mg/L), where a concentration of 1 °dH is equivalent to 17.85 ppm [20]. Berce et al. [16] reported that a higher foulant concentration universally results in greater supersaturation and thus in a quicker start of deposition and higher fouling rates. They also reported that scaling is more severe if boiling is present because of bubble formation mechanisms, which can increase the local salt concentration near the heat transfer surface by several orders of magnitude.

There are a number of studies in literature examining the effect of foulant concentration on fouling rates. Bansal et. al. [28] conducted experiments on a PHE with solutions ranging in $CaSO_4$ concentration from 2800 to 3200 mg/L. They reported that the deposition of the foulant was significantly higher with higher $CaSO_4$ concentrations. However, their solution concentration changes significantly during the experiments which they account for and readjust by adding make-up chemicals. The initial drop in concentration due to scaling and the subsequent rise in concentration due to addition of chemicals results in a fluctuating hardness value for the entire experimental run. Hence, the effect of a change in hardness value on scaling tendency cannot be accurately determined. Lee et al [29] also performed experiments on a PHE using solutions with $CaSO_4$ concentration ranging from 4000 to 6500 mg/L. They reported an increase in fouling resistance with increasing concentrations of $CaSO_4$. However, a change in solution concentration as the experiment progressed was not addressed or accounted for. Quan et al [30] ran trials on a double pipe heat exchanger with solution hardness ranging from 150 - 450 mg/L of $CaCO_3$. Their experiments also yielded a similar trend of an increase of fouling rate and fouling resistance as the concentration of $CaCO_3$ was increased. However, similar to Lee et al [29], they didn't account for any changes in $CaCO_3$ concentration during the experiment. Pääkkönen et al. [31] performed experimental tests and ran CFD simulations on test setup consisting of 2 flat stainless steel plates with a 15mm channel gap. They studied the precipitation of $CaCO_3$ by varying the $Ca+^2$ concentration in the solution between 200 to 480 ppm. Consistent with other literature, they didn't account for any change in Ca^2 concentration and reported an increase in fouling resistance with increasing Ca^2 concentrations.

Hence, it is very evident from literature that an increase in hardness or foulant concentration

in the flowing media, increases fouling rate and fouling resistance on the heat transfer surface. However, there is no definitive research studying the effect of varying the $CaCO_3$ concentration on scaling in PHEs. Additionally, majority of literature fails to account for a change in foulant concentration as scale is deposited on the plate. Hence, future work must be conducted to study the effect of varying the $CaCO_3$ concentration in the solution on scaling tendency and subsequent performance of PHEs, while ensuring a constant concentration is maintained during the entire experimental run.

2.2 Temperature

Another parameter whose effect on scaling is extensively studied in literature is temperature, both of the surface and the fluid. Together, surface and fluid temperatures are responsible for the concentration gradient, which is the main driver of diffusive transport from the solution to the surface [16].

2.2.1 Surface/Wall Temperature

The effect of surface/wall temperature on the fouling resistance of different fouling mechanism is shown in figure 6, with crystallization fouling increasing with increasing surface temperatures. Al-Otaibi et. al. [36] conducted experiments with brackish water and also reported that for a constant fluid temperature, an increase in wall temperature resulted in an increasing fouling rate for inverse solubility salts due to higher concentration gradients.

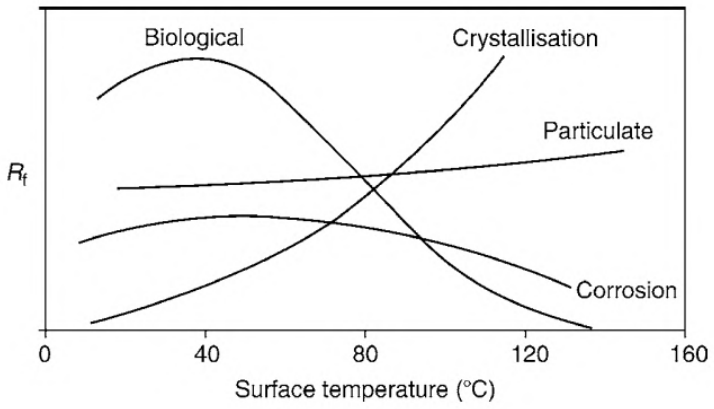

Figure 6: Effect of surface temperature on fouling resistance [12]

The surface temperature of the heat exchanging surface can be changed in multiple ways. If all other parameters are held constant, an increase in the temperature of the heating media would directly increase the temperature of the heat exchanging surface. Additionally, if the walls are heated electronically, an increase in heat flux would increase the wall temperature if all other parameters are held constant. Several experimental studies conclude that higher wall temperatures lead to higher fouling resistances. Bansal et. al. [28] conducted experiments on a PHE to study the precipitation of $CaSO_4$. Since the wall temperature in a PHE cannot be monitored due to its compact structure, they increased the heating media temperature while keeping the test solution inlet temperature constant. They reported an increase in fouling resistance and deposition rate as the heating media temperature was increased. However, they performed only 2 experiments and hence insufficient information is available to make any conclusions. Lee et al [29] also conducted experiments on a PHE to study the scaling characteristics of $CaSO_4$. Upon increasing the heating media inlet temperature, for a constant test solution inlet temperature, they reported an increase in fouling resistance. Pääkkönen et al. [32], who conducted experiments on the precipitation of $CaCO_3$ on 2 flat stainless steel plates, varied the heat flux while keeping all other operating conditions constant (Since the plates are heated electronically by

ohmic heaters, a change in heat flux is equivalent to a change in wall temperature). As the heat flux was increased from 53 kW/m^2 to 62kW/m^2, the fouling resistance increased as well. The change in fouling resistance was negligible when heat flux was varied from 53 to 59 kW/m^2, however significant fouling resistance change was observed when the heat flux changed from 59 kW/m^2 to 62 kW/m^2, in spite of a smaller increment value. This issue was unaddressed and more experiments are needed to determine the effect of change in heat flux on scaling tendency. Teng et. al. [33] also reported an increase in $CaCO_3$ fouling resistance in a stainless steel double pipe heat exchanger, when they increased the heating media inlet temperature from 50 °C to 70 °C for a constant test solution inlet temperature. Additionally, Lee et. al. [29], Bansal et. al. [28] and Pääkkönen et al. [32] reported higher foulant deposits towards the outlet of the heat exchanging surface on the test solution side. This is because both experiments used counter-current systems, in which the wall temperature increases in the direction of the test solution flow.

Hence, it can be concluded that an increase in wall temperature, would increase the amount of foulant deposited and thereby increase the fouling resistance. However, no definitive research has been done investigating the effect of wall temperature/heat flux on the precipitation of $CaCO_3$ on PHEs. Additionally, as the deposition process advances, the surface's temperature will vary as a result of the deposited layer's insulating properties and result in auto-retardation of the fouling process [16]. Since the thermal conductivities (and therefore insulating properties) of $CaCO_3$ and $CaSO_4$ are different, further research must be conducted to investigate the change in heat transfer performance due to $CaCO_3$ precipitation.

2.2.2 Fluid Temperature

For the current context, i.e. studying scaling on heat exchanging surfaces, the fluid temperature refers to the temperature at which the test solution arrives at the inlet of the heat exchanger. Therefore, fluid temperature is synonymous with test solution inlet temperature. Since $CaCO_3$ is an inverse soluble salt, its tendency to stay dissolved in the fluid decreases with increase in fluid temperature. Hence, at higher fluid temperatures, $CaCO_3$ would be more likely to precipitate and scale, if the other operating conditions were also complementing scaling.

Lee et al [29] conducted experiments on a PHE to study the effects of $CaSO_4$ scaling. When keeping the heating media temperature constant at 95 °C, an increase in test solution inlet temperature from 15 to 55 °C, resulted in an increase in fouling resistance in their study. Quan et al [30] ran trials on a double pipe heat exchanger to study the precipitation of $CaCO_3$ on a double pipe heat exchanger. Upon increasing the test solution inlet temperature from 22.5 to 44.5 °C, for a constant heating media temperature, they also noticed a significant increase in fouling resistance. Li et. al. [34] performed experiments on a PHE to study $CaCO_3$ precipitation. They performed experiments at 3 different test solution inlet temperatures ranging from 30 to 50 °C. They reported an increase in fouling resistance with increasing inlet temperatures. However, for all 3 tests, the heating media temperature and the solution hardness level was not held constant. Hence, the increase in fouling resistance is due to a number of factors and a direct correlation between fluid temperature and $CaCO_3$ precipitation on PHEs cannot be made. Due to the absence of any other definitive literature on the effect test solution inlet temperature on $CaCO_3$ precipitation in PHEs, future work must be conducted.

2.3 Flowrate

The effect of flowrate of the test solution on precipitation of $CaCO_3$ and $CaSO_4$ on heat exchanging surfaces has been studied in great detail in literature. This is because altering the flowrate simultaneously changes the turbulence, shear stress and contact time with heat exchanging surface, and therefore it's effect on foulant precipitation is not very intuitive. According to Pääkkönen et al. [37], scale formation in forced convection systems can be controlled by diffusion mass transfer, surface integration, or both. It is suggested that increasing the flow velocity would enhance mass transfer that promotes deposition, but would simultaneously also increase the shear stress that leads to deposit removal. Hence, the effect of flowrate on precipitation of the foulant is not so straightforward.

The majority of literature studying the effect of flowrate on crystallization fouling observes a decrease in fouling resistance with an increase in flow velocity. Lee et al [29] conducted experiments on a PHE to study the precipitation of $CaSO_4$. They observed that increasing the Reynolds number of the test solution from 2552 to 5578, while keeping all other operating conditions constant, resulted in a decrease in fouling resistance by a factor of 3. Teng et. al. [33] performed tests to study precipitation of $CaCO_3$ on a double pipe heat exchanger by recording the amount of $CaCO_3$ deposited on the pipe surface in g/m^2. An increase in the velocity from 0.15 to 0.45 m/sec led to a decrease in foulant deposition by a factor of two. Kho et. al. [35] also performed experiments on a PHE to study crystallization fouling of $CaSO_4$. They performed experiments for 3 different flow velocities - 0.2, 0.35 and 0.65 m/s. They observed a decrease in fouling resistance with increasing flow velocity. However, the change in fouling resistance was negligible when the velocity was increased from 0.2 to 0.35 m/s and a significant change in fouling resistance was observed when the velocity was increased from 0.35 to 0.65 m/s. Even though the second velocity increment is larger, it does not justify the huge change in fouling resistance as compared to the first velocity increment. This observation was not addressed by the authors and makes it difficult to determine the effect of change in flowrate on scaling tendency. Pääkkönen et al. [32], who conducted experiments on the precipitation of $CaCO_3$ on 2 flat stainless steel plates, observed the change in fouling resistance when the flow velocity was changed from 0.2 to 0.4 m/s. Consistent with other literature, they observed that fouling resistance was inversely proportional to flow velocity. However, the decrease in fouling resistance was significantly larger for a velocity change from 0.2 to 0.27 m/s when compared to the decrease in fouling resistance for a velocity change from 0.27 to 0.4 m/s, in spite of a larger increment value. This issue was unaddressed and the effect of change in flowrate on scaling tendency cannot be accurately predicted from these experiments.

The decrease in fouling resistance with increase in flow velocity is due to 2 factors - decreasing solution-interface temperatures and higher shear stress. Initially, when there is only deposition of the foulant and no removal, the decrease in fouling resistance with increasing velocity is primarily owing to lower solution-interface temperatures caused due to higher test solution flow rates for same heating media conditions. As the experiment proceeds and a significant fouling layer is deposited, the drop in fouling resistance is also due to a higher removal rate owing to higher shear forces [38].

From literature it is evident that an increase in test solution flow velocity decreases the fouling resistance in heat exchangers. However, no definitive literature is available on the effect of test solution flow velocity on the precipitation of $CaCO_3$ in a PHE and its further affect on its performance. Although it is likely that the same trend would be observed, further research must be conducted to confirm the hypothesis and to study its effect on PHE performance.

2.4 Surface finish & plate geometry

The material of the heat exchanging surface and the accompanying surface morphology plays an important role in the development of crystallization fouling. As for surface finish, Berce et al. [16] reported that rough surfaces exhibited higher deposition rates (increased nucleation points), shorter induction periods and stronger deposit adhesion. MacAdam and Parsons [39] demonstrated how increasing surface roughness from 0.2 µm to 0.8 µm, leads to a 30% increase in scaling rate.

The effect of surface material on scale formation is linked to the thermal conductivity of the material. Teng et. al.[33] investigated the precipitation of $CaCO_3$ on multiple double pipe heat exchangers constructed of different materials. They reported a linear growth relationship between foulant deposition and an increase in the surface's thermal conductivity. This is because a high thermal conductivity results in a higher heat transfer across the heat exchanging surface and therefore higher surface temperature on the test solution side. Additionally, surface material is also linked to surface energy. A lower surface energy results in a lower adhesion strength between calcium carbonate crystals and the surface. MacAdam and Parsons [39] reported that the scaling rate of calcium carbonate for copper was greater than aluminium which was again greater than steel.

The plate geometry also plays a major role in the formation of deposits. Fouling was found to be most prevalent in low-flow velocity zones, which heavily depends on the design of the plate of the gasketed plate heat exchanger. Additionally, fouling was observed primarily on the hot end of the plates and a strong correlation between plate design and fouling tendency was reported. [16]. To illustrate the importance of plate geometry, Bansal and Müller-Steinhagen [40] investigated the design of the flow distributors (shown in figure 7) at the entrance and the exit of the plates. The purpose of the distributors is to properly distribute the fluid over the entire plate. The results showed that there was a significant driving force for crystallization near the exit, probably as a result of the design of the particular plate they investigated. Although deposit formation in this limited area did not have any significant effect on the overall heat transfer, it did increase the pressure drop well beyond any acceptable limits.

Since plate geometry is a function on the angle, wavelength and amplitude of the corrugations, its effect on fouling is not only difficult to predict but also to difficult to experimentally study. Every PHE manufacturer employs a different plate profile and surface morphology, and therefore it is very difficult to generalise the effect of plate roughness, surface and geometry on fouling tendency. Hence, plate geometry and material was not chosen as one of the parameters whose affect on $CaCO_3$ precipitation on PHEs will be studied. In order to isolate its effects, the same plate design would be used for all experiments.

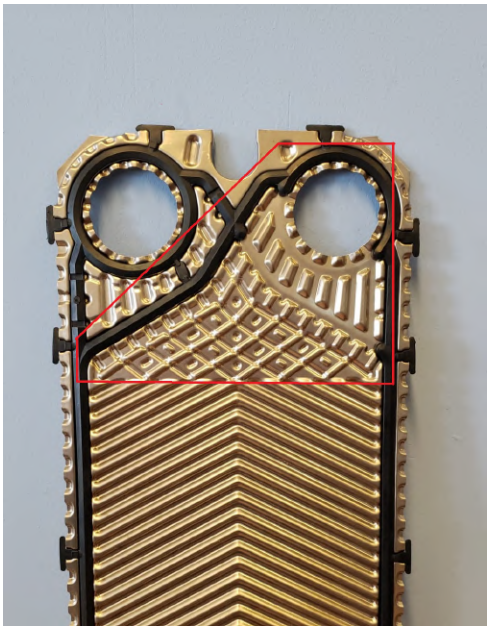

Figure 7: Example of a flow distributor at the entrance of a heat transfer plate.

2.5 pH

The effect of pH of test solution on scaling tendency is not extensively studied in literature. MacAdam and Parsons [39] reported that as the pH of water increases so does the conversion of bicarbonate to carbonate and hence the potential to form calcium carbonate. This can be seen in figure 8. Augustin and Bohnet [41] also conducted experiments to study the effect of pH on $CaCO_3$ precipitation on a heated tube. Their experiments varied pH in a range of 6-10 and measured the fouling resistance change. Consistent with the reporting of MacAdam and Parsons [27], they found that increasing the pH increased the number of free carbonate ions in the system. This increases the tendency of the solution to supersaturate and therefore the fouling resistance increases with an increase in pH.

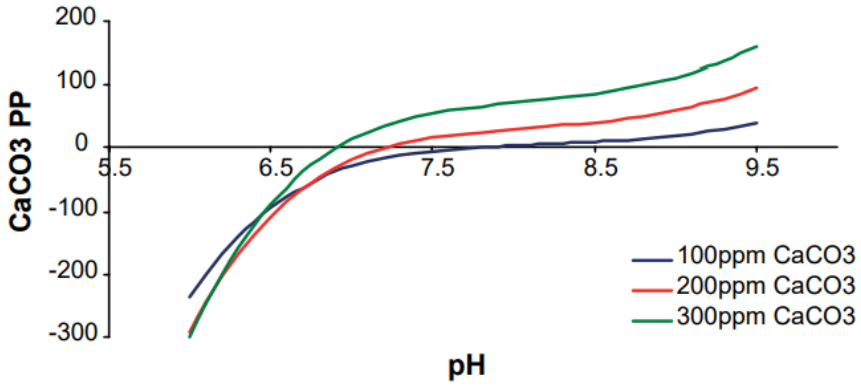

Figure 8: Effect of pH and hardness level on the calcium carbonate precipitation potential [39].

The effect of pH of test solution on $CaCO_3$ scaling in PHEs is not well studied in literature. Hence, further work must be conducted to determine its effect on scaling tendency and PHE performance. However, changing the pH of the test solution while ensuring that the hardness value of the test solution remains constant can be challenging. It would also involve adding salts or chemicals that could interfere with the $CaCO_3$ scaling process. Hence, the effect of pH on $CaCO_3$ precipitation will not be studied.

3 Research Goal, Question and Approach

3.1 Research Goal

The goal of this project is to better understand calcium carbonate scaling ($CaCO_3$) in Gasketed Plate Heat Exchangers (GPHEs). The data collected must be analysed and presented in a way that can aid GPHE manufacturing companies to better design their products and the users of GPHEs to better design their operating conditions.

3.2 Research Question

The question that this project aims to answer in order to achieve the goal is:

RQ: What is the effect of Hardness, Flowrate, Temperature and Heat Flux on Calcium Carbonate Scaling in Gasketed Plate Heat Exchangers?

SQ1: How does the performance of the GPHE change as the scale is deposited on the plate?
SQ2: Which parameter has the greatest influence on calcium carbonate scaling in GPHE?

3.3 Research Approach

This project is a quantitative study, and therefore an experimental setup will be built and experiments will be designed to determine the effect of the previously mentioned parameters on $CaCO_3$ scaling in GPHEs. The data will be analysed and a visual representation of the variation in overall heat transfer coefficient and fouling resistance with time will be plotted for each experimental run to investigate the change in GPHE performance as the scale develops. Additionally, the GPHE will be opened after every experimental run to observe and weigh the scaled plates. The images of the scaled plates will also be compared with a clean plate, to observe any patterns of scale formation on the plate. Finally, a rank list can be prepared to determine which parameter has the greatest influence on $CaCO_3$ scaling in GPHEs.

4 Methodology

The available literature indicates that numerous parameters significantly influence the formation of scale. However, quantifying these effects in general cases proves challenging, necessitating a case-specific approach to understanding the impact of parameter variations on scale formation. Accurately quantifying these effects is crucial for scaling prevention and developing detailed models of the scaling process [32]. Consequently, the subsequent phase of the study entails designing an experimental setup to investigate the influence of water hardness, inlet temperature, heat flux, and flow rate on the formation of $CaCO_3$ scale.

4.1 Selection of Geometry

Given the study's objective of examining $CaCO_3$ scale formation on gasketed plate heat exchangers (GPHEs), the chosen geometry for the investigation will be a GPHE. Since Alfa Laval is an active participant in this project, the GPHE used will be manufactured by them. Alfa Laval produces a wide variety of GPHEs tailored to specific applications, fluid media, flow rates, duties, etc. The selection of the GPHE will determine the experiments that can be run and the time it takes for scale formation to occur on the unit. For consistent initial and boundary conditions, a smaller heat exchanger with fewer plates would result in a shorter duration for the deposition of scale to begin due to a smaller overall plate area for the scale to deposit. Moreover, a smaller heat exchanger with fewer plates would be more cost-effective and easier to handle, maintain, and clean between experimental runs. The most compact GPHE design possible is one channel with the heating medium and one with the cooling medium, resulting in 3 plates. However, practical applications of GPHEs contain multiple alternate heating and cooling media channels. In such systems, each channel of a cooling medium is heated by two channels of the heating medium on either side. Hence, the most compact heat exchanger design that most accurately approximates the real-world application of GPHEs is one channel of cooling medium heated by two channels of the heating medium on each side of it, resulting in a total of 4 plates. Additionally, the GPHE would be configured in a counter-current arrangement, to replicate commonly used real-world conditions. Hence, the geometry chosen for the primary experiments is the smallest GPHE manufactured by Alfa Laval, the T2B, with the most compact design of 4 plates and configured in a counter-current arrangement. The first and third channels in the T2B would be occupied by the heating medium, whereas the second or the middle channel will be occupied by the cooling medium.

Since the T2B is designed for water-water duties, both media for the experiment will be water. Since $CaCO_3$ is an inversely soluble salt, i.e. heating the solution results in salt precipitation, the cooling medium is water with dissolved $CaCO_3$, also known as 'hard water'. As the hard water is heated in the GPHE, its temperature increases, resulting in the precipitation of $CaCO_3$ on the plate. To heat the cooling medium, the heating medium must be a constant water supply at a high temperature. However, to supply the cooling medium to the GPHE at a constant hardness, temperature, and flow rate, and to supply the heating medium at a constant temperature and flow rate, ancillary equipment is needed to form a 'cold loop' and a 'hot loop' for the cooling and heating medium, respectively. Careful selection of ancillary equipment in the two loops is essential to conduct experiments with constant initial and boundary conditions. Furthermore, to effectively investigate and quantify the effects of scale formation on the GPHE, the two loops must be equipped with suitable measuring equipment. Hence, the next step is determining the measurement methods by which the scale and its effect on the GPHE can be quantified. This allows for the appropriate selection of measuring equipment and ensures a comprehensive design of the two loops.

4.2 Measurement Methods

The experimental setup must be designed to incorporate all the essential measuring instruments required for recording the data. To determine which measuring instruments are needed, the

measuring methods with which scaling and its effect on the GPHE performance will be quantified need to be selected. It is beneficial to use more than one method to quantify scaling on the GPHE to obtain a more holistic view of the effects of scale on GPHE performance. Additionally, one or more of the methods must be able to provide data in real time, i.e. during the experimental run, so that the GPHE performance can be continuously monitored.

- **Direct weighing measurement method:**

  The amount of scale deposited on the plate can be measured by calculating the difference in the plate weight before and after each experiment. To measure the weight of the deposited $CaCO_3$ scale, and not any water collected with the scale, the plate must be dried in an oven before taking the final weight measurement so that all the water has evaporated. To use this measurement method, the only measuring equipment needed is a weighing scale. Since the amount of scale that would deposit on the plate is expected to be ≈ 0.5-1.0 gram, the resolution of the weighing scale must be at least 0.01g. Additionally, the uncertainty in the measurement from the weighing scale must be of a similar magnitude.

  The drawback of this method is that no data can be obtained in real-time, i.e. during the experimental run. To determine the amount of scale deposited, the experiment must be stopped, the GPHE must be disconnected from the system, and the entire unit must be opened to access the scaled plates and weigh them. Additionally, no information regarding the distribution of scale on the plate or the presence of any localised deposits can be retrieved using this method. It must also be noted that in order to utilize this method, de-hardened/soft water must be used in the hot loop to ensure that any change in plate weight is only due to $CaCO_3$ scaling from the hard water in the cold loop.

- **Heat transfer measurement method:**

  In this method, the effect of the deposited scale on the GPHE performance can be quantified by calculating the change in heat transferred during an experimental run. When hard water is heated in the GPHE, $CaCO_3$ would precipitate and adhere to the plate surface. Since scale has a lower thermal conductivity than stainless steel, the amount of heat transferred via the plates reduces with time as the amount of scale deposited on the plate continues to rise. If the flowrates and temperatures of both media are constantly monitored, the amount of heat transferred by the GPHE and, therefore, the overall heat transfer coefficient can be calculated for the entire experimental run duration. The rate at which the two quantities drop during an experimental run and the difference between the final and initial values of the quantities can provide useful information pertaining to scale formation. Additionally, since a lower amount of heat transferred via the plates results in a decrease in the outlet temperature of the cooling medium, the change in GPHE performance with time can be estimated in real time by monitoring the temperatures during an experimental run.

  To use this method, the mass flowrate (M) and the temperature at the inlet (T_{in}) and the outlet (T_{out}) of both media of the GPHE must be known for all times 't' of an experiment. Therefore, the measuring equipment needed is 4 temperature sensors, 2 mass flow meters and a data acquisition unit (DAQ) to receive and log the incoming signal from the temperature sensors and flow meters. With these measurements, the average heat transfer rate (Q_{avg}) of the T2B can be calculated using the following formulas

$$Q_c = M_c \cdot c_{p,c}(T_{c,out} - T_{c,in}) \tag{2}$$

$$Q_h = M_h \cdot c_{p,h}(T_{h,out} - T_{h,in}) \tag{3}$$

$$Q_{avg} = (Q_h + \dot{Q}_c)/2 \tag{4}$$

Where Q_c and Q_h denote the heat gained and heat lost by the cold and hot media, respectively and T_h and T_c denote the measured temperature of the hot and cold medium respectively. $c_{p,h}$ and $c_{p,c}$ denote the specific heat capacity of hot and cold media, respectively. These values are obtained from the National Institute of Standards and Technology (NIST) database and are based on the average temperature and pressure at the inlet and outlet of the GPHE for each set of measurements.

With the temperature measurements, the Logarithmic Mean Temperature Difference (LMTD), which is the effective driving force in the heat exchanger, can then be calculated

$$LMTD = \frac{(T_{h,in} - T_{c,out}) - (T_{h,out} - T_{c,in})}{ln\left(\frac{T_{h,in} - T_{c,out}}{T_{h,out} - T_{c,in}}\right)} \tag{5}$$

Finally, the overall heat transfer coefficient is determined in terms of the average heat transfer rate ((Q_{avg}), heat transfer surface area (A) and LMTD.

$$U = \frac{Q_{avg}}{A \cdot LMTD} \tag{6}$$

With the help of this method, it is also possible to determine the change in fouling resistance with time. Since the temperatures are constantly monitored during the experiment, the overall heat transfer coefficient for a time 't' (U_t) can be determined by calculating the average heat transfer rate and LMTD for that time 't'. Additionally, the overall heat transfer coefficient at time t=0 can be denoted as U_0. Hence, the fouling resistance at a time 't' ($R_{f,t}$) can be calculated by equation 7. These can then be plotted against time to get a fouling curve as shown in Figure 5.

$$R_{f,t} = \frac{1}{U_t} - \frac{1}{U_0} \tag{7}$$

During the startup phase of the system, when it is approaching the desired temperatures, the transient nature of the system at time t=0 poses a challenge in accurately determining the value of U_0. However, if the same experiment was run with de-hardened water as both media, the GPHE would not scale, and therefore the overall heat transfer coefficient would be constant for the entire experimental run. This overall heat transfer coefficient value, obtained by running the experiment with de-hardened water as both media, can be termed as U_0, and used in equation 7 to determine the fouling resistance at a time 't' ($R_{f,t}$).

This measurement method is relatively simple to implement but generates a large amount of data that can be used to characterise the scaling tendency of the GPHE. The change in temperatures, average heat transferred, overall heat transfer coefficient and fouling resistance with time can provide useful insights into understanding the tendency of $CaCO_3$ to precipitate and adhere to the plate as well as the change in GPHE performance due to scaling. Additionally, by monitoring the temperatures during the experiment, an indication of the presence and extent of scale formation can be obtained in real-time. However, similar to the direct weighing measurement method, a drawback of this method is that information regarding the distribution of scale cannot be obtained and that de-hardened water must be used in the hot loop to ensure that any change in the measured quantities is because of scaling from the hard water in the cold loop.

- **Visual Inspection Method:**

  The method of visual inspection will also be used to understand the scaling tendency of the plate. It aims to address the drawback of the two previous quantitative methods, i.e. information pertaining to the distribution of scale and presence of any localised deposits. In some experimental trials, the scale may be uniformly distributed across the entire plate, while in some cases, there may be regions of concentrated deposits. Additionally, as the hard water is heated in the GPHE, its temperature increases along the plate length from the inlet to the outlet. Theoretically, the amount of scale deposited on the plate must also increase along the plate length as the $CaCO_3$ is more likely to precipitate at higher temperatures. These scale distribution patterns can be observed with the help of this method. This method is fairly simple to implement, and the only measuring equipment needed for this method is a camera. At the end of each experimental trial, after the GPHE is opened and the plates are dried, photos of the scaled plate can be compared to a clean plate to observe scale distribution patterns.

4.3 Design of the Experimental Setup

The experimental setup consists of a cold and hot loop centred around the GPHE selected for this study, the T2B. Upon selecting the measuring methods and equipment needed to quantify scale, the next step is to design the two loops.

4.3.1 Design of the Cold Loop

The heat exchanger on which scaling is deposited, the T2B, must be supplied with the hard water at the required flowrate, temperature and hardness. As discussed previously, the supply of this hard water and all ancillary and measuring equipment needed for it form the 'Cold Loop'.

- **Hard Water:**

  The most important component of the cold loop is the medium flowing through it, i.e. water containing dissolved $CaCO_3$ or hard water. The test solution cannot be prepared by directly dissolving $CaCO_3$ into water. This is because $CaCO_3$ is practically insoluble in water. At 18 °C, the solubility of $CaCO_3$ in water is between 13 and 19 ppm [42], which is equivalent to a German degree hardness of 1.8 to 2.6 °dH. These hardness values are too low to cause visible or significant scaling deposits onto the heat-exchanging surface. To obtain significant amounts of $CaCO_3$ dissolved in water, Li et al. [34] and Pääkkönen et al. [32] added calcium chloride ($CaCl_2$) and sodium bicarbonate ($NaHCO_3$) in water to elicit the reaction see in equation 8, resulting in the formation of sodium chloride (NaCl) and $CaCO_3$ dissolved in water.

$$2\,NaHCO_3 + CaCl_2 \longrightarrow CaCO_3 + 2\,NaCl + CO_2 + H_2O \tag{8}$$

  In reaction 8, 2 moles of $NaHCO_3$ (168 grams) and 1 mole of $CaCl_2$ (111 grams) are added to water resulting in the formation of 1 mole of $CaCO_3$ (100 grams) dissolved in water. Hence, by following the same procedure and varying the amount of $NaHCO_3$ and $CaCl_2$ added, the required final hardness of the solution can be obtained. It must be noted that since tap water already contains some calcium and magnesium dissolved in it, it is essential to use water devoid of these salts. Using tap water to prepare the hard water can result in the formation of some magnesium carbonate ($MgCO_3$) along with $CaCO_3$ in the solution. This dissolved $MgCO_3$ would also precipitate and deposit as scale on the heat-exchanging surface along with the $CaCO_3$, thereby obscuring the final results. $MgCO_3$ scale and $CaCO_3$ scale have different properties, and the deposit of both salts simultaneously would make it difficult to determine the effect of $CaCO_3$. Additionally, since de-mineralised water could leach any metal it comes in contact with, it cannot be

used either. Hence, dehardened water, i.e. water devoid only of calcium and magnesium salts, will be used to prepare the hard water solution. This would ensure that the solution prepared is of the required hardness value since no calcium or magnesium was previously dissolved in the water.

- **Tank and Heating Jacket:**

  In order to provide a constant supply of hard water to the GPHE, the water of required hardness must be prepared and stored. Hence, the first component of the cold loop must be a tank that can store the hard water needed for the experiments. The tank must be large enough to ensure a constant supply of hard water throughout the experiment. Additionally, as the plate scales and $CaCO_3$ is deposited on the plate, the amount of salt dissolved in the tank would reduce, thereby decreasing the hardness of the hard water in the tank. This cannot be compensated for by adding excess salts prior to running the experiment, as that would alter the initial hardness value of the water in the tank. In addition, it is not possible to accurately calculate the excess salt needed, as the scaling tendency of the GPHE is not known prior to running the experiment. Hence, the tank must be chosen such that it can store a large quantity of water which would require a large amount of salts to achieve the required $CaCO_3$ concentration. As a result, the amount of $CaCO_3$ lost from the tank due to scaling would be negligible when compared to the initial quantity of $CaCO_3$ dissolved in the water. This would ensure a relatively constant $CaCO_3$ concentration in water and therefore, a relatively constant hardness value throughout the experiment.

  Apart from providing hard water at a constant hardness value, it is also important to provide it at a constant temperature. If the required supply temperature is higher than room temperature, the water in the tank must be heated. However, this cannot be done with a heating coil or an immersion heater, as the walls of the heater would reach temperatures higher than 60-70 °C resulting in $CaCO_3$ scaling on the walls of the heater. Additionally, over the course of multiple hours of the experiment, the water in the tank would constantly lose heat to the surroundings and eventually drop back to room temperature before the end of the experiment. Hence, to initially bring the water to the required temperature and also hold it at that temperature for the duration of the experiment, a heating jacket for the tank is needed. The heating jacket, that will be wrapped around the tank, must have a digital control to set the required power supply and, therefore, the heat supplied to the tank. Thus, it can be used in a way that it brings the water to the required temperature gradually so that the walls of the tank never get too hot to result in scaling on the walls. Additionally, it can be set to a lower power supply during the experimental run to cancel any losses to the atmosphere.

- **Pump, Valve and Flowmeter:**

  The hard water stored in the tank must be circulated in the cold loop at the required flowrate. This can be done using a pump and a valve to control the flow. Since the GPHE used is small, the flowrates that will be used for the experiments are not expected to be very high. Additionally, precise control over the flow is needed to ensure that the required flow of hard water is pumped through the loop. Hence, a needle valve can be placed after the pump to control the flow of hard water through the cold loop. A needle valve is a type of valve that uses a tapered needle-like stem to control fluid flow. By rotating the stem, the position of the needle changes, adjusting the opening size through which the fluid flows. This control allows for accurate regulation of flow rates, making needle valves suitable for applications that require precise fluid metering at low flowrates. Finally, a flowmeter can be placed after the pump and needle valve to monitor and determine the water's exact flow rate. The flowmeter must have a high resolution of $\approx$ 1kg/hr to detect small

changes in flowrate. Additionally, it must have a digital display for easy flow monitoring. Hence, a Coriolis flowmeter can be used since it provides highly accurate measurements without being affected by changes in fluid properties. It works by vibrating one or more tubes through which the fluid flows. As the fluid passes through these vibrating tubes, the Coriolis effect causes the fluid particles to deflect, leading to a phase shift in the tube vibration. This phase shift is measured and used to calculate the mass flow rate.

Since the flowrates required for the experiments are not expected to be high, the pump chosen does not need a high head capability. However, a pressure drop will be experienced through the piping, GPHE and other components. Additionally, to constantly stir the tank and mix the $CaCO_3$ in the water to prevent it from settling at the bottom of the tank, a bypass must be added at the outlet of the pump. The bypass allows for a portion of the hard water to be pumped back into the tank, ensuring constant mixing in the tank, while also allowing the pump to circulate the hard water through the loop. The bypass line can also be equipped with a ball valve to switch the hard water supply back to the tank 'on' or 'off'. Hence, the pump must have enough head capacity to supply the required flowrate through the cold loop, compensate for the pressure drop and constantly mix the hard water in the tank via the bypass. Since the only requirement from the pump is high reliability and efficiency, a centrifugal pump with the required head capacity can be used owing to its high efficiency, easy maintenance and low costs.

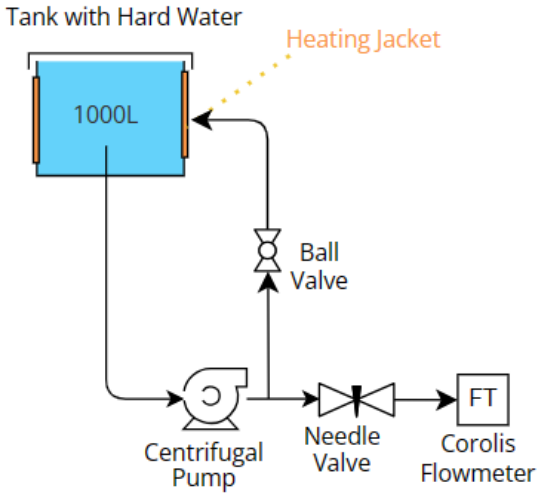

Figure 9: 1st Section of Cold Loop Design

- **Temperature Sensors and DAQ:**

  Once the hard water has been pumped at the required flowrate, the next step is to measure its temperature. This can be done with the help of a thermocouple placed in the loop. The most common thermocouple used is the Type 'K' thermocouple owing to its large temperature measuring range, good accuracy and sensitivity, and cost-effectiveness. A Type 'K' thermocouple consists of two different metal wires, usually composed of chromel (nickel-chromium alloy) and alumel (nickel-aluminium alloy). The principle behind its operation is the Seebeck effect, where a temperature gradient between the two wire junctions generates an analog output voltage. To convert the analog voltage signal to a digital temperature reading, a data acquisition unit (DAQ) is also needed. Hence, to obtain the exact temperature of the hard water, a type 'K' thermocouple must be connected to a DAQ.

- **Cold Loop channel in GPHE:**

  Once the flowrate and temperature of the hard water are determined, it can be passed into the GPHE. As mentioned in subsection 4.1, the configuration of the T2B, i.e. the GPHE selected for the experiments, consists of 4 plates and, therefore, 3 channels. The cooling medium is assigned 1 channel, whereas the heating medium is assigned 2 channels. This configuration and channel allocation is chosen for a number of reasons-

  1. By selecting a 3-channel configuration, the T2B more accurately approximates real-world GPHE applications, which consist of multiple alternate channels of heating and cooling media.
  2. Allocating only 1 channel to the hard water ensures that only the 2 plates that form the channel get scaled. This eliminates the effect of flow distribution or distance of the plate from the inlet port on the scaling tendency of the GPHE.
  3. Allocating 2 channels of the T2B to the heating medium allows for the use of the heating medium at a lower flowrate, resulting in a lower heat demand. This makes the system safer and more economical.

  The hard water entering the GPHE would therefore flow in the middle channel as it is heated by the heating medium flowing on either side. Once the hard water exits the T2B, its temperature can be determined by placing another type 'K' thermocouple connected to the same DAQ mentioned previously.

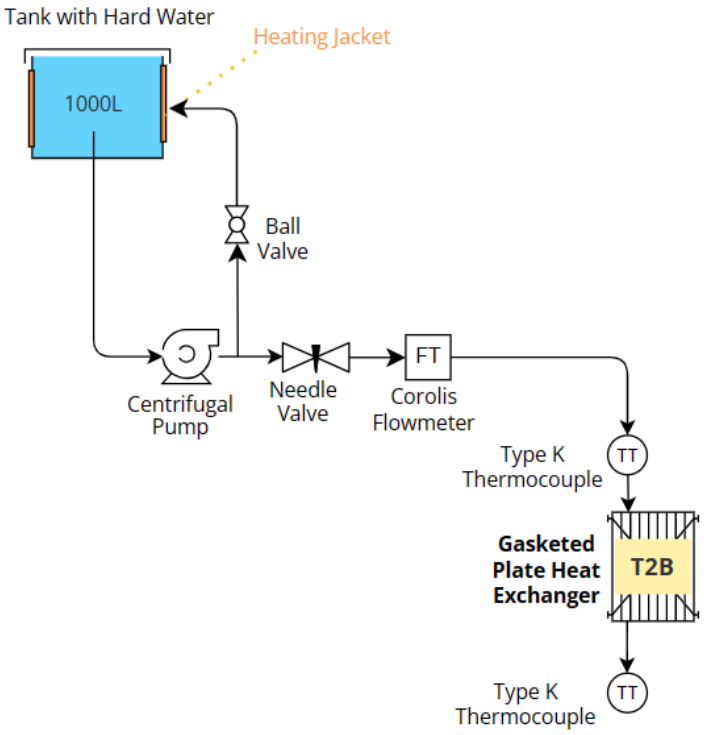

Figure 10: 1st and 2nd Section of Cold Loop Design

The primary objective of the cold loop is to circulate hard water through the T2B, at the desired flowrate, hardness, and temperature. As a result, once the hard water exits the GPHE, it must be returned to the tank to complete the cold loop. However, since the hard water gets heated in the T2B, its temperature upon exiting is much higher than when it entered. Therefore, the final step in completing the cold loop is to cool the hard water down to the tank temperature and subsequently return it to the tank.

- **Cooling Hard Water to Tank Temperature:**

  In order to run the experiment for multiple hours, the hard water exiting the T2B needs to be cooled down to the tank temperature for the entire duration of the experiment. An easy solution would be to employ a recirculating chiller with a digital control. However, this would be very expensive as a chiller capable of extracting a few kilowatts of heat can amount to several thousand euros. The laboratory in which the setup will be built is equipped with a cooling circuit that can supply water at flowrates exceeding 1000 kg/hr and at a temperature of approximately 13 - 15 °C. By using an additional GPHE after the T2B, the water from the cooling circuit can be utilised to cool down the hard water to tank temperature. Since Alfa Laval are an active part of the project, the additional GPHE needed, the TL3B, is also sourced from them. Hence, the two media of this additional GPHE will be the hard water already present in the loop, and the water from the cooling circuit of the laboratory. The cooling circuit has a ball valve to vary the flow of cooling water required. Additionally, a rotameter can be used to determine and monitor the flowrate of the cooling water. A rotameter is a type of flowmeter used to measure the flowrate of a fluid in a pipeline. It consists of a vertical tube with a tapered float inside. As the fluid flows upward through the tube, the float rises, reaching a stable position indicating the flowrate. Since a high level of precision is not needed when measuring the flowrate of cooling water, a rotameter can be used owing to its simplicity and cost-effectiveness. Additionally, a type 'K' thermocouple connected to the DAQ can also be placed along with the rotameter to determine the temperature of the cooling water entering the TL3B. Hence, by determining the exact temperature of the cooling water and selecting the correct flowrate, the hard water exiting the T2B can be cooled to the tank temperature. This can be verified by measuring the temperature of the hard water at the exit of the TL3B with another type 'K' thermocouple connected to the DAQ. The hard water can then be returned to the tank, whereas the cooling water that exits the TL3B is connected to the return line of the cooling circuit, completing the circulation within the laboratory's cooling system. Finally, a thermocouple can be placed in the tank to ensure that the tank is always at the required temperature.

- **Piping of Cold Loop:**

  After having selected all the components of the cold loop, the final step is to select the piping that will connect the components to each other. Since, at no point in the cold loop is the water expected to reach temperatures higher than 80°C, the piping for the entire loop can be chosen as rubber hoses. This makes the cold loop cheap to construct and easy to maintain. Additionally, at the highest point in the system, a de-airing valve can be added to remove any air from the cold loop. This can prevent airlocks which restrict fluid flow and prevent corrosion by minimising the presence of oxygen.

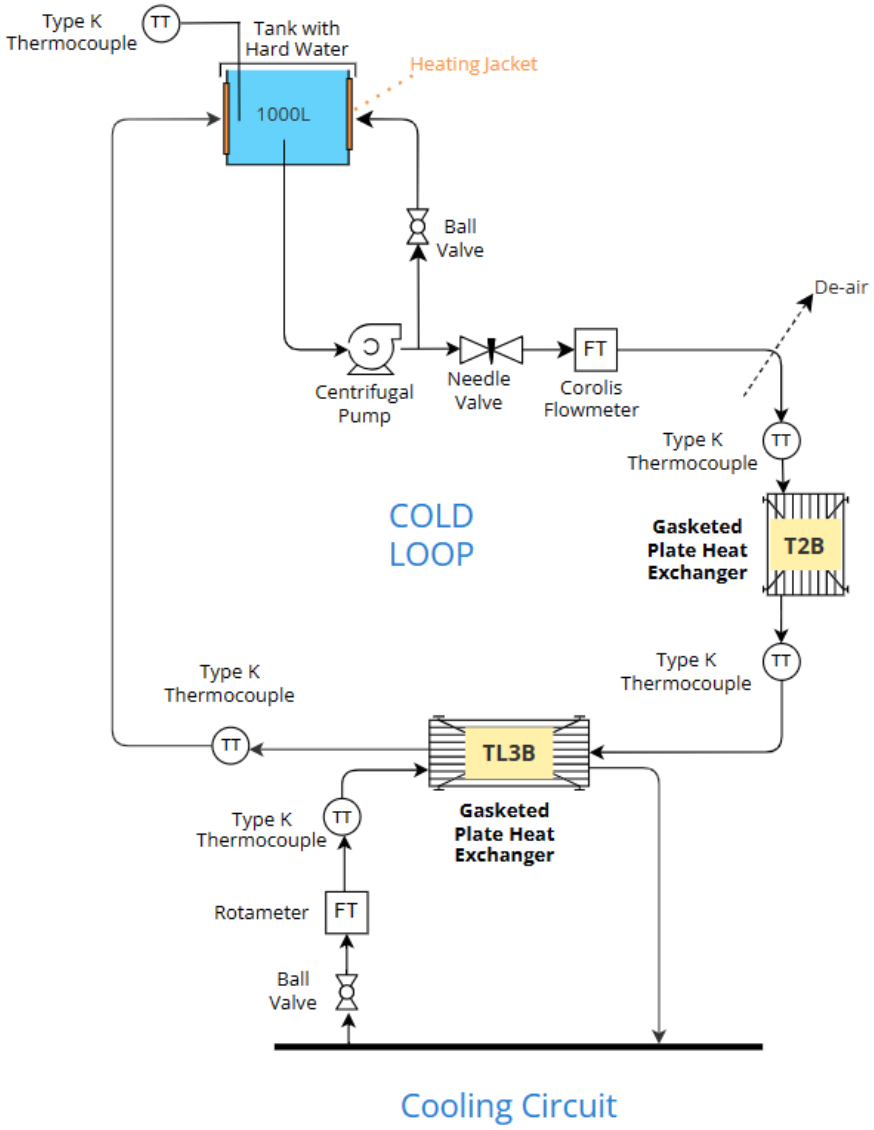

Figure 11: Complete Cold Loop Design

4.3.2 Design of the Hot Loop

The heat exchanger on which scaling is deposited, the T2B, must also be supplied with hot water at the required flowrate and temperatures. As discussed previously, the hot water supply, along with all ancillary and measuring equipment needed, forms the 'Hot Loop'.

- **De-hardened Water:**

  The most important component of the hot loop is the water flowing through it. As mentioned earlier, it is important that the water in the hot loop does not scale the plates of the T2B. This is vital to ensure that any changes in plate weight and GPHE performance are only due to scaling caused by the hard water in the cold loop. Hence, the water used in the loop must be chosen carefully to ensure that the hot medium does not scale the plates even at high temperatures. Filling the loop would tap water would result in the formation of scale, whereas filling the loop with de-mineralised water can result in the leaching of the metal. Hence, dehardened water, i.e. water devoid only of calcium and magnesium salts, must be used in the hot loop. This ensures that the plates will not scale due to the hot medium.

- **Boiler:**

  The primary purpose of the hot loop is to supply hot water to the T2B. Therefore, the key component of the hot loop is a boiler. The boiler must provide a steady stream of hot water at the desired temperature and flowrate throughout the experiment. Therefore, the boiler should allow for the selection of the outlet temperature. Additionally, the boiler should be equipped with an integrated pump to deliver the hot water. To meet these requirements, the selected boiler should have a control system connected to its own resistive heating elements, temperature and flow sensors. By determining the temperature and flowrate of the water entering the boiler, the control system can determine the amount of heat needed to achieve the set outlet temperature.

  In essence, the boiler required for the experiments consists of several essential components. These include resistive heating elements responsible for generating heat, a pump to facilitate the circulation of water, and temperature and flow sensors that provide feedback on the system's conditions. These sensors are connected to a control system, which receives the data and regulates the heat output of the resistive heating elements based on the desired outlet temperature and the flowrate of the water. The exact flowrate can be set by placing a ball valve after the boiler. This integrated setup ensures precise control and enables hot water supply at the required flowrate and temperature.

  It must also be noted that a pressure relief valve must be connected to the boiler. A pressure relief valve is a critical safety device installed to protect against excessive pressure buildup in a system. The pressure relief valve works by opening automatically when the pressure inside the boiler exceeds a set limit. When the pressure reaches a predetermined threshold, the valve's spring-loaded mechanism is activated, allowing excess pressure to escape through a discharge pipe or vent. This action reduces the pressure within the boiler and helps maintain it at a safe operating level. It thereby safeguards against the risk of overpressure, which can occur due to various factors such as malfunctions, blockages, or operator errors. By promptly releasing excess pressure, the pressure relief valve helps prevent damage to the boiler, protects the surrounding equipment and piping, and mitigates the potential for injuries and property damage.

- **Hot channel in GPHE:**

  Once the hot water at the required temperature and flowrate is obtained from the boiler, it can be passed into the T2B. As discussed previously, the T2B consists of 1 channel for the cold medium and 2 channels for the hot medium. The hot water therefore flows through two channels of the T2B, heating the hard water in the process. The hot water exiting the T2B can then be returned back into the boiler. To make the necessary calculations to quantify scaling at the end of the experiments, two type 'K' thermocouples connected to the DAQ can be placed at the inlet and outlet of the T2B, to determine and log the temperature of the hot water.

- **Piping of Hot Loop:**

  The piping arrangement of the hot loop plays a crucial role in ensuring safety. Given that the hot water circulating within this loop is expected to reach temperatures of ≈ 80-90°C, it is important to secure the positioning of the piping. Moreover, the material chosen for the piping must be able to withstand such elevated temperatures for the entire experimental run. As a result, copper pipes will be employed for constructing the hot loop's piping system, as they can withstand high temperatures and, unlike rubber hoses, will remain fixed its position even under high flowrates, provided it is well secured at both ends.

  Additionally, similar to the cold loop, a de-airing valve must be added at the highest point in the loop. This helps to remove any air to prevent airlocks which restrict fluid flow and to prevent corrosion by minimising the presence of oxygen.

- **Expansion Vessel:**

  Due to the high temperatures present in the system, the water flowing through the copper piping will undergo thermal expansion. As the water heats up, from room temperature to 80-90 °C, it expands in volume and increases pressure within the system. To accommodate this expansion and prevent potentially damaging pressure buildup, it is necessary to install an expansion vessel. An expansion vessel is a vital component in the closed-loop heating system. Its primary function is to absorb the excess pressure resulting from fluid expansion caused by temperature changes. The expansion vessel consists of a sealed chamber divided by a flexible diaphragm. One side of the diaphragm contains compressed air or gas, while the other side is connected to the system's water supply. As the water in the system heats up and expands, it compresses the gas or air within the expansion vessel. This compression allows the vessel to act as a buffer, absorbing the increased volume of water and maintaining a balanced pressure level. This prevents excessive pressure from damaging the copper piping, valves, and other system components.

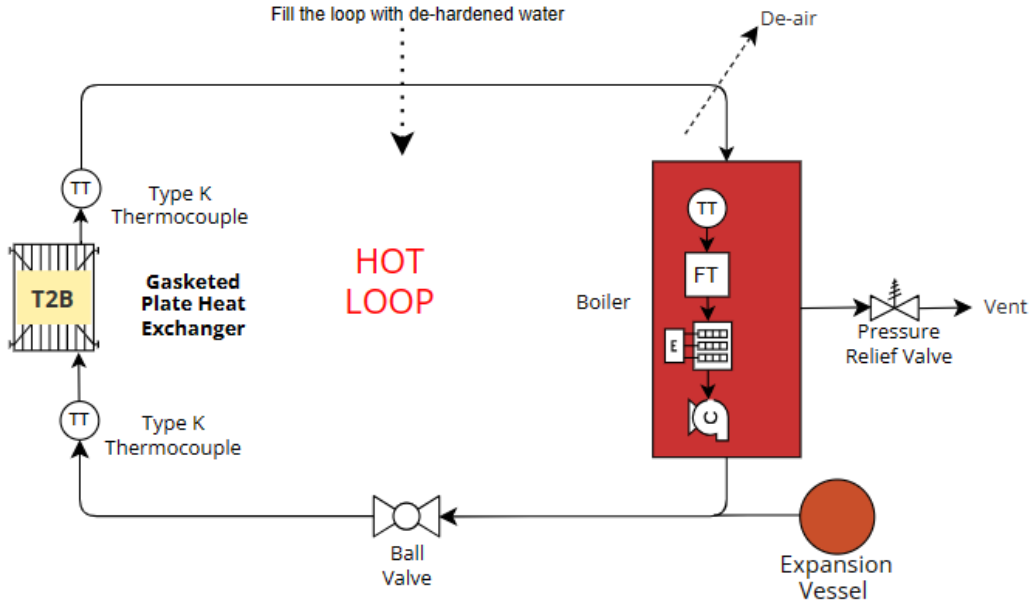

Figure 12: Complete Hot Loop Design

After completing the design of the two loops, they are assembled together with the T2B to create the experimental setup. The complete setup is seen in figure 13. The thermocouples have been assigned numerical labels to allow for easy referencing throughout the remainder of this study. The thermocouples positioned at the inlet and exit of the T2B in the hot loop are numbered $TT1$ and $TT2$, respectively. In the cold loop, the thermocouples positioned at the inlet and exit of the T2B are labelled as $TT3$ and $TT4$, respectively. The thermocouple positioned at the inlet of the TL3B in the cooling circuit is referred to as $TT5$, while the thermocouple at the exit of the TL3B in the cold loop is referred to as $TT6$. Lastly, the thermocouple positioned in the tank is labelled as $TT7$.

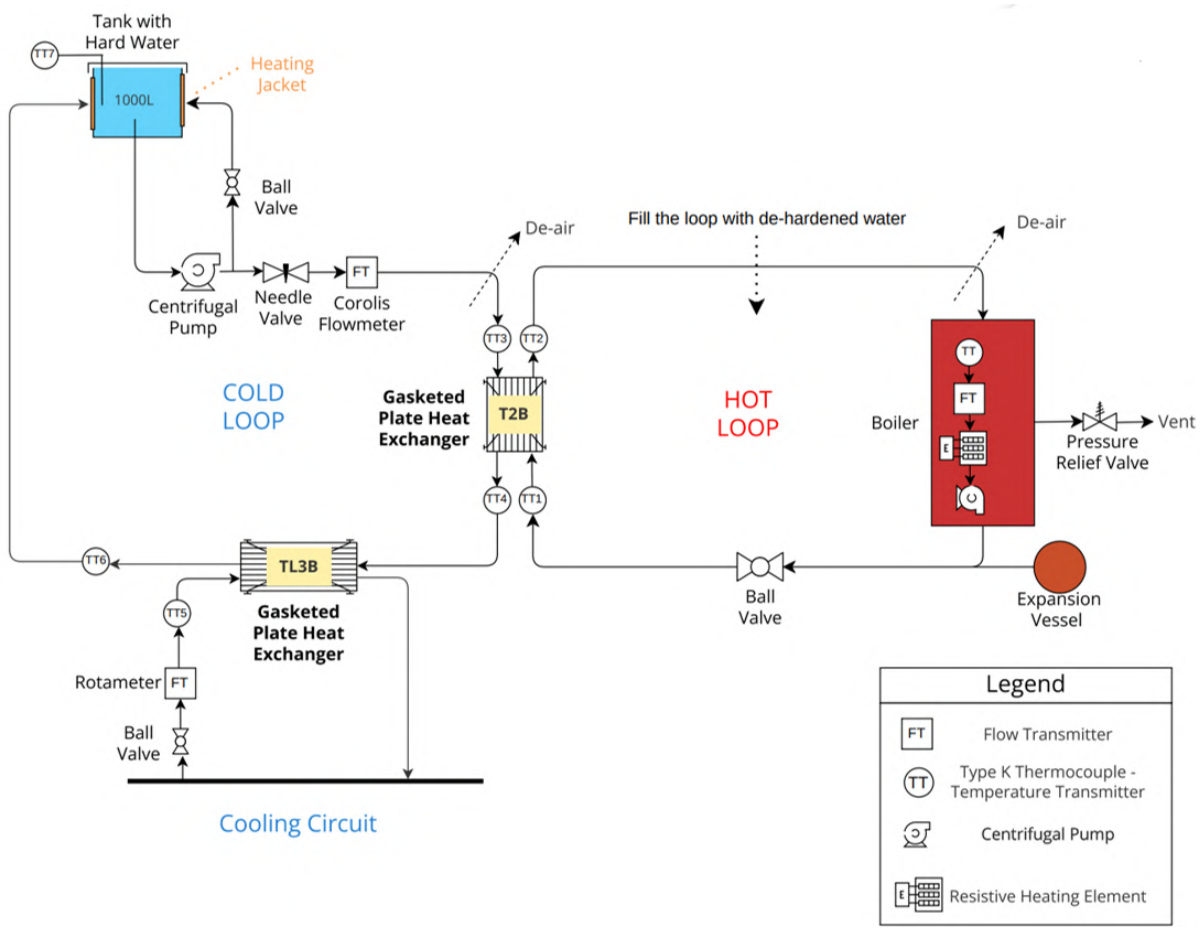

Figure 13: Complete Experimental Setup Design

4.4 Design of Experiments (DOE)

Upon selecting the equipment for the cold and hot loops and completing the overall setup design, the next step involves designing the experiments themselves. As mentioned in section 3, the research question that this study aims to answer is to determine the effect of hardness, flowrate and temperature of the hard water as well as the heat flux on $CaCO_3$ scaling in GPHEs. Since the heat transfer area is constant for all experiments, the heat flux (W/m^2) can be replaced by duty (kW) exchanged by the T2B. The experiments must be designed such that when one parameter is varied, all other parameters are held constant for the entire duration of the experiment. This approach ensures that any observed changes in the weight of scale deposited, scale distribution on the plate, and change in GPHE performance are solely attributed to the specific parameter being studied.

The initial step is to estimate the total number of experiments required for the study. Assuming a minimum of 4 variations for each parameter and considering the investigation of 4 parameters, the total number of experiments would be 4^4 = 256. However, conducting 256 experiments is impractical due to the significant amount of resources needed as well as the time constraints involved. To address this issue, a solution is to establish a 'base case' by selecting specific values for hardness, flowrate and inlet temperature of the hard water as well as the duty exchanged by the T2B. These chosen values collectively form the base case. With respect to this base case, the flowrate can be varied 3 times while keeping the hardness, inlet temperature, and duty constant. As a result, the base case along with these 3 additional experimental cases constitute a set of 4 experiments studying the effect of flowrate variation. Similarly, with respect to the base case, the inlet temperature can be varied 3 times while keeping the flowrate, hardness, and

duty constant. The base case along these 3 additional experimental cases constitute a set of 4 experiments studying the effect of inlet temperature variation. This process is repeated two more times to create sets of experiments examining the effect of variation of hardness and duty. These 4 sets of experiments collectively encompass 12 unique experiments plus the base case, resulting in a total of 13 experiments. By employing this strategy, the number of experiments is reduced from 256 to 13 while still investigating the effects of each parameter by varying them across 4 levels and keeping other parameters constant. This approach, known as fractional factorial design, allows for a more manageable and efficient experimental design while still providing valuable information about the effects of the parameters.

The next step in designing the experiments involves estimating the base case values for the hard water's flow rates, hardness, and inlet temperature. Additionally, by approximating the outlet temperature of the hard water at which scaling can be expected, the base case value of duty of the T2B can be estimated. A starting point is established for the experimental design by determining these base case values, which can then be used as a reference for varying the parameters while keeping others constant in subsequent experiments. The experiments will be designed using CAS, a tool designed by Alfa Laval to aid in heat exchanger selection. This tool, however, cannot account for scaling or fouling on the plates. Hence, the drop in outlet temperature of the cold media or the overall heat transfer coefficient of the GPHE due to scaling cannot be predicted or calculated by this software. As a result, CAS will be used to design the experiments under the assumption that no scaling will occur on the plates.

To prevent scale formation, Alfa Laval recommends that customers maintain flowrates resulting in a shear stress exceeding 50 Pa on the heat exchanger plate. According to CAS, the flowrate corresponding to a shear stress of 50 Pa on a T2B designed with 1 cold medium channel is 250 kg/hour. Since, the flowrate can be varied on either side of 250kg/hour by varying the opening of the needle valve, it can be chosen as the base value for flowrate of hard water.

Alfa Laval also noted that in many GPHE applications where cooling water is utilized, the water source is typically cooling tower water or tap water. Hence, the cooling water temperature typically falls within the range of 15 to 25°C, varying depending on the country and time of year. Considering that the temperature of tap water at TU Delft is $\approx$ 20°C, the lowest permissible water inlet temperature for the experiments is 20°C. However, 20°C cannot be set as the base case value for inlet temperature as it would be difficult to cool down the hard water in the tank to below this temperature. Hence, the base value of inlet temperature can be set to 25°C, as it allows for inlet temperature to be varied on either side of it.

To determine the base case value of water hardness, an inductive coupled plasma optical emission spectroscopy (ICP-OES) analysis was conducted on tap water. ICP-OES is an analytical technique employed for detecting chemical elements in a sample. The analysis revealed that tap water contains approximately 59 ppm of calcium ions (Ca^{+2}). Given the molar mass ratio between calcium carbonate ($CaCO_3$) and calcium (Ca) is 2.5, the concentration of calcium carbonate in water is 2.5 times the concentration of calcium ions in water (assuming all calcium in water exists as $CaCO_3$). Therefore, tap water comprises approximately 148 ppm of $CaCO_3$, which corresponds to a German degree hardness of 8.26°dH. Using tap water and therefore setting the base value hardness as 8.26°dH, poses a few problems. Firstly, reducing the hardness value of tap water would not be straightforward as that would involve removing calcium carbonate from tap water. Additionally, considering that the duration of a single experiment may only be a few hours or a maximum of 1 day, it is unlikely that significant scaling would be observed in such a short duration with a hardness value of 8.26°dH. This may lead to difficulties when comparing the results of 2 different experiments as the weight of the scale deposited and

the change in GPHE performance would be negligible. Hence, as an initial estimate, the base value hardness can be chosen as 3 times that of tap water, i.e. 25°dH. This would ensure that the plate is scaled considerably during an experiment. Additionally, selecting the base value hardness as 25°dH, allows for variation of hardness value in either direction.

Finally, the base case value of the duty exchanged by the T2B can be estimated by selecting an approximate outlet temperature of the hard water such that the plates will experience scaling. Alfa Laval advises their customers to limit their cooling water outlet temperature to 50°C to prevent scaling. However, due to the potential short duration of the experiment, significant scaling may not be observed when limiting the outlet temperature of the base case to 50°C. Additionally, for the same duty when the flowrate is increased or the inlet temperature is decreased, the outlet temperature will drop below 50°C, further lowering the possibility of the plate to scale. Hence, for the base case, the outlet temperature can be selected as 60°C, as this leaves enough room for the outlet temperatures to decrease below 60°C in other experiments while still resulting in a high probability to experience scale formation. Therefore, for a base case value of flowrate and inlet temperature of 250kg/hour and 25°C respectively, the duty required for an outlet temperature of 60°C can be estimated using equation 9, as 10kW.

$$\begin{aligned} \dot{Q} &= \dot{m} \cdot cp \cdot \Delta T \\ \dot{Q} &= \left(\frac{250}{3600}\right) \cdot 4.18 \cdot (60 - 25) \\ \dot{Q} &\approx 10\,\text{kW} \end{aligned} \tag{9}$$

After selecting the base case values for the flowrate, hardness and inlet temperature of hard water, as well as the duty exchanged by the T2B, the base case design on the cold loop side is complete. For the design of the remaining experiments, each parameter needs to be varied 3 times with respect to the base case in order to form a set of 4 experiments studying the effect of variation of a parameter. To keep the sets of experiments consistent with each other, the value of the parameter will be reduced once and increased twice with respect to the base case. Additionally, the difference between the 2 values of the parameter will always be kept constant.

In order to achieve the required duty for the chosen flowrate and inlet temperature of the hard water, the hot medium also needs to be designed for each experiment. Considering that the hot medium is not susceptible to scaling and that this study focuses on the effect of variation of parameters of the hard water, the flowrate and temperature of the hot medium can be selected, for each experiment, in a manner that delivers the required duty to the cold medium. The selection of the hot medium conditions can be made with the help of Alfa Laval's heat exchanger design and selection tool, CAS. Since the flow conditions of the cold medium and the GPHE as well its configuration are fixed, it must be supplied as an input to CAS. Additionally, the tool allows for the selection of the 'margin' parameter. The margin, expressed as a percentage, indicates how oversized or undersized a GPHE is for the case it is being configured for. If the margin is positive, the GPHE is oversized, which means that the GPHE possess excess heat transfer area than needed for that particular case. As a result, when the plate initially scales, and the plate surface area available for heat transfer reduces, the excess area of the GPHE compensates for this loss in plate surface area, resulting in a negligible change in GPHE performance. Conversely, if the margin is negative, the GPHE is undersized, which means that the GPHE possess insufficient heat transfer area than needed for that particular case. As a result, when the plate initially scales, and the plate surface area available for heat transfer reduces, the change in GPHE performance is very large due to a further reduction in plate surface area. To avoid both these extreme situations, the margin for every experiment will be set to zero, making the heat transfer surface area perfect for every case.

- **DOE - Effect of Change in Flowrate:**

  To conduct experiments focused on studying the effect of flowrate on scaling tendency and GPHE performance, it is necessary to maintain a constant hardness and inlet temperature of the hard water, as well as a constant duty exchanged by the T2B throughout all experiments. As previously mentioned, the base case is configured with a hard water inlet temperature of 25°C, flowrate of 250kg/hr, hardness of 25°dH and an approximate duty of 10kW with a margin of 0. Additionally, the GPHE for the experiments is a T2B with 2 hot medium channels and 1 cold medium channel, resulting in a total of 4 plates. It is also known from Alfa Laval that the plate for the T2B is made of alloy 316 stainless steel and has a plate thickness of 0.5mm. These conditions are supplied to CAS with a guess for the inlet temperature and flowrate of the hot medium. After a few iterations, the base case is configured as seen in figure 14.

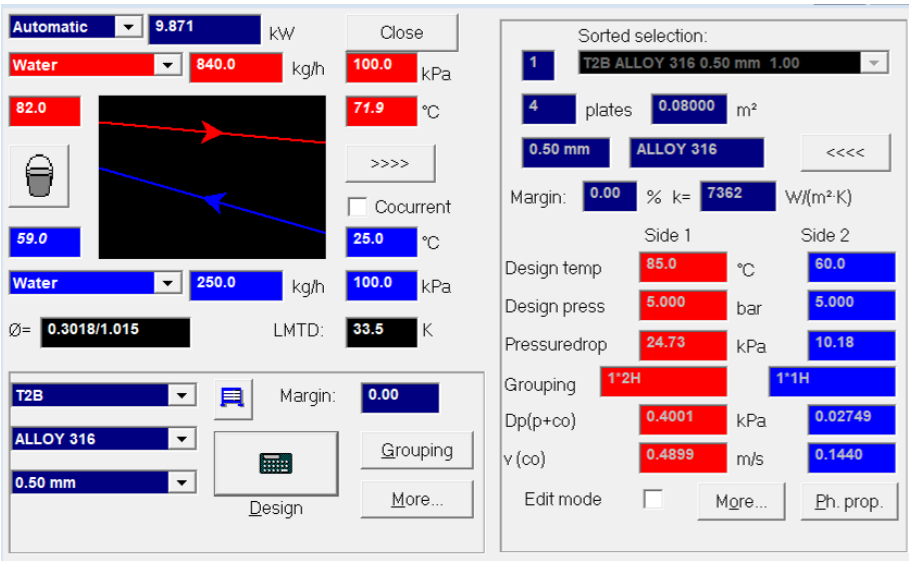

Figure 14: Configuration of Base Case on CAS

In figure 14, all data concerning the hot medium is placed in red boxes and data concerning the cold medium is paced in blue boxes. The case is configured for the T2B with 4 plates resulting in a total heat transfer area of 0.08 m^2. Under 'Grouping' it is visible that the GPHE has 2 channels for the hot medium and 1 channel for the cold medium. For the cold medium, the flowrate is 250kg/hour, the inlet temperature is 25 °C, and the outlet temperature is 59 °C. For the hot medium, the flowrate is 840 kg/hour, the inlet temperature is 82 °C and outlet temperature is 71.9 °C. It must be noted that it was not possible to configure the T2B with a 0 margin as well as a 10kW duty. Hence, the margin was set to 0 and a duty of ≈ 9.8kW was chosen for the base case. Therefore, all other cases will be configured with the same duty.

After configuring the base case, the other 3 cases in the set of experiments studying effect of variation of flowrate can be designed. As stated previously, the value of the parameter will be varied reduced once and increased twice with the respect to the base case. Additionally, the difference between 2 values of the parameter must always be held constant. An appropriate step size for these set of experiments can be set to 20% of the flowrate of the base case, i.e. 50kg/hour. Hence, the 4 flowrates can be selected as 200, 250, 300 and 350kg/hr. For each flowrate, the case must be configured in CAS for a constant inlet temperature of 25 °C, duty of 9.8kW and margin of 0. Additionally, the hardness of the cold medium for every case will be set to 25 °dH. All 3 cases are configured in CAS and all relevant details pertaining to the cold and hot media for the set of experiments

studying the effect of flowrate variation are noted in table 1. The images of the configured cases in CAS are seen in Appendix A.

Table 1: DOE - Effect of change in Flowrate

		Cold Medium				Hot Medium		
Case No.	**Duty kW**	**Flowrate kg/hr**	**Inlet Temp °C**	**Hardness °dH**	**Outlet Temp °C**	**Flowrate kg/hr**	**Inlet Temp °C**	**Outlet Temp °C**
Effect of Change of Flowrate								
1	9.87	200	25	25	67.5	1350	85	78.7
2 Base Case		250			59	840	82	71.9
3		300			53.4	735	79	67.4
4		350			49.3	670	77	64.3

- **DOE - Change in Inlet Temperature:**

  To conduct experiments focused on studying the effect of inlet temperature on scaling tendency and GPHE performance, it is necessary to maintain a constant hardness and flowrate of the hard water, as well as a constant duty exchanged by the T2B throughout all experiments. The value of inlet temperature for the base case was chosen as 25°C. Similar to the experiments studying effect of flowrate variation, the step size for the change in inlet temperature can be set to 20% of the value of the base case inlet temperature, i.e. 5°C. Hence, the 4 inlet temperatures can be selected as 20, 25, 30 and 35°C. For each inlet temperature, the case must be configured in CAS for a constant flowrate of 250 kg/hour, duty of 9.8kW and a margin of 0. Additionally, the hardness of the cold medium for every case will be set to 25 °dH. All 3 cases are configured in CAS and all relevant details pertaining to the cold and hot media for the set of experiments studying the effect of inlet temperature variation are noted in table 2. The images of the configured cases in CAS are seen in Appendix A.

Table 2: DOE - Effect of change in Inlet Temperature

		Cold Medium				Hot Medium		
Case No.	**Duty kW**	**Flowrate kg/hr**	**Inlet Temp °C**	**Hardness °dH**	**Outlet Temp °C**	**Flowrate kg/hr**	**Inlet Temp °C**	**Outlet Temp °C**
Effect of Change of Inlet Temperature								
5	9.87	250	20	25	54	750	79	67.7
6 Base Case			25		59	840	82	71.9
7			30		64	1080	84	76.1
8			35		69	1500	86	80.4

- **DOE - Effect of Change in Duty:**

  To conduct experiments focused on studying the effect of duty on scaling tendency and GPHE performance, it is necessary to maintain a constant hardness, inlet temperature and flowrate of the hard water, throughout all experiments. The value of duty for the base case was chosen as 9.8 kW. Similar to the experiments studying effect of flowrate variation, the step size for the change in duty can be set to 20% of the value of the base case duty, i.e. 1.77 kW. Hence, the 4 duties can be selected as 7.89, 9.8, 11.84 and 13.81 kW . For

each duty, the case must be configured in CAS for a constant flowrate of 250 kg/hour, inlet temperature of 25 °C a margin of 0. Additionally, the hardness of the cold medium for every case will be set to 25 °dH. All 3 cases are configured in CAS and all relevant details pertaining to the cold and hot media for the set of experiments studying the effect of change in duty are noted in table 3 The images of the configured cases in CAS are seen in Appendix A.

Table 3: DOE - Effect of change in Duty

		Cold Medium				**Hot Medium**		
Case No.	**Duty kW**	**Flowrate kg/hr**	**Inlet Temp °C**	**Hardness °dH**	**Outlet Temp °C**	**Flowrate kg/hr**	**Inlet Temp °C**	**Outlet Temp °C**
Effect of Change of Duty								
9	7.89	250	25	25	52.2	675	75	63.5
10 Base Case	9.87				59	840	82	71.9
11	11.84				65.8	1950	85	79.8
12	13.81				87.9	2300	93	87.9

- **DOE - Effect of Change in Hardness:**

  To conduct experiments focused on studying the effect of hardness on scaling tendency and GPHE performance, it is necessary to maintain a constant inlet temperature and flowrate of the hard water, as well as a constant duty exchanged by the T2B throughout all experiments. The value of hardness for the base case was chosen as 25 °dH. Similar to the experiments studying effect of flowrate variation, the step size for the change in hardness can be set to 20% of the value of the base case hardness i.e. 5 °dH. Hence, the 4 hardness values can be selected as 20, 25, 30 and 35°dH. For each hardness value, the case will be identical to the base case, apart from the hardness value of the hard water. Hence, the individual cases do not need to be configured in CAS. The relevant details pertaining to the cold and hot media for the set of experiments studying the effect of change in hardness are noted in table 4.

Table 4: DOE - Effect of change in Hardness

		Cold Medium				**Hot Medium**		
Case No.	**Duty kW**	**Flowrate kg/hr**	**Inlet Temp °C**	**Hardness °dH**	**Outlet Temp °C**	**Flowrate kg/hr**	**Inlet Temp °C**	**Outlet Temp °C**
Effect of Change of Hardness								
13	9.87	250	25	20	59	840	82	71.9
14 Base Case				25				
15				30				
16				35				

4.5 Sizing the Loops

Once the design of the two loops and the experiments are completed, the next step is to appropriately size the equipment within the loops. The equipment must be selected such that it allows for the successful execution of the designed experiments on the T2B.

In the cold loop, the equipment needs to handle the flow of hard water at the desired flowrate, hardness, and temperature. The tank must be selected such that it can accommodate and supply the hard water for the entire experimental run and the heating jacket must be chosen such that it allows for the hard water to be pumped at the required temperature. The 2nd GPHE, the TL3B, must be configured such that it removes all the heat supplied to the hard water in the T2B. Additionally, other supporting equipment such as pumps and valves should be selected to ensure efficient circulation and control of the hard water within the loop.

Similarly, in the hot loop, the equipment should be sized to meet the temperature, flow and safety requirements of the hot medium. This includes selecting a boiler with an integrated pump, temperature and flow sensors, and a control system, that is capable of supplying the necessary temperature to achieve the desired duty in the T2B. Additionally, the expansion vessel and valves should be chosen to ensure safety, reliable operation and control of the hot medium within the loop.

4.5.1 Sizing the Cold Loop

- **Hard Water:**

  Before sizing the equipment in the cold loop, it is important to determine the quantity of salt and de-hardened water required to prepare the hard water for a single experiment. The objective is to ensure a continuous and consistent supply of hard water to the T2B at the desired flowrate, while maintaining a relatively constant concentration of $CaCO_3$ throughout the experiment, in spite of scaling on the GPHE. As mentioned earlier, using a large quantity of de-hardened water would require a substantial amount of salt to achieve the desired $CaCO_3$ concentration in the prepared hard water. As a result, the amount of $CaCO_3$ lost from the hard water due to scaling would be negligible when compared to the initial quantity of $CaCO_3$ dissolved in the water. This ensures a relatively constant $CaCO_3$ concentration and therefore a relatively constant hardness value throughout the experiment.

  In the current configuration of the T2B, the cold medium, i.e. the hard water, passes through a single channel. As a result, only 2 plates come in contact with the hard water. From Alfa Laval, it is known that the area of one side of the plate on which scale can deposit is 0.02 m^2. Therefore, in the current configuration, the area available for scale to deposit is 0.04 m^2. It is also known that the free channel length, or the distance between 2 plates, is 2.4mm. By using this information and making some assumptions, the maximum amount of scale that is expected to deposit on the plates can be calculated. This value also represents the maximum amount of $CaCO_3$ lost from the tank due to scaling. Hence, this information can be used to determine the initial amount of $CaCO_3$ that must be dissolved in the tank to ensure a constant hardness value in the tank for the entire experimental run.

  The first assumption that can be made is that the entire plate area will not scale in an experiment run for a duration of less than 24 hours. A majority of the scaling will be observed at the exit of the plates. This is because the hard water will heat up and increase in temperature as it flows along the plate towards the exit. Hence, the temperature of the hard water in the channel will be highest at the exit and lowest at the inlet. Since $CaCO_3$ is inverse soluble, the tendency of the plate to scale will increase as the hard water is closer to the exit. As a result, the inlet of the plate will not suffer from scaling in a short experiment. It is therefore assumed that only the final 75% of the plate length will scale in an experiment. Hence the total effective area available for the scale to deposit is 75% of 0.04 m^2 = 0.03 m^2. The next assumption can be made regarding the thickness of the scale that will deposit on the plates. In an experiment run for a short time duration,

significant blockage of the channel is not expected. Thus, it can be assumed that in the most extreme case, 5% of the free channel length, i.e. 5% of 2.4mm = 0.12mm, will be blocked by the scale. Based on this assumption, each plate must have a 0.06mm thick layer of scale deposited onto it. From the previous 2 assumptions, the maximum volume of scale that can be deposited on the plates is 1.8 cm^3, as determined by equation 10.

$$\begin{aligned}\text{Volume of scale deposited} &= \text{Maximum thickness of scale deposited} \times \text{Effective area of plate} \\ &= (\frac{0.06}{1000}) \times 0.03 \\ &= 0.0000018\,m^3 \\ &= 1.8\,cm^3\end{aligned} \tag{10}$$

The density of $CaCO_3$ is between 2.7 and 2.95 g/cm^3 [43]. By using the mean value of 2.825 g/cm^3, the maximum total mass of scale that can deposit on the plates is 1.8 × 2.825 ≈ 5 grams. For the base case hardness of 25 °dH, the concentration of $CaCO_3$ needed is 0.446 g/L. Hence, if 500L of de-hardened water is used for an experiment, the amount of $CaCO_3$ in the water will drop from 223 grams to 218 grams if the maximum scaling condition is achieved. This corresponds to a change in hardness from 25 °dH to 24.4 °dH. This drop in hardness can be considered negligible, making 500L of de-hardened water an optimal choice for the experiments.

As per equation 11, the addition of 2 moles of $NaHCO_3$ (168 grams) and 1 mole of $CaCl_2$ (111 grams) to water results in the formation of 1 mole of $CaCO_3$ (100 grams).

$$2\,NaHCO_3 + CaCl_2 \longrightarrow CaCO_3 + 2\,NaCl + CO_2 + H_2O \tag{11}$$

Thus, if a volume of 500L of de-hardened water needs to be brought to a hardness level of 25 °dH, 223 grams of $CaCO_3$ needs to be formed in water. This would require 374.6 grams of $NaHCO_3$ and 247.5 grams of $CaCl_2$. Similarly, for experiments requiring lower or higher hardness values, the calculations can be performed accordingly.

- **Tank and Heating Jacket:**

  Once the volume of de-hardened water and, therefore, the total volume of the hard water needed for an experiment is known, the tank can be sized. A tank commonly used to hold large volumes of liquids is an intermediate bulk container (IBC). The standard capacity of an IBC tank is 1000L and is made of high-density polyethylene (HDPE), a thermoplastic polymer. A 1000L IBC tank, as seen in figure 15, is available in the lab at TU Delft, where the experiments will be conducted. Since the capacity of this tank is more than sufficient to hold 500L of de-hardened water, and the tank material can safely handle liquids in the temperature range of 20 - 35 °C, it was chosen as the tank to house the hard water.

  To ensure that the water in the tank is at the required inlet temperature of the experiment and to cancel any heat losses from the tank to the surroundings during the experimental run, a heating jacket is needed for the tank. The heating jacket should be designed for a 1000L IBC tank to ensure a good fit around the tank. Additionally, the heating jacket must have its own temperature sensors and a heating element connected to a control system that can heat the tank to the set temperature. For the highest inlet temperature needed for the experiments, 35 °C, the heating jacket needs to heat 500 L of water from room temperature (≈ 20 °C) to 35 °C overnight. Hence, the heating jacket needs to supply heat of 31350 J, as calculated in equation 12, in ≈ 16 hours. Hence, the power supply of the heating jacket must be 31350/16 ≈ 2kW.

$$\begin{aligned} Q &= m \cdot cp \cdot \Delta T \\ &= 500 \cdot 4.18 \cdot (35 - 29) \\ &= 31350\,\text{J} \end{aligned} \tag{12}$$

In line with the requirements, the heating jacket chosen for the experiments is the *IBC-J90-Pro* from the manufacturer *Frank Berg*, as seen in figure 16. It is designed for a 1000L IBC tank, has a power supply of 2kW and is made of polyester insulation that helps in cancelling losses to the environment. Since the jacket has integrated temperature sensors and a control system, it can be set to heat the tank up to a temperature of 90 °C via digital control. Since the required inlet temperatures of the hard water can be achieved using this heating jacket, and the heat loss of the atmosphere can be cancelled during the experimental run, it is an appropriate selection for the experiment.

Figure 15: IBC 1000L Tank

Figure 16: Frank Berg Heating Jacket

- **Pump and Flowmeter:**

  The next step in sizing the cold loop is to size the centrifugal pump. The primary purpose of the pump is to ensure the circulation of hard water within the loop and effectively mix the hard water in the tank utilizing a bypass line. Consequently, the hard water being pumped is divided into two portions, with one portion entering the T2B and the other portion returning back into the tank. Once the flowrate of the hard water entering the T2B is fixed based on the ongoing experiment, the remaining flow is directed back into the tank. Therefore, a higher power rating for the pump results in an increased flow back into the tank. Since the mixing of the tank is aided by a large flowrate of water returned back to the tank, it is beneficial to use a pump with as high as a power rating as possible.

  In order to optimize cost and minimize project timelines, it was decided to use one of the pumps present in the lab at TU Delft. After carefully considering all available options, it was decided to use the centrifugal pump *CDXM 90/10* from the manufacturer *Ebara*, as seen in figure 17. It has a nominal power of 1.2kW and a maximum head rating of 30m. From CAS, it is known that the pressure drop in the cold medium channel of the T2B is expected to be between 0.1 - 0.3 bar, depending on the flowrate of the hard water. This

corresponds to a head of 1-3 metres. By assuming a similar pressure drop in the additional GPHE, and due to the valves, flow sensors, and temperature sensors, it can be concluded that the maximum head rating of the pump is more than sufficient to deliver the required flowrates and mix the hard water in the tank. The pump is, therefore an appropriate selection for the cold loop.

Since the properties of the medium in the cold loop and its flowrates are known, the flowmeter needed for the experiments can be selected. During the design of the cold loop, it was decided to use the Coriolis flowmeter owing to its highly accurate measurements without being affected by changes in fluid properties. Additionally, a high resolution of ≈ 1kg/hr and a digital display would enable accurate and easy monitoring of the flow. Hence, the Coriolis flowmeter *RHM-08* from the manufacturer *Rheonik*, as seen in figure 18, was selected. It has a high resolution of 0.36 kg/hr with a measuring range of 0 - 3000kg/hr. Additionally, it has a digital display to easily monitor the flow. Since the flowmeter meets all the requirements, it is an appropriate selection for the cold loop.

Figure 17: Ebara Pump

Figure 18: Rheonik Flowmeter

- **Temperature Sensors and DAQ:**

  In order to measure the temperature at various points in the cold loop, type K thermocouples were selected during the design phase. Moreover, considering that these thermocouples produce an analog output voltage, a data acquisition system (DAQ) is required to convert the voltage into a digital temperature reading. Consequently, the manufacturer *Omega*'s *5TC Series* type K insulated wire thermocouples were selected for this application. As the name suggests, an insulated wire thermocouple is equipped with an insulating material that surrounds and protects the two metal wires along their entire length. This insulation serves to electrically isolate the two wires from each other and the surrounding environment, preventing unwanted electrical interference and ensuring accurate temperature measurements. Additionally, to display and log the temperature readings, the *OM-DAQ-USB-2400* data acquisition system, also manufactured by *Omega*, was chosen. The DAQ with connected thermocouples is seen in figure 19. It allows for 8 differential analog inputs and is powered by connecting to a laptop. To facilitate the display and logging of the temperature readings, the DAQ also comes with software that can be installed on the laptop. With the DAQ and software combination, the temperature readings can be conveniently displayed in real-time and saved for future analysis.

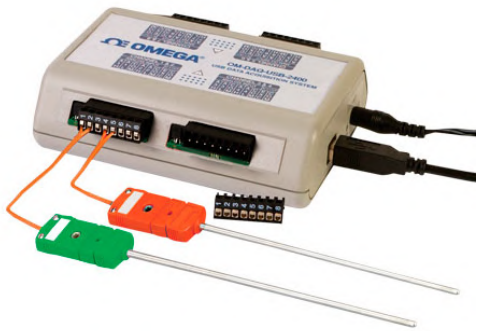

Figure 19: Omega thermocouples and DAQ

- **Cooling Hard Water to Tank Temperature:**

  In order to cool down the hard water exiting the T2B to tank temperature, the cold loop was designed with an additional GPHE from Alfa Laval, the TL3B, connected to the cooling circuit in the lab at TU Delft. The cooling circuit can provide water to the TL3B at a temperature of 13-15 °C and at flowrates of over 1000 kg/hr. The TL3B was chosen as the area of a TL3B plate is more than 3.5 times the area of a T2B plate, thereby resulting in a higher heat transfer capability of the GPHE. Additionally, to further increase the available area for heat transfer, the TL3B can be configured with more plates than the T2B. This further increases the heat transfer capacity of the GPHE, allowing for effective cooling with reduced cooling water consumption. Since Alfa Laval had a readily available 8 plate TL3B GPHE, it was configured on CAS for the base case, to check if it meets the requirements of the experimental design. As seen in figure 20, the hard water leaving the T2B at 250 kg/hr and 59 °C, is cooled to 25 °C, with only 220 kg/hr of cooling water at 14 °C. Hence, the 8 plate TL3B is more than capable of cooling the hard water down to tank temperature, making it an appropriate selection for the cold loop.

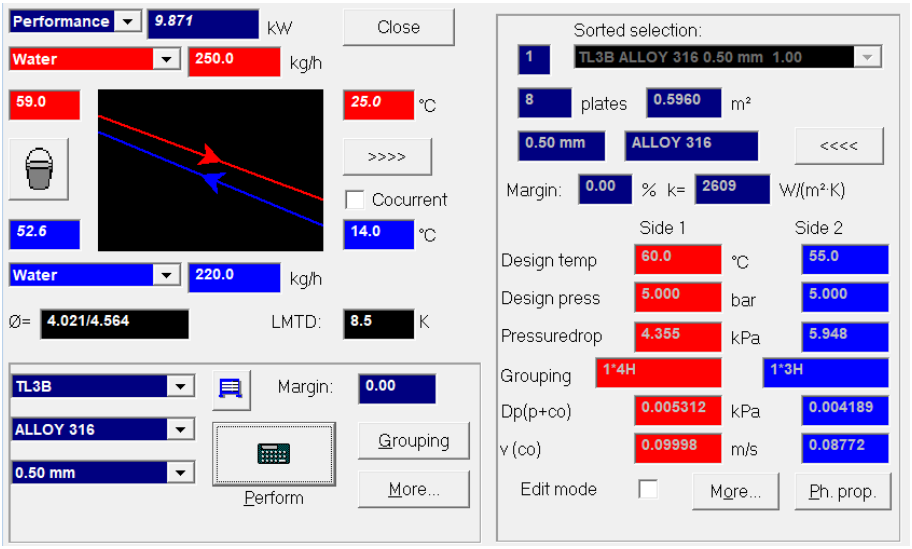

Figure 20: Configuration of the TL3B for the base case on CAS

In order to monitor the flowrate of water from the cooling circuit to the TL3B, a rotameter was positioned in between the two. From figure 20, it is known that the flowrate of cooling water needed for the base case is 220kg/hr. While each experiment has its own unique design, the cooling demands for the TL3B remain relatively consistent. Therefore, the flowrate of cooling water is expected to be similar across all experiments. Accordingly, a rotameter capable of monitoring flows ranging from 0 to 500 kg/hr would be an appropriate choice. Since, the *KSK* rotameter from the manufacturer *Kobold*, with a measuring range of 0-1200 kg/hr, was available in the lab at TU Delft, it was selected for the experiment. The rotameter selected is seen in figure 21.

Figure 21: Kobold Rotameter

4.5.2 Sizing the Hot Loop

- **Boiler:**

  The key component in the hot loop that requires proper sizing is the boiler. As mentioned earlier, the boiler should encompass heating elements, an integrated pump, and temperature and flow sensors connected to a control system. Additionally, the boiler must be able to supply a maximum of ≈ 14kW of heating duty to the T2B at the required flowrates and temperatures, as specified in the design of experiments. Finally, the boiler must be completely electric to avoid the use of gas for the production of hot water. After a thorough evaluation of available options, the *Calida Compact* electric central heating boiler from the manufacturer *Masterwatt*, as seen in figure 22, was selected. This boiler features 6 heating elements and can deliver a maximum power of 24kW. It includes its own pump and temperature, pressure, and flow sensors integrated with a control system. Furthermore, the boiler incorporates an in-built pressure relief valve. If the pressure in the system exceeds 3 bar, the valve opens to release the water from the loop. Given that the boiler fulfils all the specified requirements, it is a suitable choice for the hot loop.

Figure 22: Calida compact boiler

- **Expansion Vessel:**

  The final component that needs to be sized for the hot loop is the expansion vessel. To determine the volume of the expansion vessel, the volume of water in the hot loop, the expansion coefficient of water and the minimum and maximum temperature of water in the loop need to be determined. The volume of hot water in the loop is expected to be between 1-2 litres. The minimum temperature (T_{min}) in the loop will be room temperature, i.e. ≈ 20°C. As per the design of experiments, the maximum temperature (T_{max}) in the loop will be 85°C. Finally, the expansion coefficient, calculated by inverse of the temperature value, can be chosen at the mean value of the minimum and maximum temperature, i.e. 52.5°C. Hence, the volume of the expansion vessel needed is 2.5 litres, as calculated by equation 13.

$$\begin{aligned} \text{Expansion Volume} &= \text{Hot Loop Volume} \times \text{Expansion Coefficient} \times (T_{max} - T_{min}) \\ &= 2 \times (1/52.5) \times (85 - 20) \\ &= 2.5 \text{ litres} \end{aligned} \tag{13}$$

  For added safety measures, an expansion vessel with a volume larger than 2.5 litres must be installed in the hot loop. Hence, the 4 litre expansion vessel *Flexcon*, from the manufacturer *Flamco*, as seen in figure 23, was chosen for the hot loop. This expansion vessel is pre-charged at 0.5 bar. Hence, the minimum operating pressure in the hot loop must always be higher than 0.5 bar.

Figure 23: Flamco expansion vessel

Upon completing the of sizing both loops, the components can be sourced and connected to build the experimental setup. The flowmeter and all the thermocouples were calibrated before

installing them in the setup. The calibration curves can be seen in Appendix B. The two GPHEs used in the setup are seen in figures 24 and 25. Even though the T2B is configured with only 4 plates, the GPHE needs a thicker plate pack to be tightly screwed. Hence, 26 plates were added after the end plate to form a 30 plate pack. These additional plates do not have any flow through them as the hot and cold media are blocked by the 4th plate, i.e. the end plate in this case. The TL3B does not need additional plates and hence, a 8 plate TL3B was added in the experiment setup. The complete experimental setup, with all components labelled, is seen in the figure 26.

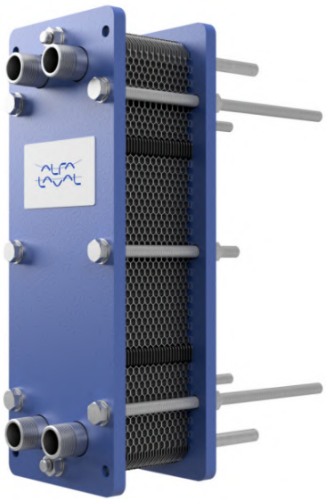

Figure 24: Alfa Laval T2B GPHE

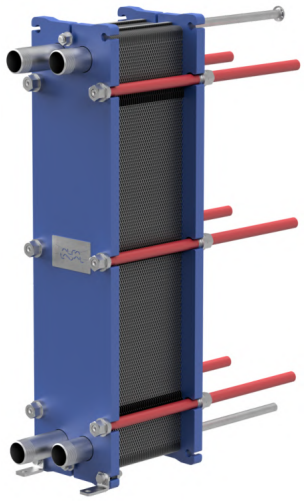

Figure 25: Alfa Laval TL3B GPHE

Figure 26: Complete Experimental Setup

4.6 Practical Considerations and Limitations

After assembling the setup, but before conducting the initial experiments, the equipment within the setup underwent testing to verify if their performance aligned with the expectations. Although the majority of the setup operated as anticipated, it is important to acknowledge discrepancies that arose during the testing phase and take them into consideration when analyzing the results.

- **Boiler:**

  The boiler that is selected for the hot loop exhibits a modulating behavior, whereby the boiler operates in a cyclical pattern to maintain the desired water temperature set-point. When the boiler is switched on and the desired water temperature is selected, the boiler continues to heat the water till it reaches the set-point. When the set point is reached, the boiler switches off. However, due to the thermal inertia of the system, the water temperature continues to rise momentarily, reaching a couple of degrees higher than the set point, before gradually starting to decline. Once the water temperature drops to a few degrees below the set point, the boiler switches on again, re-initiating the heating process. The boiler remains active until the water temperature rises back to the desired set point temperature °C, after which it switches off again. This cyclic operation repeats for the entire duration of an experiment. As a result, over a short period of time, the supply temperature of the hot medium is unstable. However, on average, the boiler is supplying a relatively constant temperature to the T2B.

  It was also observed that the boiler supply temperature was limited to a maximum of 85°C. Additionally, flowrates exceeding 1350 kg/hr result in inconsistent heating cycles of the boiler. The temperature fluctuations deviate from the expected cyclical pattern and exhibit erratic behaviour. Consequently, it is necessary to revise the experiments that involve flowrates higher than 1350 kg/hr or a hot medium supply temperature higher than 85 °C in order to comply with the limitations of the boiler. This adjustment will ensure that the experiments align with the operational capabilities of the system and facilitate accurate and reliable data collection.

- **Thermocouple placement:**

  As per the setup design, one thermocouple was installed in the tank, while six thermocouples were placed in the two loops. The positioning of the six thermocouples within the loops offered two options: direct contact with the flowing medium or placement on the surface of the brass pipe connections. Placing the thermocouple in direct contact with the flowing medium would provide a more accurate temperature measurement but required drilling a hole in the pipe connection, inserting the thermocouple, and sealing the hole to prevent leaks. This approach was tedious and prone to failure. Alternatively, the thermocouple could be attached to the surface of the brass pipe connection using a hose clamp, with the addition of insulating material in between the thermocouple and the hose clamp to minimize heat loss. However, this method would result in a less precise temperature measurement due to the insulating layer created by the brass pipe connection, which hindered the heat transfer. To determine the most suitable approach for the current setup, a test was conducted comparing the temperature measurements obtained from both methods. As depicted in Figure 27, at lower and relatively stable temperatures, the measurements from both thermocouples were similar. However, at higher and fluctuating temperatures, the thermocouple on the brass pipe connection yielded significantly lower readings as compared to the thermocouple in direct contact with the medium. Consequently, the thermocouples located before the T2B in the cold loop (TT3), before

the TL3B in the cooling circuit (TT5), and after the TL3B in the cold loop (TT6), were placed on the brass pipe connections, as these temperatures remained relatively low and constant throughout an experiment. Conversely, the thermocouples positioned in the hot loop (TT1, TT2) and the thermocouple at the exit of the T2B in the cold loop (TT4) were installed in direct contact with the medium, as these temperatures were relatively high and exhibited fluctuations due to the modulating behavior of the boiler.

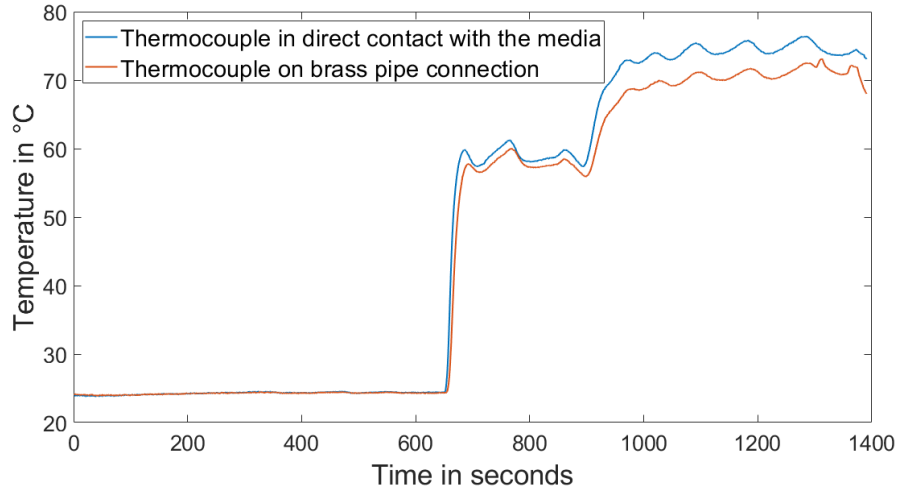

Figure 27: Comparison of temperature measurements: Thermocouple placement in direct contact with medium vs. on brass pipe connection

- **Cooling Water Supply Temperature:**

  The cooling water sourced from the TU Delft lab, intended for use in the TL3B, was not at a constant temperature throughout the day. Initially, when the supply of water from the cooling circuit is switched on, the temperature is between 13.5 and 14°C. However, as the cooling water flows through the TL3B, it accepts heat from the hard water and exits at a much higher temperature than the inlet temperature. This heated water is returned back into the circuit via the return line. Since the cooling mechanism of the circuit is incapable of extracting the amount of heat being introduced by the TL3B, the temperature of the cooling water supply gradually rises over the course of the day. During a test run, where the cooling water was used to extract 9.8kW of heat from the TL3B for 8 hours, the temperature of the cooling water gradually increased from 13.5°C at the start of the test run to 17°C at the end of the run. As a result, in order to return the hard water back to the tank from the TL3B at the tank temperature for an 8 hour experiment, the flowrate of the cooling water must be consistently increased during the experiment to keep up with the drop in supply temperature. This makes it difficult to maintain a constant tank temperature and inlet temperature of the T2B.

- **Pump:**

  When the pump in the cold loop is switched on, during the initial 30-45 minutes, it imparts a significant amount of heat into the water being circulated. Consequently, the temperature of the water after passing through the pump is elevated by 2-3 °C when compared to the temperature in the tank. However, towards the end of the first hour, the heat input from the pump decreases substantially, and the temperature difference before and after the pump drops to 0.3-0.5°C. Therefore, it is crucial to allow the pump to operate for a minimum of one hour before initiating any experiment. This ensures that the pump stabilizes and minimizes its impact on the temperature of the water being circulated.

- **Absence of Cooling Tower:**

  As previously mentioned, in many industrial applications where cooling water is used, the common sources are cooling tower water or tap water. In this setup, the intention was to use cooling tower water as the source of hard water, as it is the more prevalent choice. However, due to the presence of Legionella bacteria in the cooling tower at TU Delft, it was not accessible for use. Consequently, the hard water needed for the experiments had to be prepared artificially. This involved adding salts to the water to facilitate the formation of $CaCO_3$.

- **Fluctuation in hardness value:**

  During the testing phase, 25 °dH hard water solution was prepared in the tank by adding the necessary salts in the correct proportions to 500 litres of water. Once the hard water solution was prepared, a sample was taken, and a test run was initiated. Throughout the test run, samples were collected every 2 hours over an 8-hour period to monitor the consistency of water hardness. However, upon analyzing the samples using ICP-OES, it was observed that despite the initial hardness being 25 °dH, the hardness gradually decreased throughout the day to approximately 16 °dH. This decrease in hardness can be attributed to two main factors. Firstly, $CaCO_3$ is highly insoluble in water, with a solubility range of 13-19 ppm. Consequently, some of the $CaCO_3$ formed in the water gradually precipitates and settles at the bottom, resulting in a reduction in overall hardness. Secondly, the presence of a bypass valve, intended to facilitate mixing in the tank, only effectively mixes the upper half of the tank, while the lower half remains relatively stagnant. As a result, the settled $CaCO_3$ at the bottom of the tank is not properly re-suspended, further contributing to the gradual decrease in water hardness over time. Due to the observed decrease in water hardness over time, the planned experiments that aimed to investigate the effects of varying hardness were excluded from the study. The inability to maintain a consistent hardness level throughout an experiment rendered it impractical to use hardness as a controllable parameter.

- **Time duration of each experiment:**

  To ensure comparability of results, it is important to run each experiment for the same duration. However, given the uncertainty of when significant scaling may occur on the plates, it is necessary to allow the experiment to run for as long as possible. Considering the lab rules at TU Delft, which permit access between 8:00 and 18:00, and taking into account the preparation time for the hard water and the required hour of pump operation before each experiment, the duration for each experiment was fixed at 8 hours. This ensures consistent experimental conditions throughout all experiments while adhering to the lab regulations.

To accommodate the limitations posed by the boiler and the inability to maintain a constant hardness value in the tank, the design of experiments has been revised. In Case 8, the maximum inlet temperature has been adjusted from 35 °C to 33 °C. Furthermore, for the experiments examining the impact of varying duty, the step size has been modified to 1 kW, and the maximum duty has been capped at 11.31 kW. Lastly, the experiments studying the effect of variation of hardness were eliminated. These changes result in a total of 10 experimental cases (9 unique experiments plus the base case) that need to be conducted, as seen in table 5. The revised set of experiments were configured in CAS and updated in Appendix A

Table 5: Updated Design of Experiments

		Cold Medium				Hot Medium		
Case No.	**Duty kW**	**Flowrate kg/hr**	**Inlet Temp °C**	**Initial Hardness °dH**	**Outlet Temp °C**	**Flowrate kg/hr**	**Inlet Temp °C**	**Outlet Temp °C**
Effect of Change of Flowrate								
1	9.87	200	25	25	67.5	1350	85	78.7
2 Base Case		250			59	840	82	71.9
3		300			53.4	735	79	67.4
4		350			49.3	670	77	64.3
Effect of Change of Inlet Temperature								
5	9.87	250	20	25	54	750	79	67.7
6 Base Case			25		59	840	82	71.9
7			30		64	1080	84	76.1
8			33		67	1350	85	78.7
Effect of Change of Duty								
9	8.87	250	25	25	55.6	675	79	67.7
10 Base Case	9.87				59	840	82	71.9
11	10.87				62.5	1050	85	76.1
13	11.31				64	1350	85	77.8

4.7 Error and Uncertainty

The final step, before conducting the experiments, is to quantify the error in the measured value and determine the uncertainty in the final results. The error refers to the difference between the measured and the true value, whereas uncertainty quantifies the range of possible values that the true value of a measurement or calculated result may fall within. Calculating and reporting both error and uncertainty is crucial for understanding the reliability and quality of measurements and calculations. Quantifying these factors allows for proper interpretation of results and enables accurate comparisons between different experiments.

In the present experimental setup, the parameters measured consist of flowrate, determined by the flowmeter, and temperature, obtained from the thermocouples. The flowrate value is obtained directly via the digital display of the flowmeter in the cold loop and via the digital display of the boiler in the hot loop. According to the manufacturer's specifications, the flowmeter in the cold loop exhibits an error of 0.2% of the measured flowrate, which corresponds to an error range of 0.4 to 0.7 kg/hr for the flowrates in the range of 200 to 350 kg/hr. Given that this error is negligible in comparison to the overall flowrate, it can be disregarded in subsequent calculations. Similarly, the flowmeter in the hot loop, which operates within a flowrate range of 670 to 1350 kg/hr, has a specified error of 0.3% of the flowrate value. This translates to an error range of 2 to 4 kg/hr, depending on the specific flowrate. Similar to the flowmeter in the cold loop, this error is considered insignificant relative to the overall flowrate and can be disregarded in future calculations.

As for the temperature measurement, the reading from the thermocouple is obtained via the DAQ. Consequently, potential sources of error in the measured temperature values include the error in the thermocouples themselves and the error in the DAQ system. According to the manufacturer's specifications, the thermocouples have an uncertainty of ±1.1 °C, while the DAQ system's cold junction compensation accuracy is ±1 °C. To determine the total uncertainty in the

temperature measurement, these individual uncertainties can be combined using equation 14. Thus, considering the thermocouple error and the DAQ system's cold junction compensation accuracy as the only sources of uncertainty, the overall uncertainty in the final temperature reading is approximately ±1.48 °C, as determined by equation 14.

$$\begin{aligned} \text{Total uncertainty} &= \sqrt{(\text{Thermocouple uncertainty})^2 + (\text{DAQ uncertainty})^2} \\ &= \sqrt{(1.1)^2 + (1)^2} \\ &= 1.48°\text{C} \end{aligned} \tag{14}$$

These temperature readings will be used to make further calculations, such as the average heat transferred in the T2B (Q_{avg}), the logarithmic mean temperature difference ($LMTD$), and finally, the overall heat transfer coefficient (U). Consequently, the computed values will inherently possess uncertainty in their final results. This uncertainty can be calculated using the propagation of uncertainty or propagation of error theory, which allows the determination of the uncertainty/error in a calculated quantity based on the uncertainties/errors in the input variables. According to the uncertainty propagation theory, for a function $f(x_1, x_2, \ldots, x_n)$ that depends on n input variables with uncertainties $\Delta x_1, \Delta x_2, \ldots, \Delta x_n$, respectively, the uncertainty in the quantity f is determined by equation 15.

$$\Delta f = \sqrt{\left(\frac{\partial f}{\partial x_1}\right)^2 \cdot (\Delta x_1)^2 + \left(\frac{\partial f}{\partial x_2}\right)^2 \cdot (\Delta x_2)^2 + \ldots + \left(\frac{\partial f}{\partial x_n}\right)^2 \cdot (\Delta x_n)^2} \tag{15}$$

In this formula $\frac{\partial f}{\partial x_1}, \frac{\partial f}{\partial x_2}, \ldots, \frac{\partial f}{\partial x_n}$ represent the partial derivatives of the function f with respect to each of the input variables and $\Delta x_1, \Delta x_2, \ldots, \Delta x_n$ represent the uncertainties in each of the input variables.

- **Uncertainty in average heat transferred:**

  Upon establishing equation 15 to determine the uncertainty in a calculated quantity, the uncertainty in the average heat transferred (Q_{avg}) by the T2B can be calculated. Q_{avg} for the T2B, can be calculated using equations 16 - 18.

$$Q_c = M_c \cdot c_p \cdot (T4 - T3) \tag{16}$$

$$Q_h = M_h \cdot c_p \cdot (T1 - T2) \tag{17}$$

$$Q_{\text{avg}} = \frac{Q_c + Q_h}{2} \tag{18}$$

  Q_c and Q_h denote the heat gained and heat lost by the cold and hot medium, respectively and M_h and M_c denote the mass flow rate of the hot-side and cold-side respectively. $c_{p,h}$ and $c_{p,c}$ denote the specific heat capacity of hot and cold fluid, respectively. T_1 and T_2 denote the inlet and outlet temperatures of the hot medium, respectively and T_3 and T_4 denote the inlet and outlet temperatures of the cold medium respectively. Since M_h, M_c, $c_{p,h}$ and $c_{p,c}$ are constant throughout the experiment we can substitute $(M_h \cdot c_{ph})$ as 'h' and $(M_c \cdot c_{pc})$ as 'c'.

$$\text{Hence, } Q_h = h \cdot (T_1 - T_2) \text{ and } Q_c = c \cdot (T_4 - T_3)$$

  For the following calculations, Q_{avg} will be referred to as Q for ease of notation. Let the errors in $T1$, $T2$, $T3$, and $T4$ be $\Delta T1$, $\Delta T2$, $\Delta T3$, and $\Delta T4$, respectively. Hence, the error in Q (ΔQ), can be calculated using equation 19.

$$\Delta Q = \sqrt{\left(\frac{\partial Q}{\partial T1}\right)^2 \cdot (\Delta T1)^2 + \left(\frac{\partial Q}{\partial T2}\right)^2 \cdot (\Delta T2)^2 + \left(\frac{\partial Q}{\partial T3}\right)^2 \cdot (\Delta T3)^2 + \left(\frac{\partial Q}{\partial T4}\right)^2 \cdot (\Delta T4)^2} \tag{19}$$

The partial derivatives of Q with respect to $T1$, $T2$, $T3$, and $T4$ can be computed as follows:

Partial derivative of Q with respect to $T1$:

$$\frac{\partial Q}{\partial T1} = \frac{\partial((Qh + Qc)/2)}{\partial T1} = \frac{\partial(h/2(T1 - T2))}{\partial T1} = \frac{h}{2}$$

Partial derivative of Q with respect to $T2$:

$$\frac{\partial Q}{\partial T2} = \frac{\partial((Qh + Qc)/2)}{\partial T2} = \frac{\partial(h/2(T1 - T2))}{\partial T2} = -\frac{h}{2}$$

Partial derivative of Q with respect to $T3$:

$$\frac{\partial Q}{\partial T3} = \frac{\partial((Qh + Qc)/2)}{\partial T3} = \frac{\partial(c/2(T4 - T3))}{\partial T3} = -\frac{c}{2}$$

Partial derivative of Q with respect to $T4$:

$$\frac{\partial Q}{\partial T4} = \frac{\partial((Qh + Qc)/2)}{\partial T4} = \frac{\partial(c/2(T4 - T3))}{\partial T4} = \frac{c}{2}$$

Now, substituting these partial derivatives and the respective errors into equation 19, the error in Q (ΔQ) can be calculated as seen in equation 20

$$\Delta Q = \sqrt{\left(\frac{h}{2}\right)^2 \cdot (\Delta T1)^2 + \left(-\frac{h}{2}\right)^2 \cdot (\Delta T2)^2 + \left(-\frac{c}{2}\right)^2 \cdot (\Delta T3)^2 + \left(\frac{c}{2}\right)^2 \cdot (\Delta T4)^2} \tag{20}$$

- **Uncertainty in logarithmic mean temperature difference:**

The next step is to determine the error in the logarithmic temperature difference (LMTD) of the T2B. The LMTD can be calculated using equation 21.

$$LMTD = \frac{(T1 - T4) - (T2 - T3)}{\ln\left(\frac{T1-T4}{T2-T3}\right)} \tag{21}$$

Similar to the previous calculation, considering the errors in $T1$, $T2$, $T3$, and $T4$ to be $\Delta T1$, $\Delta T2$, $\Delta T3$, and $\Delta T4$, respectively, the error in the $LMTD$ ($\Delta LMTD$) can be calculated using equation 22.

$$\Delta LMTD = \sqrt{\left(\frac{\partial LMTD}{\partial T1} \cdot \Delta T1\right)^2 + \left(\frac{\partial LMTD}{\partial T2} \cdot \Delta T2\right)^2 + \left(\frac{\partial LMTD}{\partial T3} \cdot \Delta T3\right)^2 + \left(\frac{\partial LMTD}{\partial T4} \cdot \Delta T4\right)^2} \tag{22}$$

The partial derivatives of $LMTD$ with respect to $T1$, $T2$, $T3$, and $T4$ can be computed as follows:

Partial derivative of $LMTD$ with respect to $T1$:

$$\frac{\partial LMTD}{\partial T1} = \frac{\ln\left(\frac{T1-T4}{T2-T3}\right) - \frac{(T1-T4)-(T2-T3)}{T1-T4}}{\ln^2\left(\frac{T1-T4}{T2-T3}\right)}$$

Partial derivative of $LMTD$ with respect to $T2$:

$$\frac{\partial LMTD}{\partial T2} = -1 \cdot \left[\frac{\ln\left(\frac{T1-T4}{T2-T3}\right) - \frac{(T1-T4)-(T2-T3)}{T2-T3}}{\ln^2\left(\frac{T1-T4}{T2-T3}\right)} \right]$$

Partial derivative of $LMTD$ with respect to $T3$:

$$\frac{\partial LMTD}{\partial T3} = \frac{\ln\left(\frac{T1-T4}{T2-T3}\right) - \frac{(T1-T4)-(T2-T3)}{T2-T3}}{\ln^2\left(\frac{T1-T4}{T2-T3}\right)}$$

Partial derivative of $LMTD$ with respect to $T4$:

$$\frac{\partial LMTD}{\partial T4} = -1 \cdot \left[\frac{\ln\left(\frac{T1-T4}{T2-T3}\right) - \frac{(T1-T4)-(T2-T3)}{T1-T4}}{\ln^2\left(\frac{T1-T4}{T2-T3}\right)} \right]$$

Substituting these partial derivatives and the respective errors into equation 22, the error in the $LMTD$ can be computed.

- **Uncertainty in overall heat transfer coefficient:**

  The final step is to determine the error in the overall heat transfer coefficient (U). It is defined as the ration of Q_{avg} and $LMTD$, as seen in equation 23.

$$U = \frac{Q}{\text{LMTD}} \tag{23}$$

  By denoting the error in Q as ΔQ and the error in $LMTD$ as $\Delta LMTD$, the error in the overall heat transfer coefficient (ΔU), can be calculated using equation 24.

$$\Delta U = \sqrt{\left(\frac{\partial U}{\partial Q}\right)^2 \cdot (\Delta Q)^2 + \left(\frac{\partial U}{\partial \text{LMTD}}\right)^2 \cdot (\Delta \text{LMTD})^2} \tag{24}$$

  The partial derivatives of U with respect to Q and $LMTD$ can be calculated as follows:

  Partial derivative of U with respect to Q:

$$\frac{\partial U}{\partial Q} = \frac{1}{\text{LMTD}}$$

  Partial derivative of U with respect to $LMTD$:

$$\frac{\partial U}{\partial \text{LMTD}} = -\frac{Q}{\text{LMTD}^2}$$

  Substituting these partial derivatives and the respective errors into equation 24, the error in the overall heat transfer coefficient (ΔU) can be computed as seen in equation 25.

$$\Delta U = \sqrt{\frac{\Delta Q^2}{\text{LMTD}^2} + \frac{Q^2}{\text{LMTD}^4} \cdot \Delta \text{LMTD}^2} \tag{25}$$

5 Results and Discussions

This study aims to determine the effect of various parameters on the scaling tendency and performance of the GPHE. The change in GPHE performance due to scaling can be quantified by determining the change in overall heat transfer coefficient(U) and fouling resistance (R_f) during an experiment. These quantities can be computed at all times 't' of an experiment and plotted against time to visualise the extent and rate of the drop due to scaling. However, to compute the fouling resistance (R_f), the overall heat transfer coefficient at time t=0 (U_0) is needed. As mentioned previously, this value can be difficult to estimate as, at time t=0, the system is highly transient as it is starting up and the temperatures are approaching their desired values. Hence, for a particular experimental case, the value of U_0 can be determined by operating the GPHE under the required boundary conditions but with de-hardened water as both the cooling and heating media. This ensures that the plates do not scale, resulting in a relatively constant GPHE performance for the entire experiment duration. This overall heat transfer coefficient value obtained by running the experiment with de-hardened water as both media, can be termed as U_0. For every experimental case designed, U_0 can be calculated, and a reference can be established, which, when compared against the experimental case run with the cooling medium as hard water, allows for the determination of the change in GPHE performance due to the presence of scale.

To summarise, the strategy that will be used to quantify the effect of scale on GPHE performance is to run all 10 unique experimental cases with de-hardened water as both the cooling and heating media to determine the reference overall heat transfer coefficient (U_0) for every case. Subsequently, all 10 unique experimental cases are rerun with hard water as the cooling medium and de-hardened water as the heating medium. For each case, the overall heat transfer coefficient for all times 't' of an experiment (U_t) can be determined and plotted against time to visualise the extent and rate of drop in the overall heat transfer coefficient during the experimental run. Finally, by using the corresponding value of U_0 and the fouling resistance ($R_{f,t}$) can be determined for all times 't' of the experiment and plotted against time to determine the effect of scaling on GPHE performance.

The last step is to calculate the time for 'onset of scaling' for each experiment. As discussed previously, Berce et. al. [16] noted that during the initial stages of scale formation, the thickness of the deposited scale is negligible and therefore, no drop in the overall heat transfer coefficient is noticed. In fact, the sparse scale deposits induce roughness-induced turbulence, thereby temporarily increasing the overall heat transfer coefficient. However, as the experiment proceeds and the thickness of the deposited scale continues to grow, the overall heat transfer coefficient begins to drop and eventually falls below the value of U_0. The time at which the overall heat transfer coefficient drops below the value of U_0, can be termed as the 'onset of scale' as beyond this point, the scale is detrimental to GPHE performance.

5.1 Determining the reference overall heat transfer coefficient (U_0)

The determination of the reference overall heat transfer coefficient (U_0) for every experimental case involves conducting all 10 distinct experiments utilizing de-hardened water as both the heating and cooling media. Since no performance variation is expected, each experiment does not need to be conducted for an extensive duration. However, due to the modulating behaviour of the boiler, it is necessary to run the experiments for a sufficient period to acquire an adequate number of temperature readings for computing a reliable average value. Consequently, all 10 experiments were conducted for a duration of 3 hours each, with the temperature being measured by the thermocouples at one-second intervals. The first experiment conducted was the base case. The temperature is obtained from the thermocouples every second and plotted against time, as seen in figure 28.

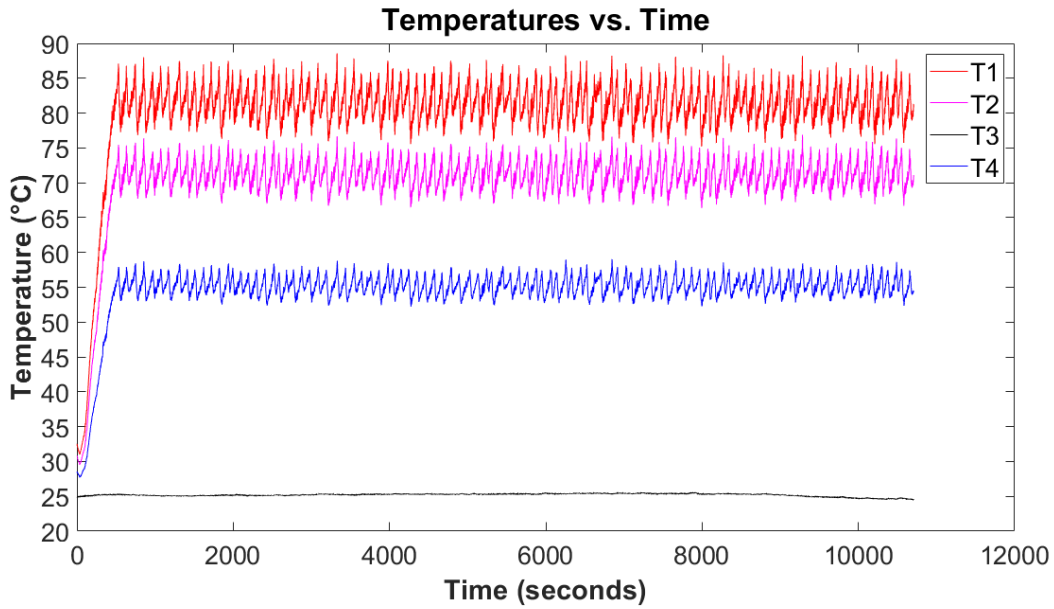

Figure 28: Temperature (°C) vs time (seconds) for the base case

In figure 28, only $T1$, $T2$, $T3$ and $T4$ are plotted, as the other three thermocouples present in the cold loop are only used to control the system and do not influence the calculations of average heat transferred, LMTD and overall heat transfer coefficient. As mentioned earlier, $T1$ and $T2$ denote the inlet and outlet temperature of the hot medium, whereas $T3$ and $T4$ denote the inlet and outlet temperature of the cold medium. The modulation of the boiler is evident by the fluctuations noticed in $T1$ and $T2$. Additionally, since the hot medium is transferring most, but not all, of its heat to the cold medium, the fluctuations in $T4$ are evident but not as pronounced as $T1$ and $T2$. Finally, no fluctuations in $T3$ are observed as the temperature of the tank was held relatively constant for the entire duration.

To mitigate the influence of fluctuations and facilitate the interpretation of the data, the recorded temperatures were subjected to an averaging process at 10-minute intervals. The resulting averaged values were plotted against time and are presented in Figure 29. In addition, the uncertainties associated with the temperature readings were determined by calculating the standard deviation within each 10-minute window. These uncertainties are visually represented in figure 29 as a shaded region surrounding each temperature curve. It accounts for the variability of the temperature measurements within each window and provides a 68% confidence interval by adding and subtracting the standard deviation once.

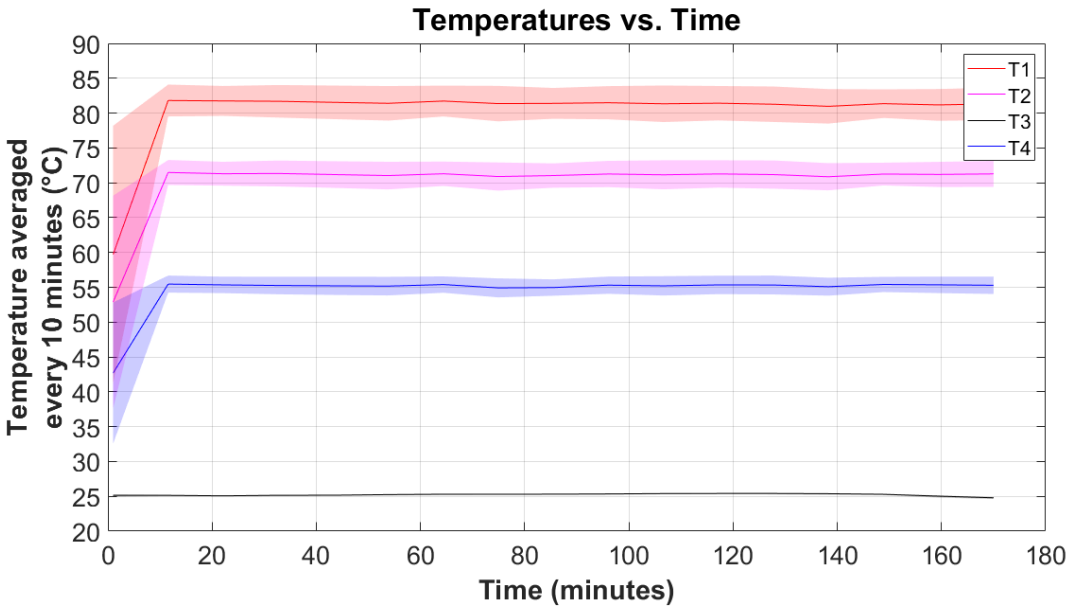

Figure 29: Temperature (°C) averaged every 10 minutes vs time (minutes) for the base case

In order to compute the average heat transferred (Q_{avg}), logarithmic mean temperature difference ($LMTD$) and finally, the overall heat transfer coefficient (U_0), the first step is to compute the average of the temperatures $T1$, $T2$, $T3$ and $T4$. As seen in figure 29, the average of $T1$, $T2$, $T3$ and $T4$ is 82°C, 71.85°C, 25.1°C, and 55.75°C respectively. Additionally, The specific heat capacity of the hot medium (cp_h), calculated at the average temperature of $T1$ and $T2$, i.e. 76.9 °C, is 4.19 kJ/(kg K). Similarly, the specific heat capacity of the cold medium (cp_c) calculated at the average temperature of $T3$ and $T4$, i.e. 40.4 °C, is 4.18 kJ/(kg K). The mass flowrate of the cold and hot medium is 250kg/hr and 840 kg/hr, respectively. Hence, the heat lost by the hot medium (Q_h) and the heat gained by the cold medium (Q_c) can be calculated as 9.9 and 8.9 kW, respectively, using equations 16 and 17. The average heat transferred by the T2B (Q_{avg}), calculated using equation 18, is 9.4 kW. Additionally, since the errors in the temperatures are known for each 10-minute window, the uncertainty in Q_{avg} can be calculated for every 10-minute window using equation 20. The uncertainties across each 10-minute window can be averaged to determine the average uncertainty in Q_{avg}. Therefore, the final Q_{avg} result can be expressed as 9.4 ± 1.4 kW.

Since the average temperatures are known, the LMTD can be calculated using equation 21 as 35.5K. Additionally, since the errors in the temperatures are known for each 10-minute window, the uncertainty in LMTD can be calculated for every 10-minute window using equation 22. The uncertainties across each 10-minute window can be averaged to determine the average uncertainty in LMTD. Therefore, the final LMTD result can be expressed as 35.5 ± 1.4K.

Finally, by using the average heat transferred by the T2B (Q_{avg}) and the LMTD, the overall heat transfer coefficient (U_0) for the base case run with dehardened water as both the cooling and heating media is 3309.8 W/m^{2}K, as determined by equation 23. Using the errors in the temperatures in each 10-minute window, the error in the uncertainty can be calculated using equation 25 for each of these windows. The uncertainties across each 10-minute window can be averaged to determine the average uncertainty in the overall heat transfer coefficient. Therefore the final U_0 can be expressed as 3309.8 ± 43.5W/m^{2}K.

It must be noted that the average heat transferred by the T2B is 0.4 kW or ≈ 4% lower than the designed duty of 9.8 kW. Additionally, there is a 1kW difference between the heat lost by

the hot medium (Q_h) and the heat gained by the cold medium (Q_c), in spite of supplying the T2B with the hot and cold media at their designed flowrate and supply temperatures. This is primarily because of the configuration of the T2B. The T2B is designed with 3 channels, configured such that the hot medium flows in channels 1 and 3, whereas the cold medium flows in channel 2. As a result of this configuration, the hot media in channel 1 loses heat to the cold media on one side, and to the atmosphere via the start plate on the other side. Similarly, the hot media in channel 3 loses heat to the cold media on one side, and to the rest of the plate pack on the other side. This results in a higher heat loss and, therefore, a lower hot medium outlet temperature than the design outlet temperature. Similarly, the lower heat transferred from the hot medium to the cold medium results in a lower heat gain of the cooling medium and, therefore, the observed outlet temperature of the cold medium is lower than the design outlet temperature. Additionally, the error in the flowrates and media temperatures further contributes to the difference between Q_h and Q_c. Since insulating the T2B was not possible and the errors in the measurements cannot be accounted for, the difference between Q_h and Q_c was accepted as a limitation of the system.

To ensure the repeatability of the system, the base case was repeated 2 more times. The average heat transferred (Q_{avg}) and overall heat transfer coefficient (U_0) was calculated as 9.43 ± 1.5 kW and 3334 ± 45.1 W/m^{2}K for the first repetition and 9.39 ± 1.48 kW and 3316 ± 43.5 W/m^{2}K for the second repetition. Since all three base case runs resulted in similar values of Q_{avg} and U_0, the system was considered repeatable. Hence, the remaining 9 experiments were conducted, and the value of U_0 was determined for each case. The plots for averaged temperature vs time for the two repetitions of the base case and for the additional 9 experiments are seen in Appendix C.

5.2 Performing experiments with hard water as the cooling medium

Once the reference overall heat transfer coefficient (U_0) is determined for every experimental case, the experiments with hard water as the cooling medium can be conducted. Similar to the previous experiments, the temperatures from the thermocouples will be retrieved every second. The recorded temperatures will then be subjected to an averaging process at 10-minute intervals. In addition, the uncertainties associated with the temperature readings will be determined by calculating the standard deviation within each 10-minute window. Finally, by using the average value of the temperatures and their uncertainties, the average heat transferred (Q_{avg}), logarithmic mean temperature difference ($LMTD$), overall heat transfer coefficient (U) and fouling resistance (R_f) along with their uncertainties can be determined for each experimental case. This allows for the quantification of the effect of each parameter on the GPHE performance by using the heat transfer measurement method. To implement the direct weighing measurement method, the plate weights must be noted before each experiment. After the completion of an experiment, the GPHE can be opened, and the scaled plates can be dried in the oven and weighed. By subtracting the weight of the clean plates, the weight of the scale deposited on the plates can be determined. This helps determine the effect of each parameter on the tendency of $CaCO_3$ to deposit on the plate. Finally, to implement the visual inspection method and observe the distribution of the scale on the plate, photos of the scaled plate can be taken after every experiment and compared to the image of the clean plate. The implementation of the 3 methods together provides a holistic view of the effects of each parameter on the overall operational efficiency of the GPHE.

The first experiment performed with hard water as the cooling medium is the base case. As mentioned in the design of experiments, the base case is configured with a cold medium flowrate of 250kg/hr, an inlet temperature of 25°C and a hardness value of 25°dH. The hot medium is configured such that the T2B duty is 9.8kW. The experiment is performed for a duration of 8 hours, and the plot of temperatures averaged every 10 minutes vs time, along with their uncertainties indicating a 68% confidence interval, is seen in figure 30. As seen in the figure, the

supply temperatures of the hot and cold media (T1 and T3) are relatively constant for the entire duration of the experiment. On the other hand, a drop in the cold medium outlet temperature (T4) is visible throughout the duration of the experiment. This indicates a gradual build-up of scale on the plates, hindering heat transfer from the hot medium to the cold medium, thereby reducing the outlet temperature of the cold medium throughout the experiment. In spite of the lower amount of heat transferred from the hot medium to the cold medium, a gradual increase in the outlet temperature of the hot medium (T2) is not noticed. This is possibly due to additional heat lost from the hot medium to the atmosphere and the remaining plate pack.

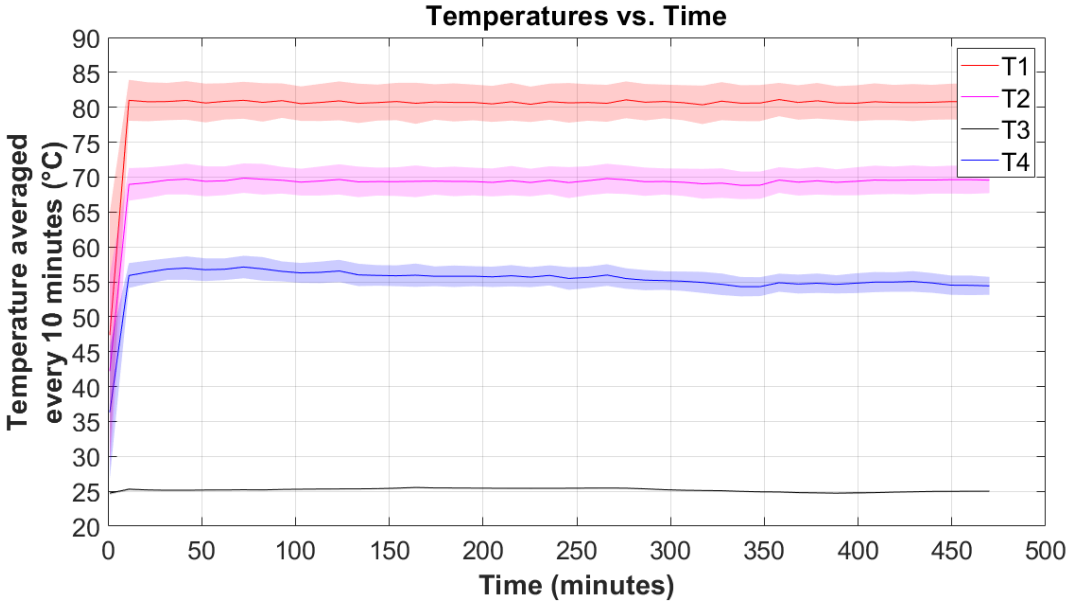

Figure 30: Temperature (°C) averaged every 10 minutes vs time (minutes) for the base case performed with hard water

Once the temperatures and their uncertainties are determined for each 10-minute window, the $LMTD$ and Q_{avg} can be calculated to determine the value of U. The values of U and their uncertainties, indicating a 68% confidence interval, are plotted in figure 31. The plot also includes the reference value of the overall heat transfer coefficient (U_0) for the base case. As seen in figure 31, the value of U decreases throughout the duration of the experiment. This is due to the build-up of the scale on the plates, which results in a decrease in the outlet temperature of the cold medium. It must also be noted that, the value of U seems to begin at infinity and rapidly drops to a finite value. This corresponds to the rapid increase in hot and cold media temperatures as the system approaches the desired temperatures. Additionally, for most of the experiment duration, the value of U is greater than the value of U_0. This is because the initial deposits of scale induce roughness-induced turbulence, which increases the value of U of the GPHE. As the thickness of the deposited scale increases during the experiment, the value of U begins to drop and falls below the value of U_0 at the 354th minute. The onset of scale for the base case, as per its definition for this study, is therefore at ≈ minute 354.

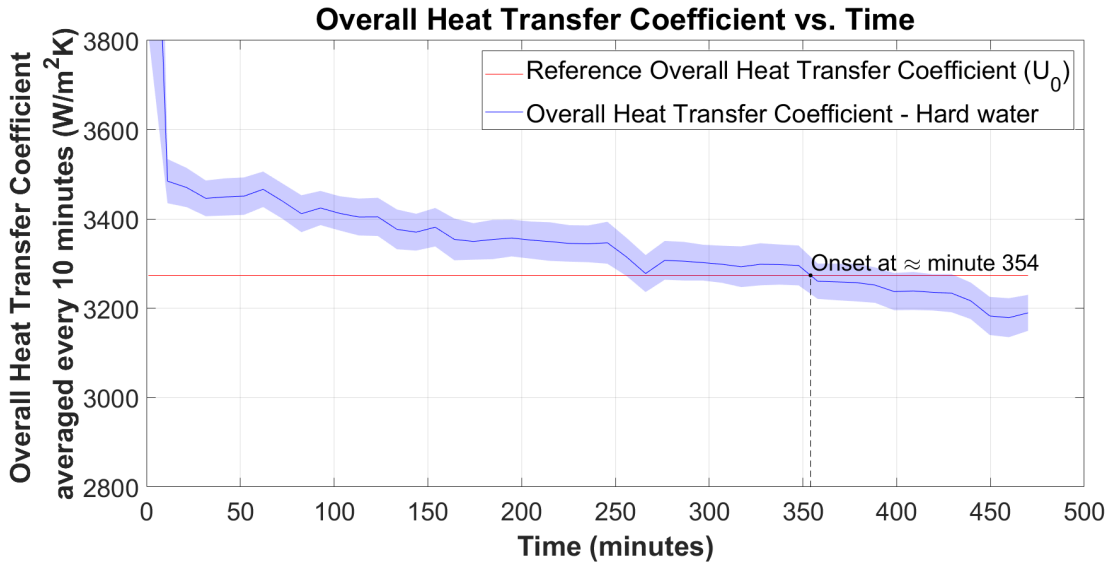

Figure 31: Overall heat transfer coefficient (W/m^{2}K) averaged every 10 minutes vs time (minutes) for the base case

The next step is to determine the fouling resistance (R_f) for the entire experiment. Using the uncertainty propagation formula (equation 15) and ignoring the uncertainty in the value of U_0, the uncertainty in the fouling resistance can be calculated as $\Delta U/U^2$, where ΔU is the uncertainty in U. This is plotted against time as seen in figure 32. As seen in the figure, the value of R_f is below 0 for the majority of the experiment. This indicates that rather than hindering heat transfer, the scale is promoting heat transfer in the GPHE, as the resistance due to fouling is negative. Similar to figure 31, at ≈ minute 354 the fouling resistance value exceeds 0. Beyond this point, the resistance due to fouling is positive, and therefore, the scale is detrimental to the GPHE performance. Hence, the 'onset of scale' condition is achieved at ≈ minute 354.

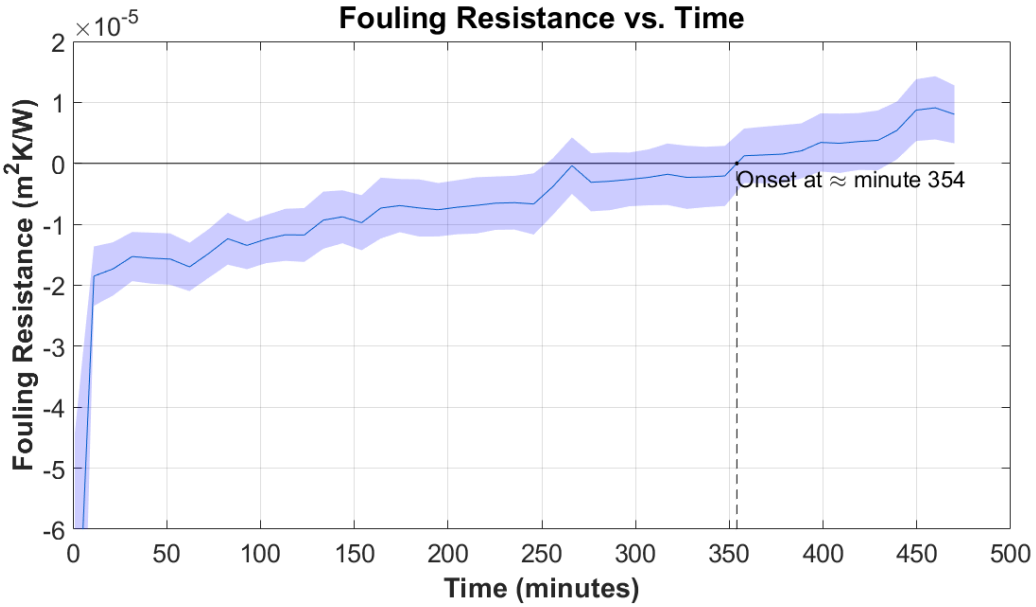

Figure 32: Fouling Resistance (m^{2}K/W) averaged every 10 minutes vs time (minutes) for the base case

After conducting the experiment, the GPHE was opened, the scaled plates were dried in an oven and subsequently weighed. The weight difference between the scaled and clean plates was 0.49 grams. Since the uncertainty in the measurement of the weighing scale used is 0.01g, the final weight of the deposited scale can be expressed as 0.49 ± 0.01 g. A sample of the scale was also extracted from the plate. ICP-OES was conducted on the sample and the results indicated that the solid scale deposited on the plates is $CaCO_3$. Subsequently, photos of the scaled and clean plates were taken and compared in figures 33 and 34. As seen in the images, the amount of scale deposited on the plate increases from the bottom to the top. This is because the cold medium, i.e. the hard water, enters at the bottom of the T2B, increases in temperature as it flows along the plate length and exits at the top. Since $CaCO_3$ is an inverse soluble salt, and its tendency to precipitate increases with temperature, maximum scale deposits are visible at the top of the plate. This phenomenon is clearly visible in both figures.

Figure 33: Comparison of the first scaled plate vs clean plate for the base case

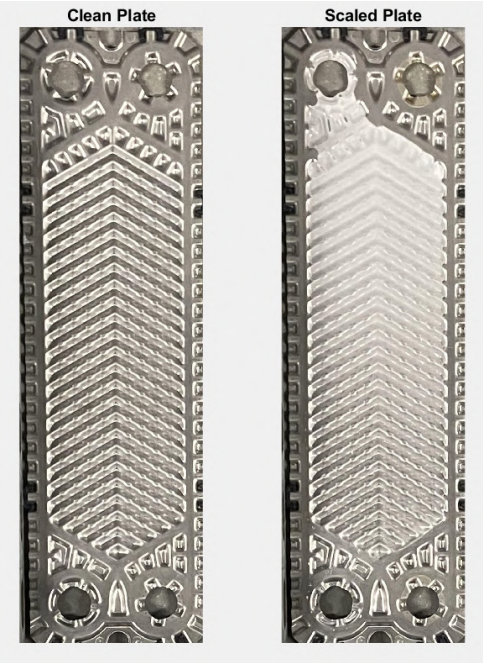

Figure 34: Comparison of second scaled plate vs clean plate for the base case

In order to obtain a better understanding of the scale deposited on the plate, the photos of the scaled plates are imported to MATLAB to conduct rudimentary image analysis. Using MATLAB, the image of the scaled plate is 'subtracted' from the image of the clean plate to highlight the difference in the two images as a heatmap. Since the only difference in the images is the deposited scale, the heatmap is able to indicate the regions and extent of scale on the plates. The heatmaps for the two scaled plates are seen in figures 35 and 36. As seen in the figures, the maximum difference in the images is at the top of the plate, i.e. where the cold medium exits and is at its highest temperature. The difference in the images gradually decreases towards the bottom, i.e. where the cold medium enters and is at its lowest temperature.

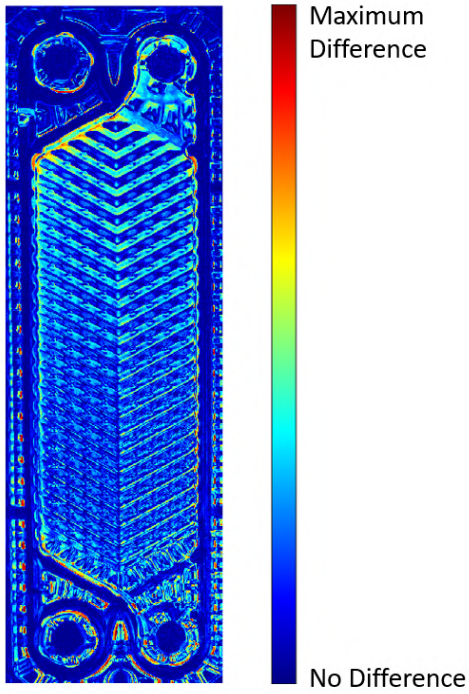

Figure 35: Heatmap indicating differences in images of the first scaled plate for the base case

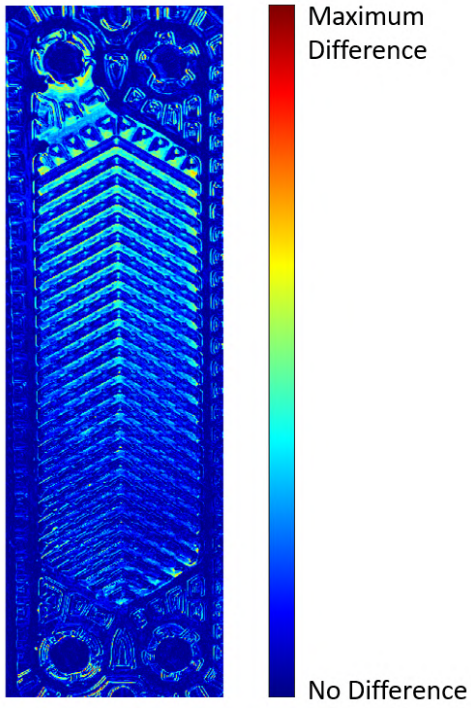

Figure 36: Heatmap indicating differences in images of the second scaled plate for the base case

After conducting the experiment, new plates were added to the GPHE and it was reconnected to the system. The entire cold loop was then flushed with de-hardened water at a flowrate of 900kg/hr for ≈ 30 minutes. This ensured that any scale in the piping of the cold loop and on the TL3B is removed from the system before the next experiment. Subsequently, to ensure the repeatability of the system, the base case performed with hard water was repeated 2 more times. The time for onset of scale and the total weight of scale deposited on the plates was calculated

as ≈ 360 minutes and 0.47 ± 0.01 g for the first repetition and ≈ 348 minutes and 0.53 ± 0.01 g for the second repetition. Since all three base case runs resulted in similar values of time for the onset of scale and weight of scale deposited, the system was considered repeatable. As a result, the remaining 9 experiments were performed with hard water and similar analyses were conducted for each experiment. Before beginning each experiment, the plates of the GPHE were replaced and the system was flushed with de-hardened water. The plots for averaged temperature vs time, overall heat transfer coefficient vs time, and fouling resistance vs time for the two repetitions of the base case are seen in Appendix D.

5.2.1 Effect of Change in Flowrate

The first set of experiments performed with hard water is the effect of variation flowrate. For these experiments, the hardness and inlet temperature of the hard water as well as the duty of the T2B remains constant, whereas the flowrate is varied from 200kg/hr to 350 kg/hr in steps of 50kg/hr. For each experiment, the plots of averaged temperature vs time, overall heat transfer coefficient vs time, and fouling resistance vs time are generated. Additionally, the time for onset of the scale and weight of the deposited scale is recorded. To gain further insights into the distribution and extent of scale on the plate, photos of the scaled plates are compared with those of a clean plate. Subsequently, rudimentary image analysis using MATLAB is performed to visualize the scale distribution on the plate as a heat map.

The plots of overall heat transfer coefficient vs time, indicating the time for onset of scaling, for cases 1, 3 and 4, corresponding to flowrates of 200kg/hr, 300kg/hr and 350kg/hr respectively, are seen in figures 37 - 39. As seen in the figures, the overall heat transfer coefficient for all three cases decreases with time, owing to the formation of scale during the experiment. Additionally, as the flowrate increases, the rate of decline of the overall heat transfer coefficient (U) decreases. As a result, the time for the onset of scale increases with an increase in flowrate, as seen in figure 40. The drop in GPHE performance with a decrease in flowrate is also visible in the plots of temperatures vs time and fouling resistance vs time, as seen in Appendix D. Hence, it can be concluded the performance of the GPHE decreases, with a decrease in flowrate.

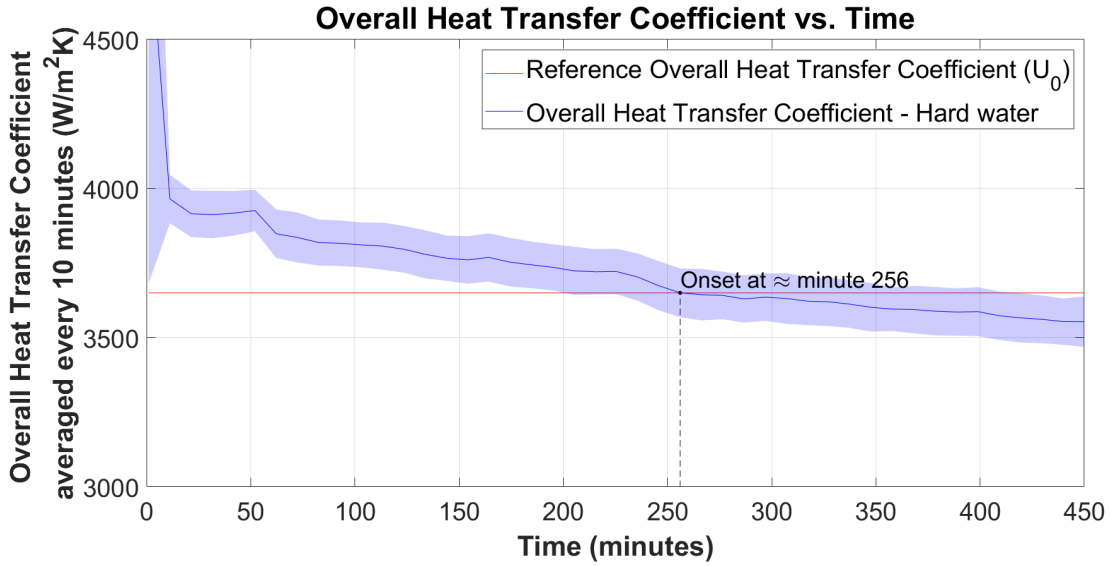

Figure 37: Overall heat transfer coefficient (W/m^2K) averaged every 10 minutes vs time (minutes) for case 1

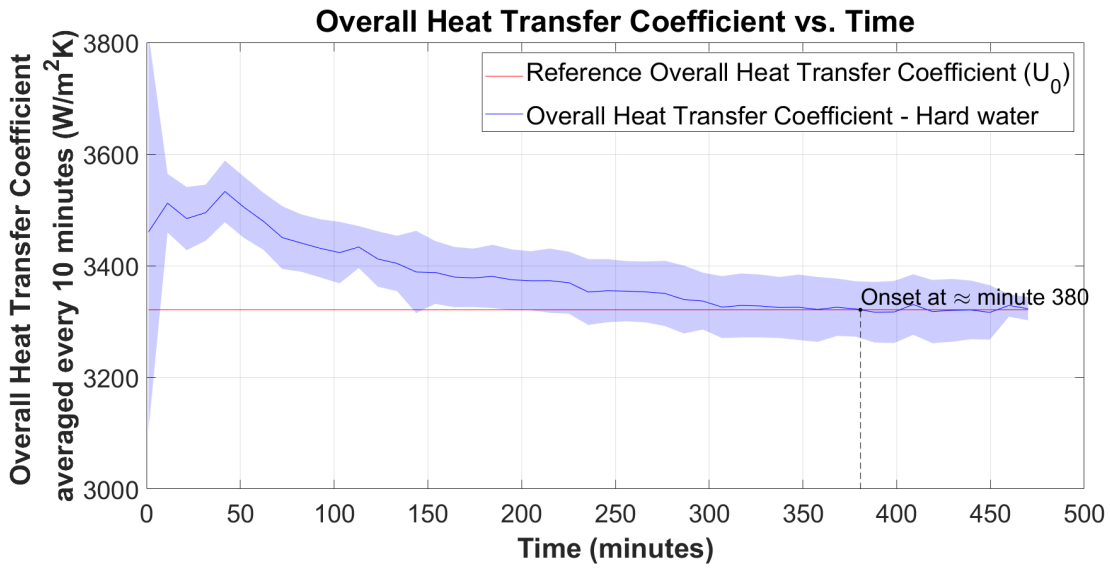

Figure 38: Overall heat transfer coefficient (W/m^{2}K) averaged every 10 minutes vs time (minutes) for case 3

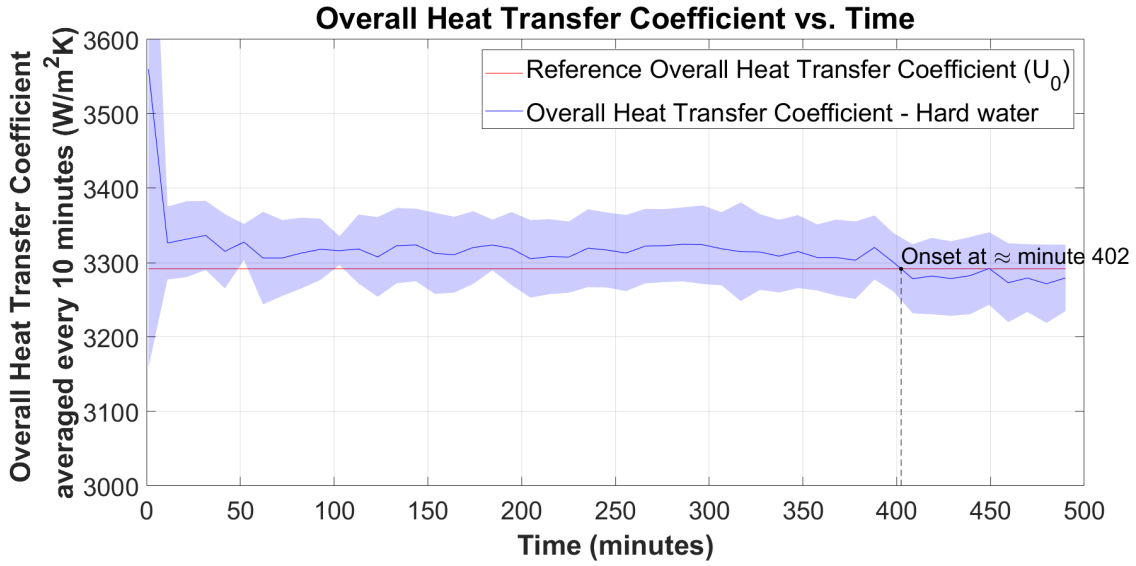

Figure 39: Overall heat transfer coefficient (W/m^{2}K) averaged every 10 minutes vs time (minutes) for case 4

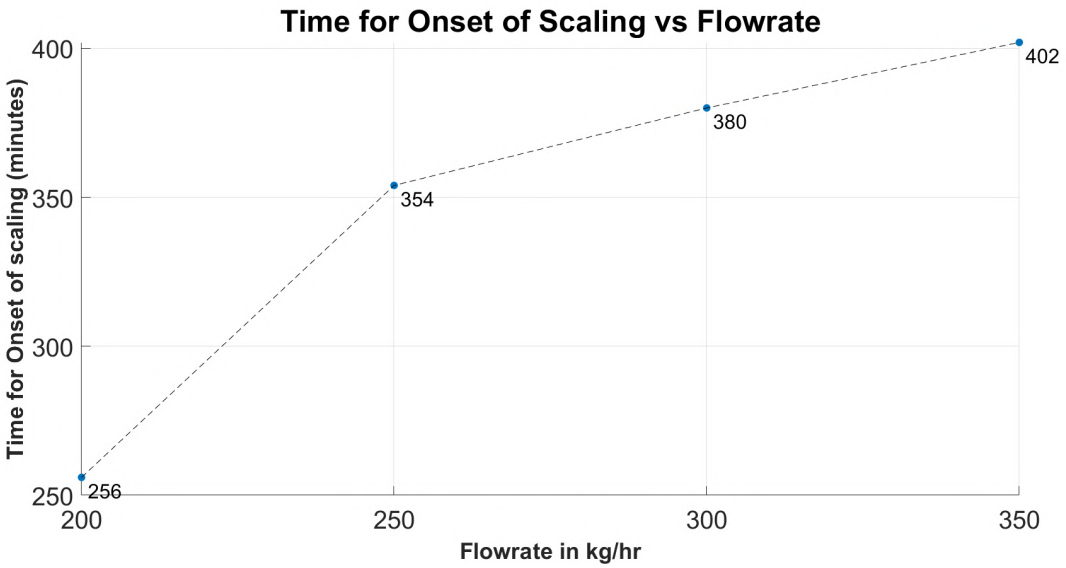

Figure 40: Time for onset of scale (minutes) vs flowrate (kg/hr)

For each case, images of the scaled plates are taken after the experiment. Figure 41 compares the scale distribution on the first plate as the flowrate is increased from 200 kg/hr to 350kg/hr. Figure 42 compares the extent of scale deposition as a heat map, as the flowrate is increased from 200 kg/hr to 350kg/hr. In both figures, the decrease in scale formation with an increase in flowrate is clearly visible. Hence, the tendency of the scale to precipitate increases with a decrease in flowrate. This observation is in accordance with the literature and is due to the higher shear stress on the wall at higher flowrates, which hinders the ability of the scale to adhere to the plate surface.

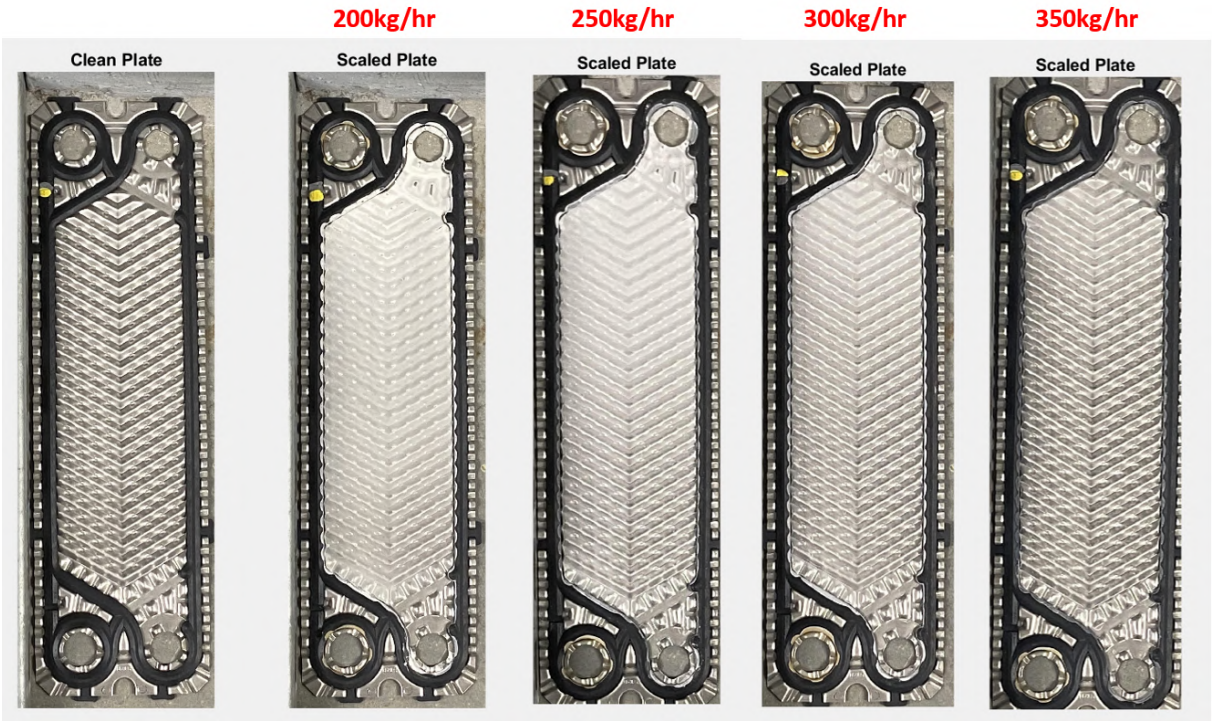

Figure 41: Comparison of scale distribution on the first scaled plate with change in flowrate

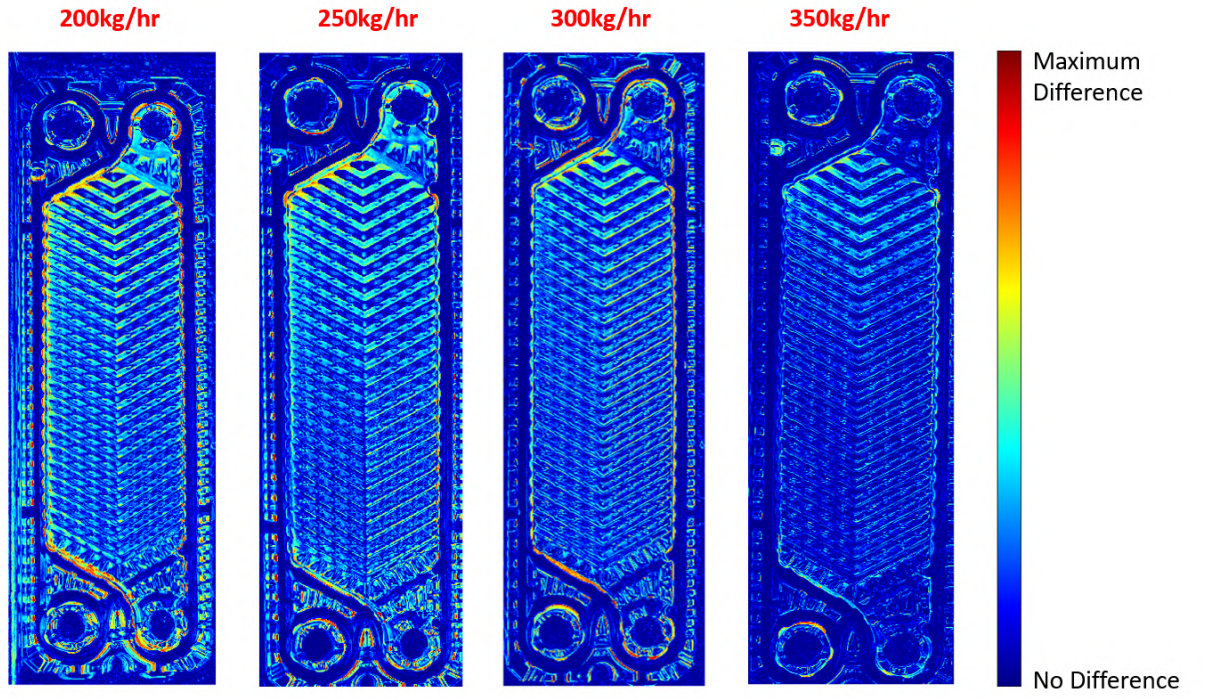

Figure 42: Comparison of scale distribution on the first scaled plate as a heatmap with change in flowrate

Similarly, for the second scaled plate, the scale distribution and extent of scale deposition as a heat map is compared for the different flowrates in figure 43 and figure 41, respectively. In both figures, a decrease in the tendency of the scale to deposit on the plate surface with an increase in flowrate is observed. This further supports the conclusion that the tendency of the scale to form on the plate increases with a decrease in flowrate.

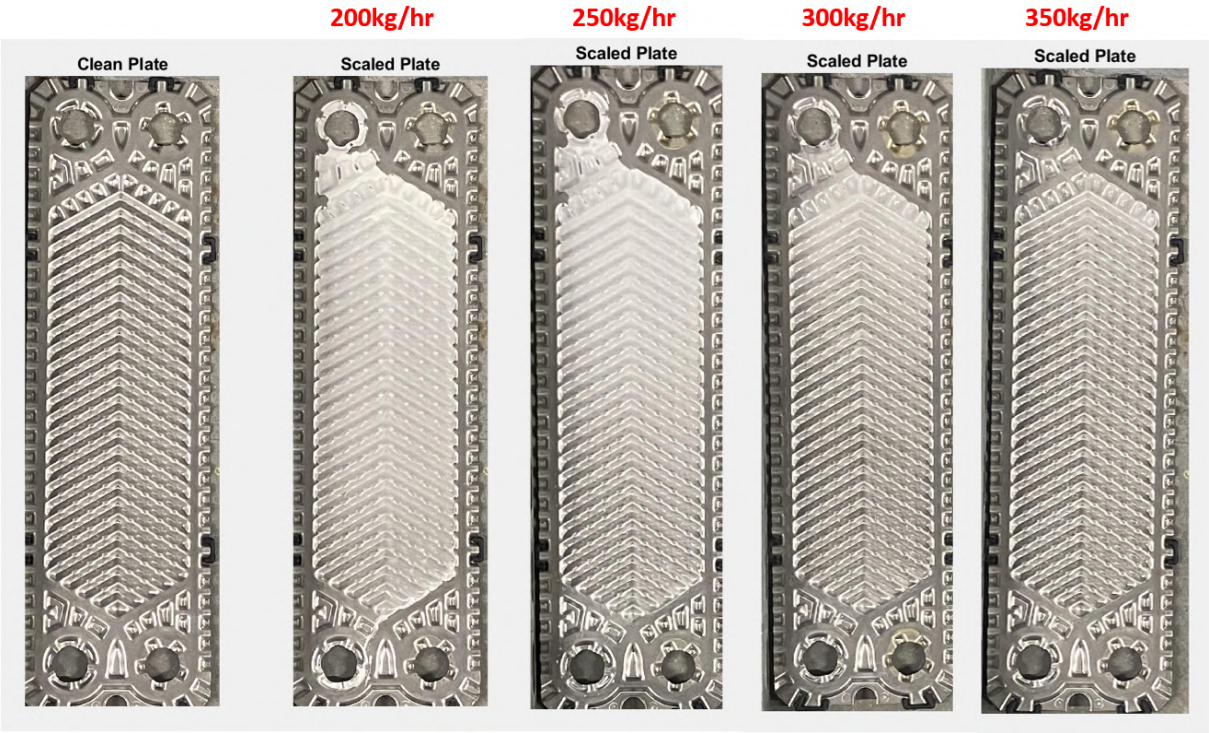

Figure 43: Comparison of scale distribution on the second scaled plate with change in flowrate

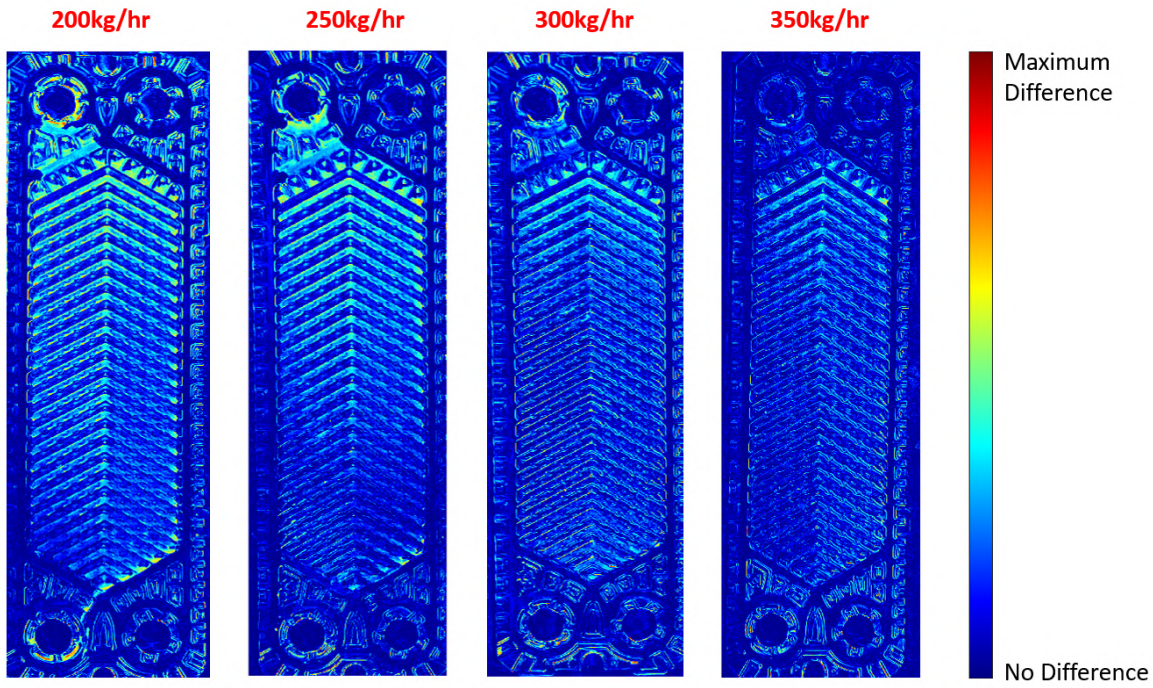

Figure 44: Comparison of scale distribution on the second scaled plate as a heatmap with change in flowrate

Finally, the total weight of the scale deposited on the two plates for each experiment is plotted in figure 45. For the lowest flowrate of 200 kg/hr, a total of 2.51 grams of the scale was deposited on the two plates, as compared to only 0.14 grams of scale for the highest flowrate of 350 kg/hr. As visible in the figures 41 - 44, the area of the plates covered by scale decreases with an increase in flowrate. Hence, the weight of the scale deposited on the plate also decreases with an increase in flowrate.

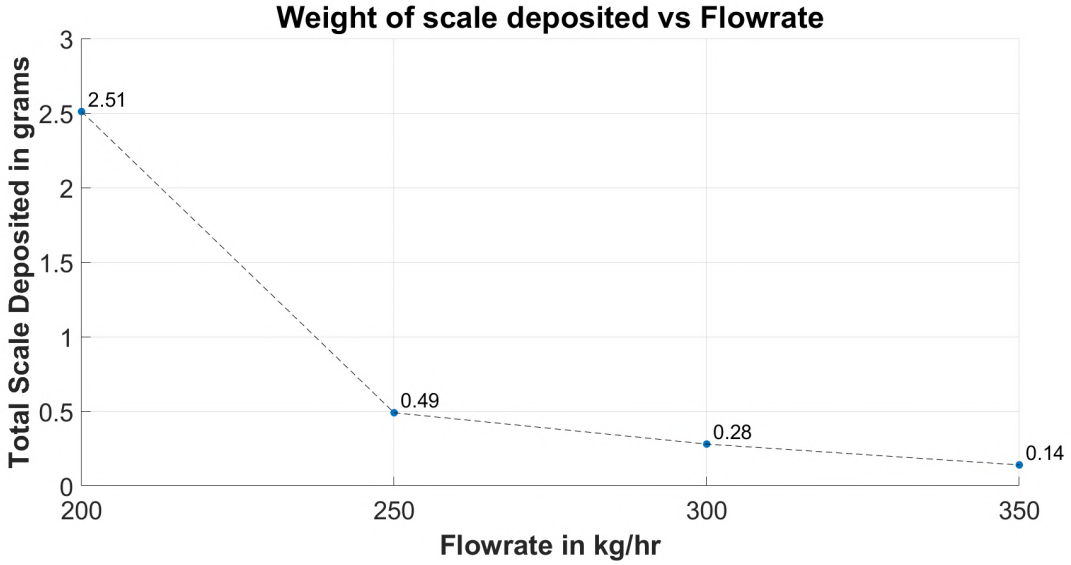

Figure 45: Weight of scale deposited (grams) vs Flowrate (kg/hr)

Based on the results obtained from the four experiments investigating the effect of flowrate variation on the onset of scaling, it can be concluded that the performance of the GPHE is directly proportional to the flowrate of the cold medium, while keeping the inlet temperature,

hardness value, and duty exchanged by the GPHE constant. This is because a lower flowrate results in a lower shear stress on the wall, resulting in scale formation on a larger area of the plate. Consequently, the increased scale formation at lower flowrates results in higher resistance to heat transfer, ultimately leading to a decrease in the overall performance of the GPHE.

It must also be noted, that as the flowrate is varied from 250kg/hr to 350kg/hr, the change in weight of scale deposited and time for onset of scale is fairly linear. However, when the flowrate is increased from 200kg/hr to 250kg/hr, the change in the two parameters is exponential. As mentioned previously, the flowrate of 250kg/hr corresponds to a shear stress of 50Pa on the plate. Hence, to avoid scale formation in the current system, the flowrate must be chosen such that the shear stress on the plate is equal to or higher than 50Pa.

5.2.2 Effect of Change in Inlet Temperature

The next set of experiments performed with hard water is the effect of variation inlet temperature. For these experiments, the hardness and flowrate of the hard water as well as the duty of the T2B remains constant, whereas the inlet temperature is varied from 20 °C to 33 °C. Similar to the previous set of experiments, the plots of averaged temperature vs time, overall heat transfer coefficient vs time, and fouling resistance vs time are generated for each case. Additionally, the time for onset of the scale and weight of the deposited scale is recorded. Finally, photos of the scaled plates are compared with those of a clean plate and MATLAB is used to visualize the scale distribution on the plate as a heat map.

The plots of overall heat transfer coefficient vs time, indicating the time for onset of scaling, for cases 5, 7 and 8, corresponding to inlet temperatures of 20 °C, 30 °C and 33 °C respectively, are seen in figures 46 - 48. As seen in the figures, the overall heat transfer coefficient for all three cases decreases with time, owing to the formation of scale during the experiment. A drop in outlet temperature of the cold medium and an increase in fouling resistance during an experiment is also visible in the plots of temperatures vs time and fouling resistance vs time, as seen in Appendix D. Additionally, the time for the onset of scale decreases with an increase in the inlet temperature, as seen in figure 49. Since increasing the inlet temperature results in an earlier time for onset of scale, it can be concluded the performance of the GPHE decreases with an increase in inlet temperature.

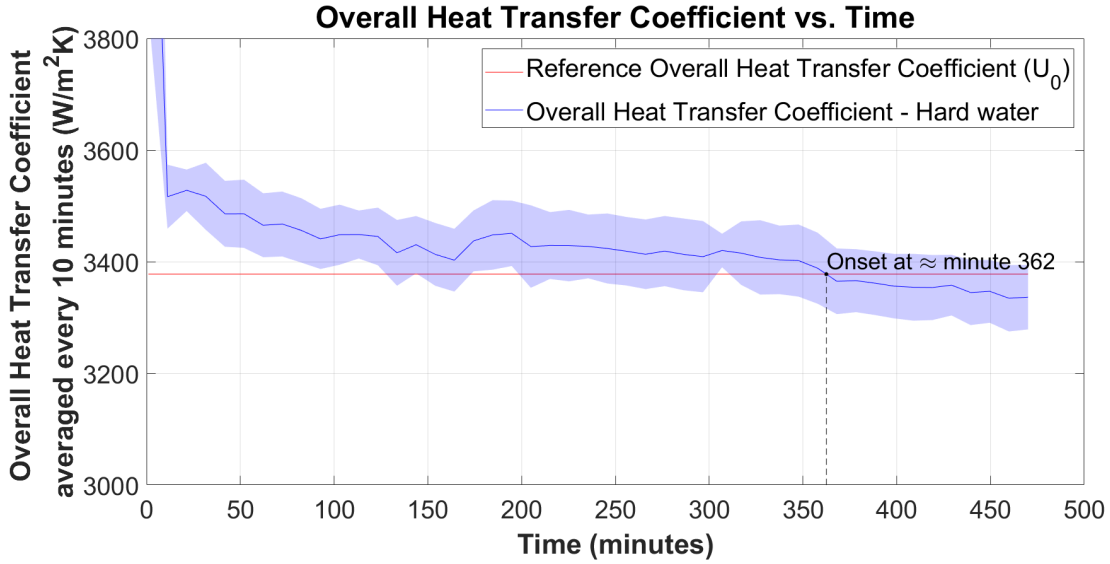

Figure 46: Overall heat transfer coefficient (W/m^{2}K) averaged every 10 minutes vs time (minutes) for case 5

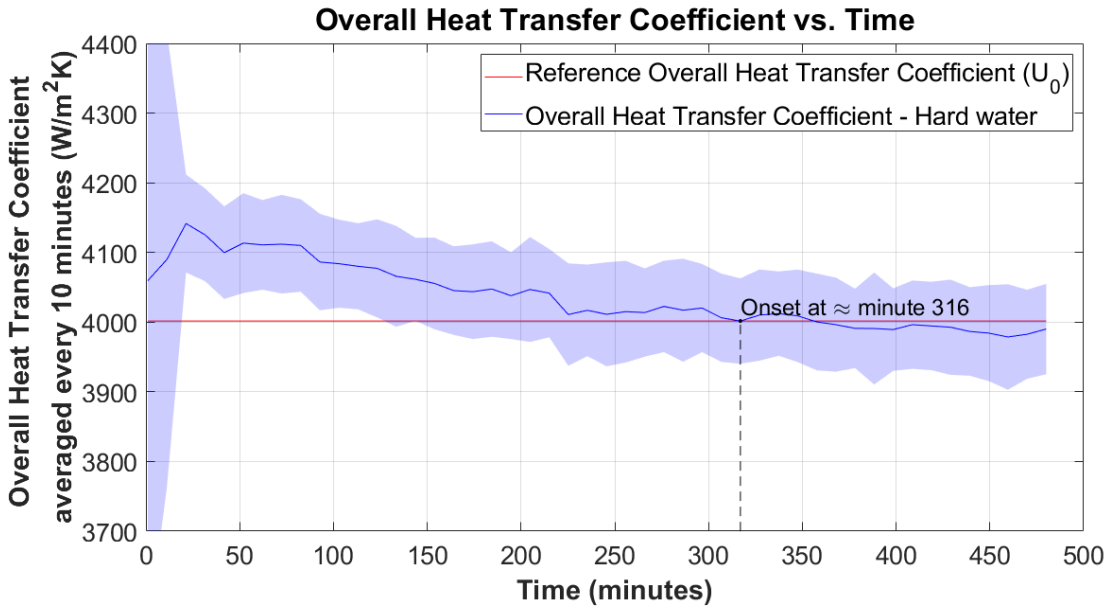

Figure 47: Overall heat transfer coefficient (W/m^{2}K) averaged every 10 minutes vs time (minutes) for case 7

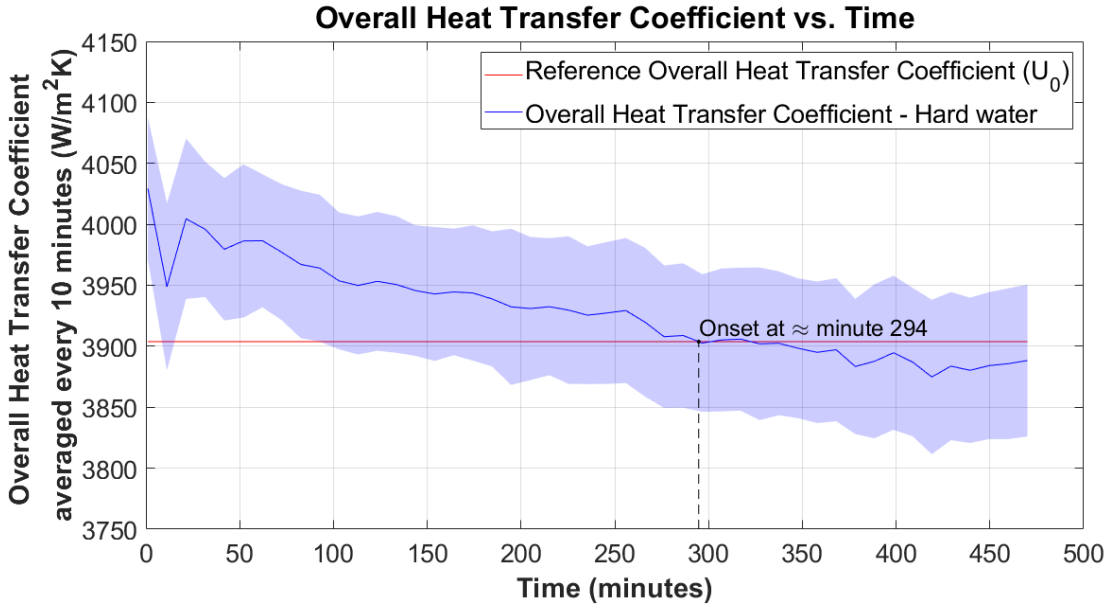

Figure 48: Overall heat transfer coefficient (W/m^{2}K) averaged every 10 minutes vs time (minutes) for case 8

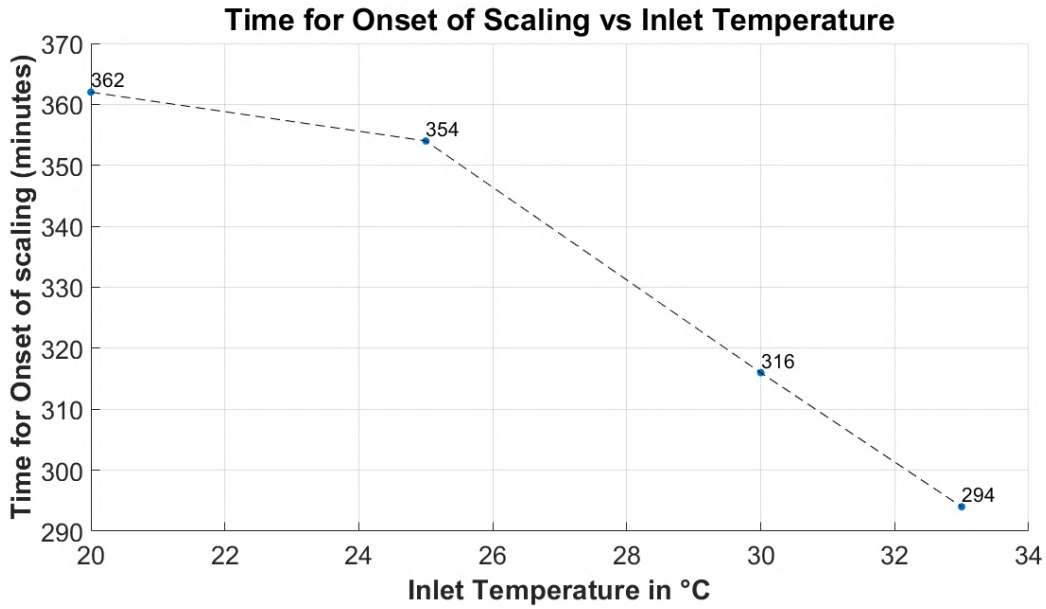

Figure 49: Time for onset of scaling (minutes) vs inlet temperature (°C)

For each case, images of the scaled plates are taken after the experiment. Figures 50 and 52 compare the scale distribution on the first and second plate as the inlet temperature is increased from 20 °C to 33 °C. Figure 51 and 53 compare the extent of scale deposition as a heat map, as the inlet temperature is increased from 20 °C to 33 °C. In all four figures, an increase in scale formation with an increase in inlet temperature is observed. Hence, the tendency of the plate to scale is directly proportional to the inlet temperature. This observation is in accordance with the literature and is due to the inverse soluble nature of $CaCO_3$. A higher inlet temperature for the same flowrate and duty of the GPHE results in higher temperatures of the hard water, and therefore a greater tendency of the $CaCO_3$ to precipitate and adhere to the plate surface.

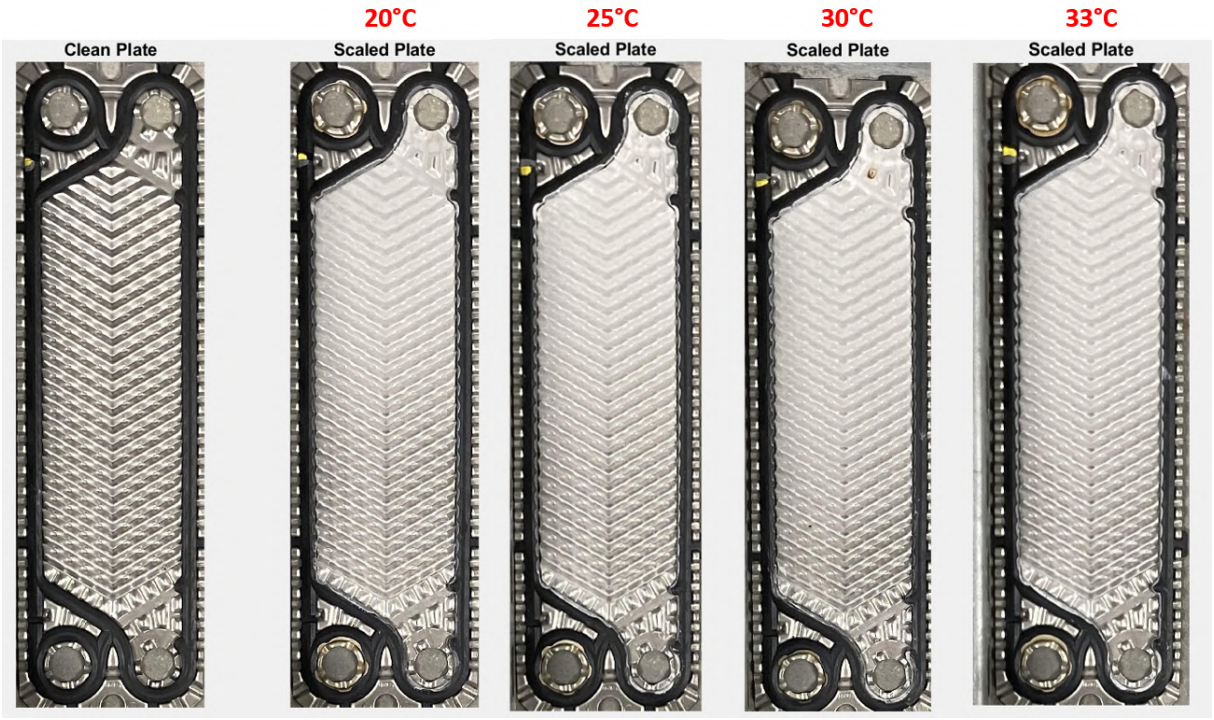

Figure 50: Comparison of scale distribution on the first scaled plate with change in inlet temperature

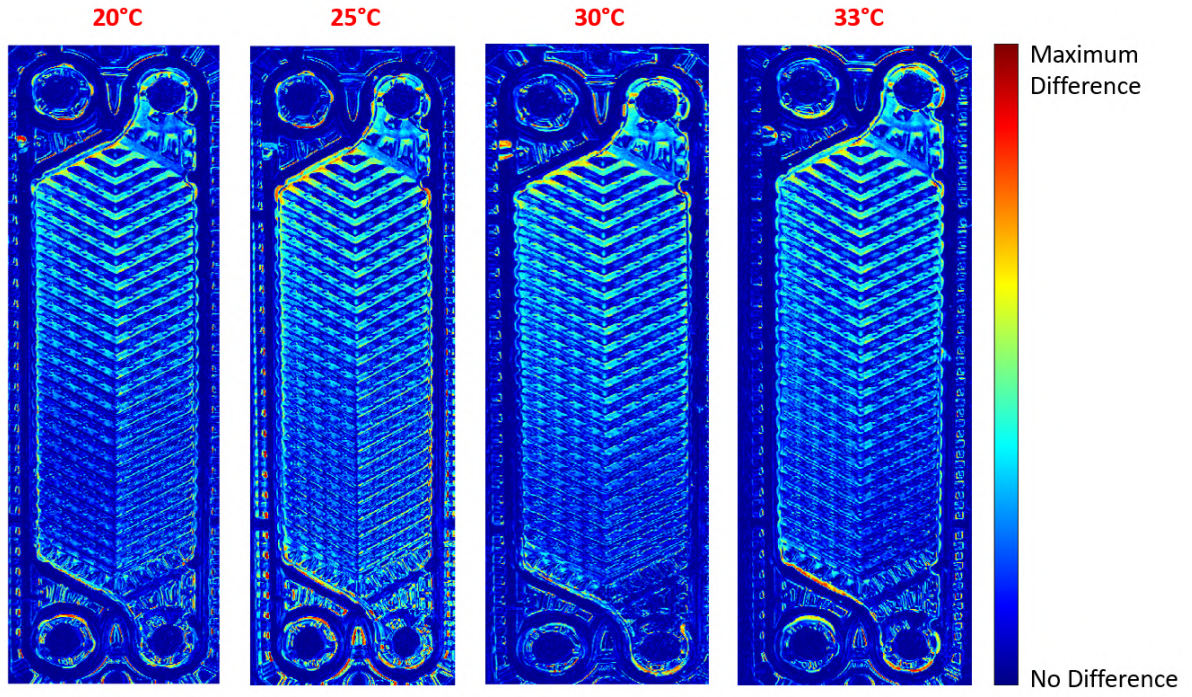

Figure 51: Comparison of scale distribution on the first scaled plate as a heatmap with change in inlet temperature

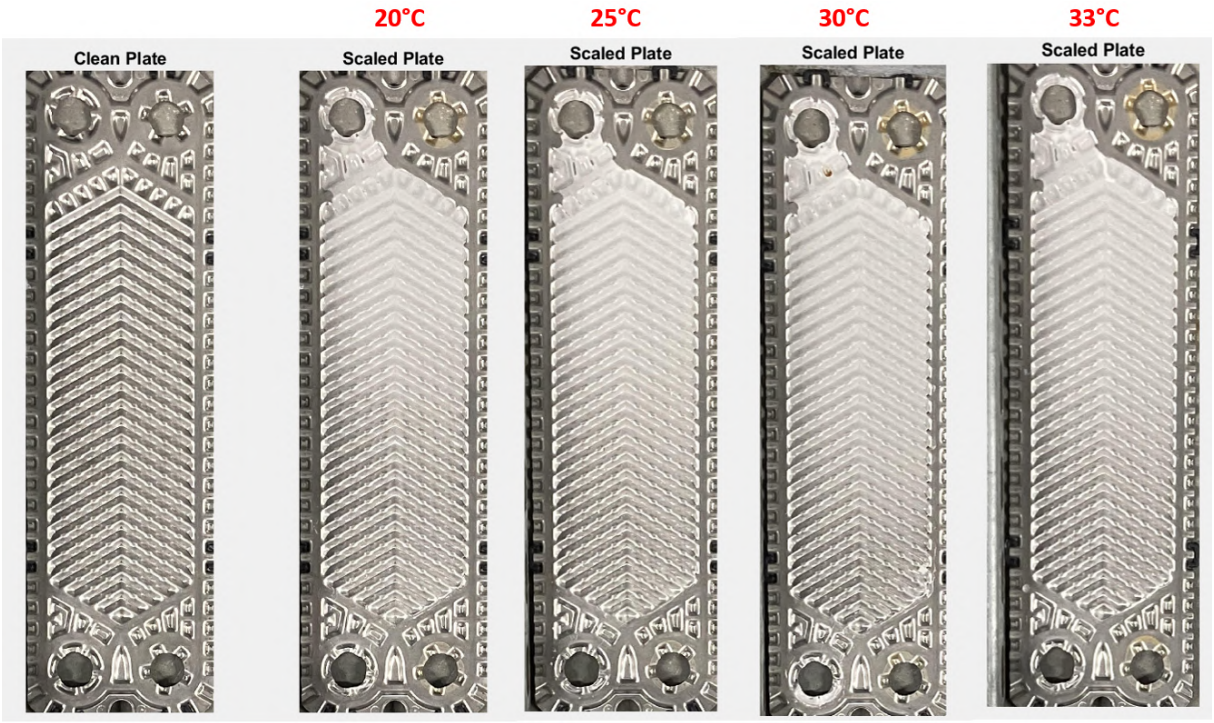

Figure 52: Comparison of scale distribution on the second scaled plate with change in inlet temperature

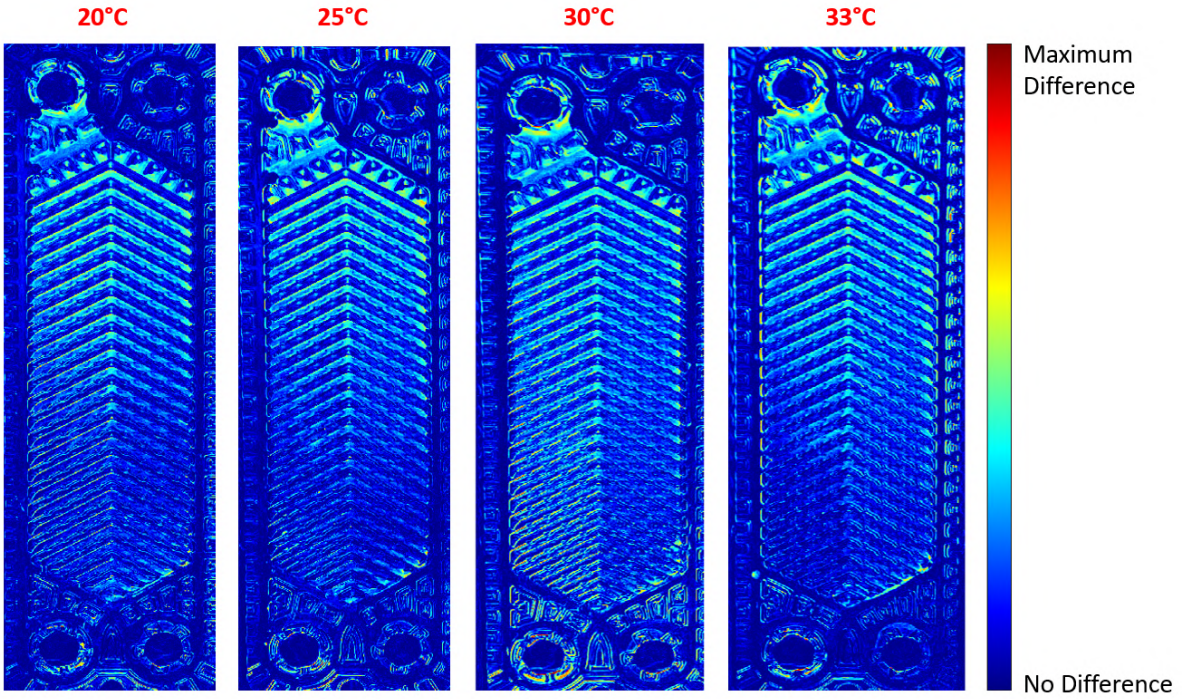

Figure 53: Comparison of scale distribution on the second scaled plate as a heatmap with change in inlet temperature

Finally, the total weight of the scale deposited on the two plates for each experiment is plotted in figure 54. For the highest inlet temperature of 33 °C, 0.79 grams of scale was deposited on the two plates, as compared to 0.36 grams of scale for the lowest inlet temperature of 20

°C. This finding is in line with the observations made from figure 41 - 44, i.e., higher inlet temperatures result in a larger scaled area of the plate, therefore resulting in a greater amount of scale deposited on the plates.

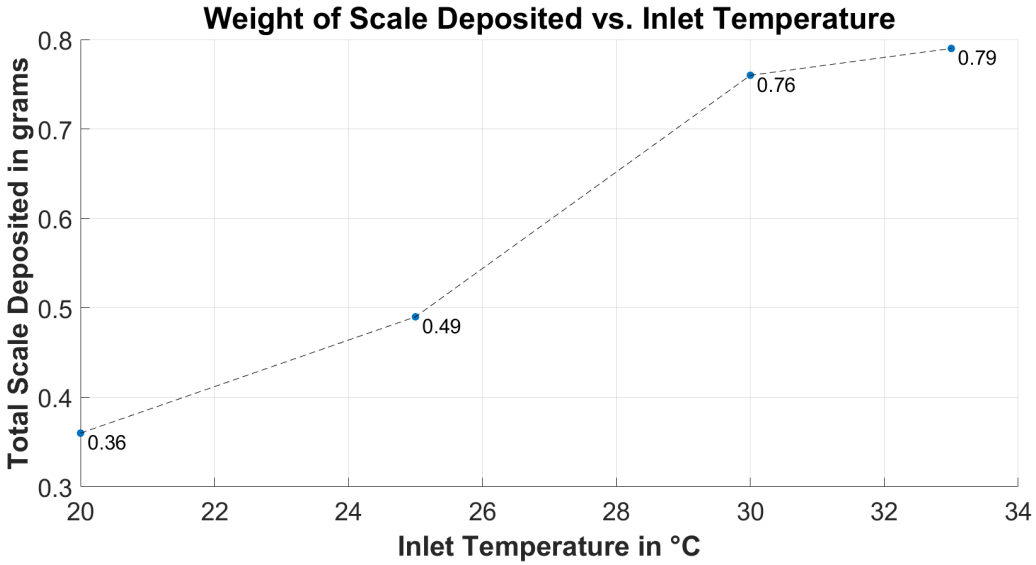

Figure 54: Weight of scale deposited (grams) vs inlet temperature (°C)

Based on the results obtained from the four experiments investigating the effect of inlet temperature variation on the onset of scaling, it can be concluded that the performance of the GPHE is inversely proportional to the inlet temperature of the cold medium, while keeping the flowrate, hardness value, and duty exchanged by the GPHE constant. This is because a higher inlet temperature results in higher temperatures of the cold medium throughout the entire plate length. These higher temperatures coupled with the inverse soluble nature of $CaCO_3$ results in scale formation on a larger area of the plate. Consequently, the increased scale formation at higher inlet temperatures results in higher resistance to heat transfer, ultimately leading to a decrease in the overall performance of the GPHE. Hence, to avoid scale formation in the current system, the lowest possible inlet temperature for the cold medium must be chosen.

5.2.3 Effect of Change in Duty

The final set of experiments performed with hard water is the effect of variation in the GPHE duty. For these experiments, the hardness, flowrate, and inlet temperature of the hard water remain constant, whereas the duty is varied from 8.87kW to 11.31 kW. Similar to the previous set of experiments, the plots of averaged temperature vs time, overall heat transfer coefficient vs time, and fouling resistance vs time are generated for each case. Additionally, the time for onset of the scale and weight of the deposited scale is recorded. Finally, photos of the scaled plates are compared with those of a clean plate and MATLAB is used to visualize the scale distribution on the plate as a heat map.

The plots of overall heat transfer coefficient vs time, indicating the time for onset of scaling, for cases 9, 11 and 12, corresponding to a duty of 8.87 kW, 10.87kW and 11.31 kW respectively, are seen in figures 55 - 57. As seen in the figures, the overall heat transfer coefficient for all three cases decreases with time, owing to the formation of scale during the experiment. A drop in outlet temperature of the cold medium and an increase in fouling resistance during an experiment is also visible in the plots of temperatures vs time and fouling resistance vs time, as seen in Appendix D. Additionally, as seen in figure 58, a reduction in time for the onset of scaling is observed as the duty of the GPHE is increased. Hence, it can be concluded the performance of the GPHE decreases with an increase in GPHE duty.

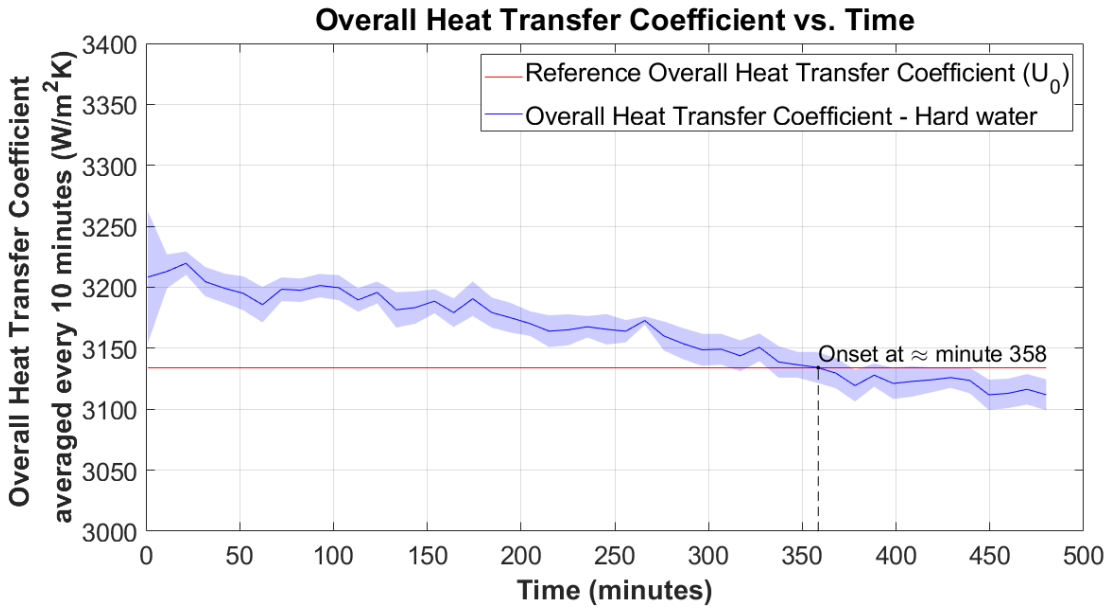

Figure 55: Overall heat transfer coefficient (W/m^{2}K) averaged every 10 minutes vs time (minutes) for case 9

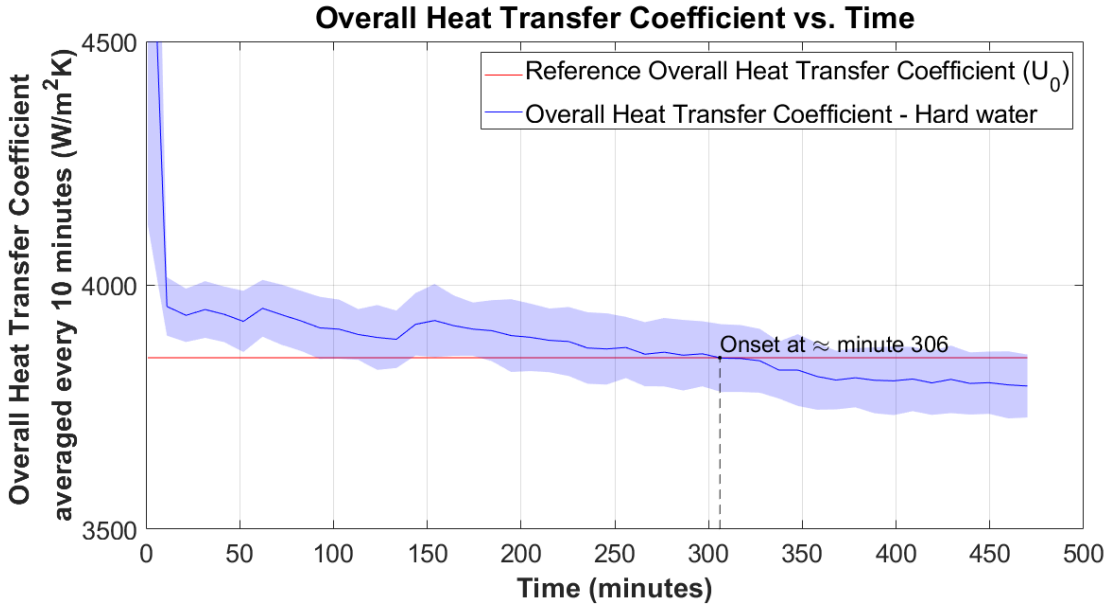

Figure 56: Overall heat transfer coefficient (W/m^{2}K) averaged every 10 minutes vs time (minutes) for case 11

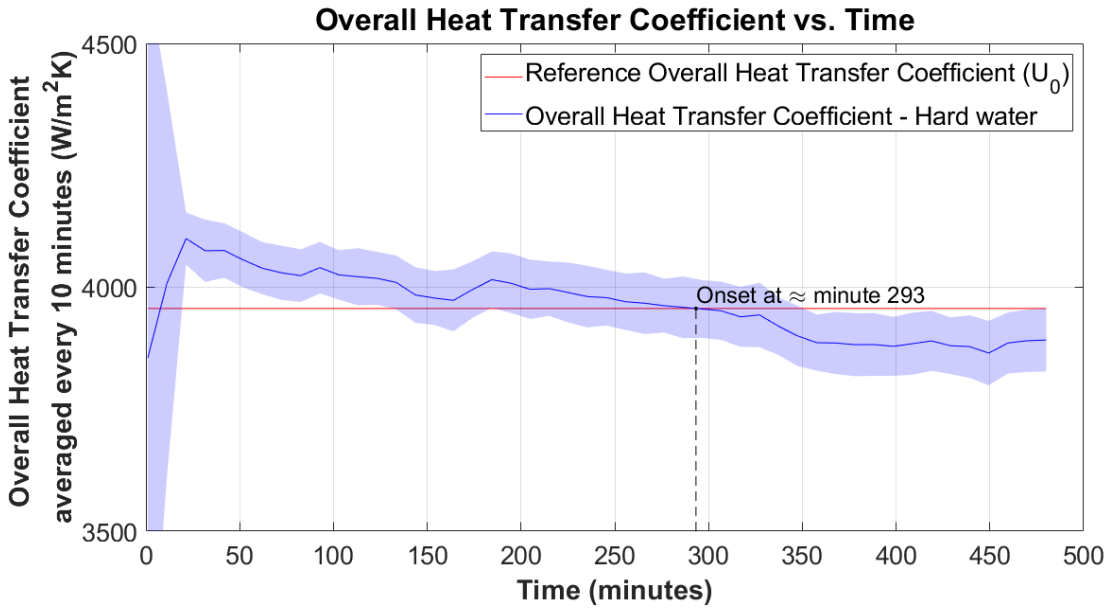

Figure 57: Overall heat transfer coefficient (W/m^{2}K) averaged every 10 minutes vs time (minutes) for case 12

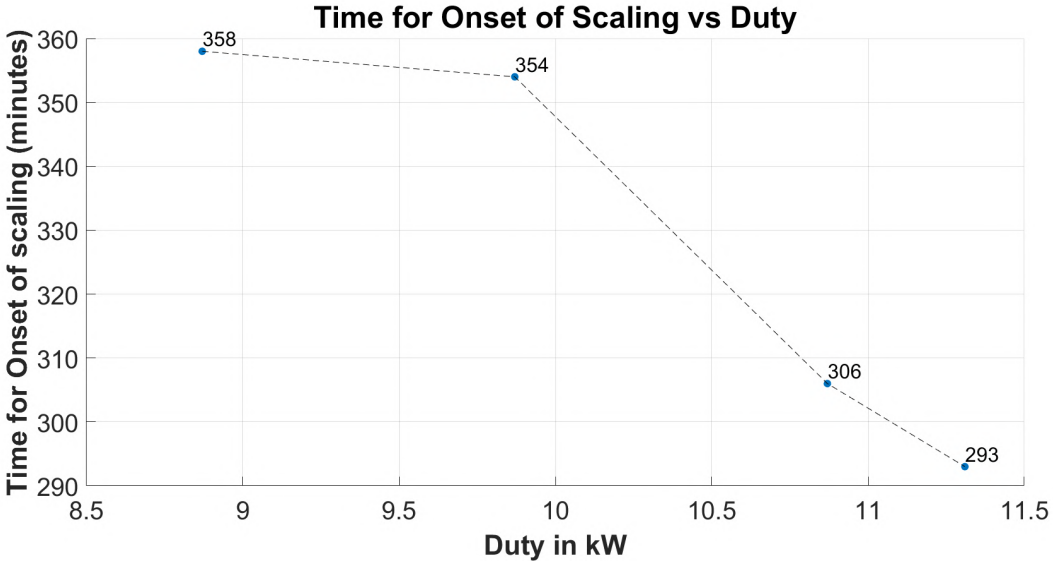

Figure 58: Time for onset of scale (minutes) vs duty (kW)

For all four cases, images of the scaled plates are taken after the experiment. Figures 59 and 61 compare the scale distribution on the first and second plate as the duty is increased from 8.87 kW to 11.31 kW. Figure 60 and 62 compare the extent of scale deposition as a heat map, as the duty is increased from 8.87 kW to 11.31 kW. In all figures, an increase in scale formation with an increase in duty is observed. This is because for a constant hard water flowrate and inlet temperature, an increase in duty results in an increase in the temperature of the hard water as it flows along the length of the plate. Since, $CaCO_3$ is inverse soluble, the higher temperatures result in greater precipitation of the scale. Hence, the tendency of the plate to scale is directly proportional to the duty.

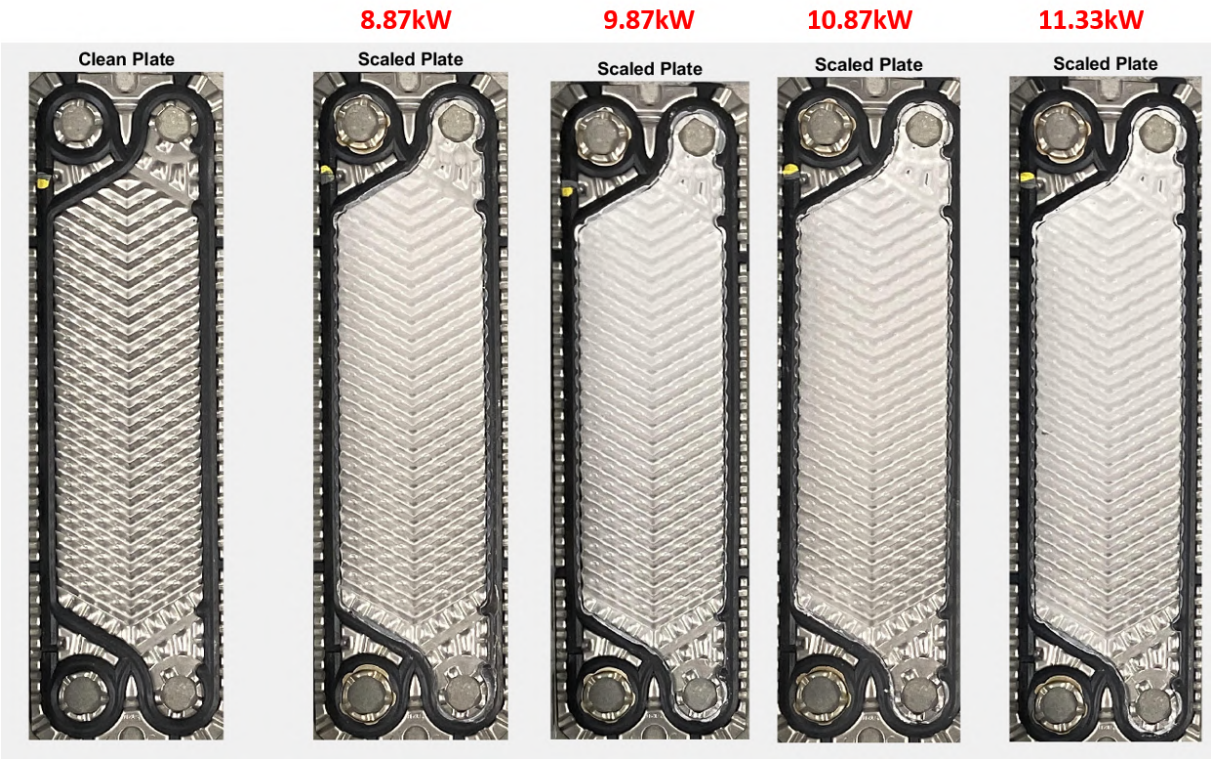

Figure 59: Comparison of scale distribution on the first scaled plate with change in duty

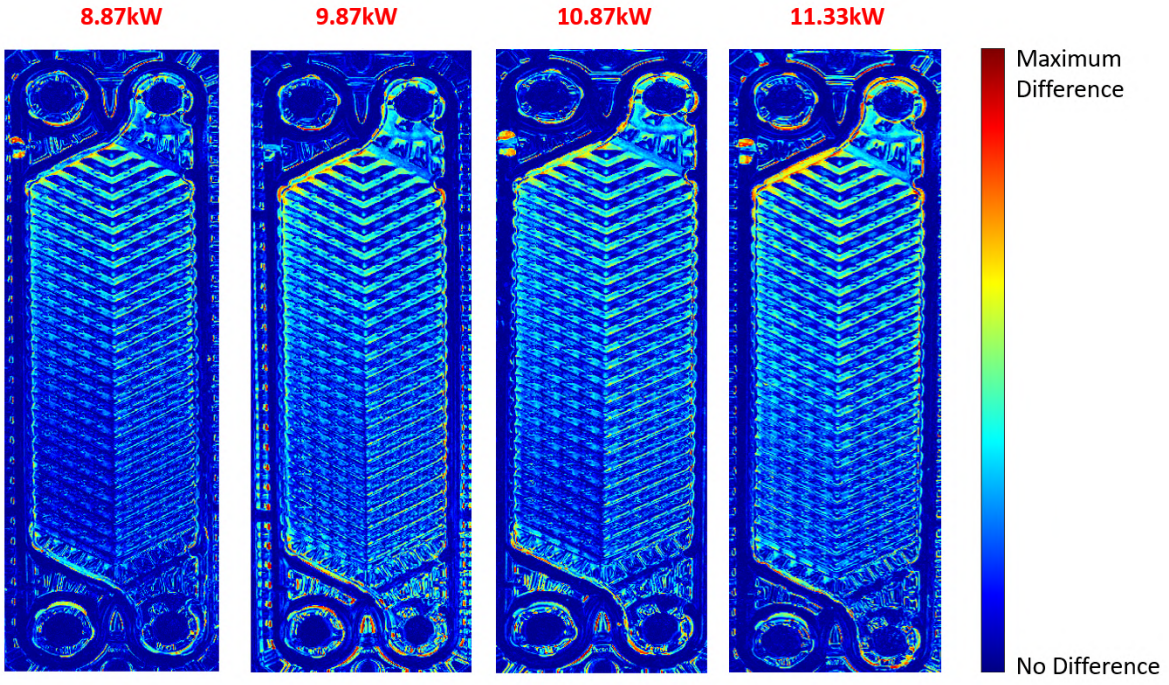

Figure 60: Comparison of scale distribution on the first scaled plate as a heatmap with change in duty

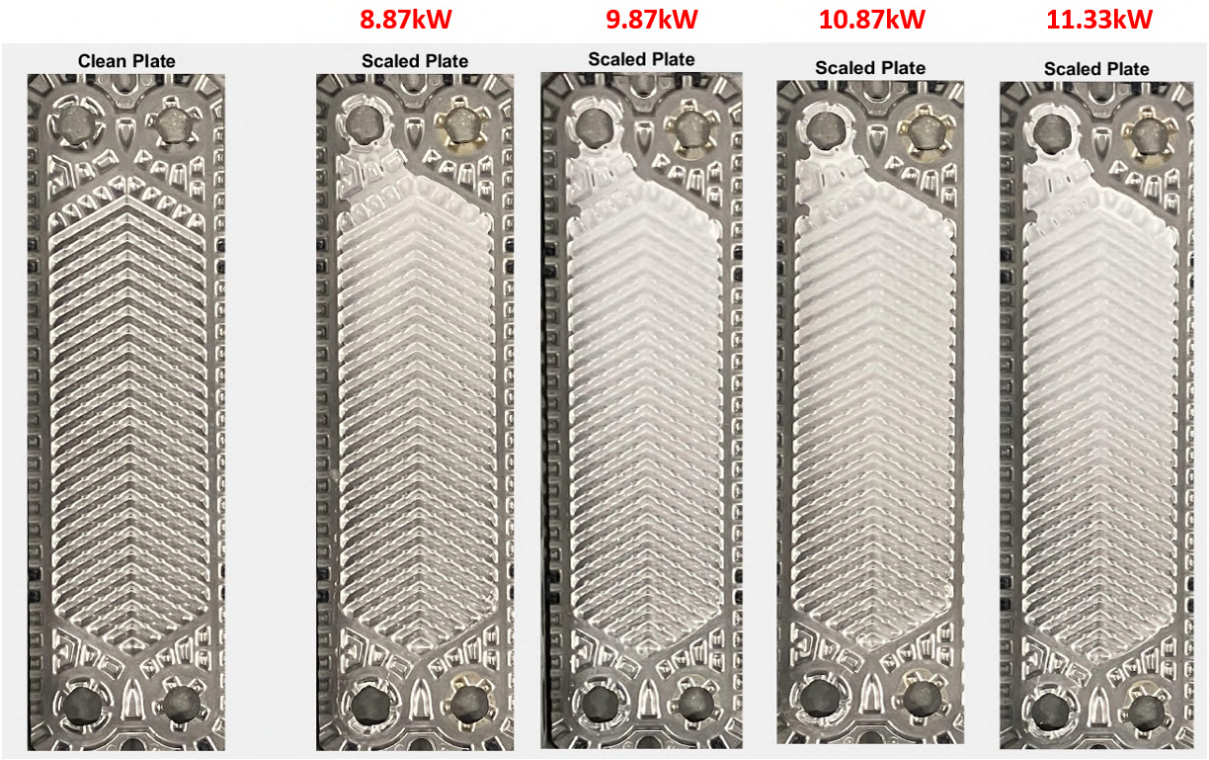

Figure 61: Comparison of scale distribution on the second scaled plate with change in duty

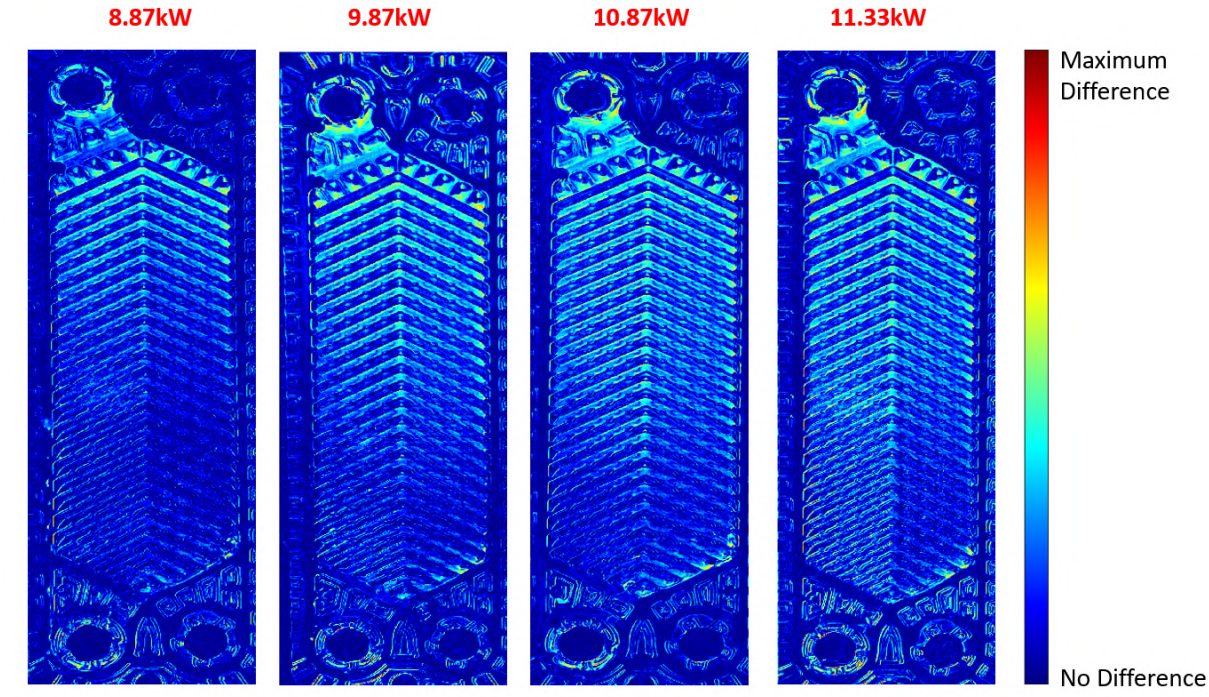

Figure 62: Comparison of scale distribution on the second scaled plate as a heatmap with change in duty

Finally, the total weight of the scale deposited on the two plates for each experiment is plotted in figure 63. For the highest duty of 11.31 kW, 1.11 grams of scale was deposited on the two plates, as compared to 0.39 grams of scale for the lowest duty of 8.87 kW. This finding is in line

with the observations made from figure 41 - 44, i.e., higher GPHE duty results in a larger scaled area of the plate, therefore resulting in a greater amount of scale deposited on the plates.

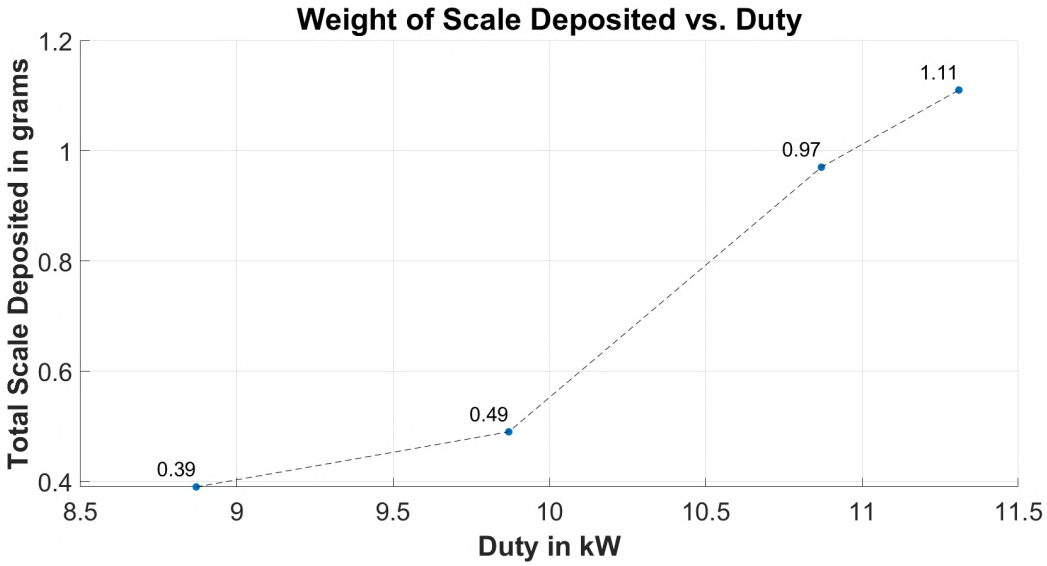

Figure 63: Weight of scale deposited (grams) vs duty (kW)

Based on the results obtained from the four experiments investigating the effect of variation of duty on the onset of scaling, it can be concluded that the performance of the GPHE is inversely proportional to the duty exchanged by the GPHE, if the flowrate, inlet temperature and hardness value of the cold medium is held constant. This is because a higher duty results in a greater amount of heat transferred to the cold medium, and therefore higher temperatures of the cold medium along the plate length. These higher temperatures coupled with the inverse soluble nature of $CaCO_3$ results in scale formation on a larger area of the plate. Consequently, the increased scale formation at higher duties results in higher resistance to heat transfer, ultimately leading to a decrease in the overall performance of the GPHE. Hence, to avoid scale formation in the current system, the lowest possible duty for the GPHE must be chosen.

5.3 Determination of the parameter with the greatest influence on scaling

Upon conducting all 10 unique experiments with de-hardened water as well as with hard water as the cooling medium, the parameter that has the greatest influence on the onset of $CaCO_3$ scaling can be determined. This is possible because the experiments were designed such that when one parameter is changed, all other parameters are held constant for the entire experimental run. As a result of this approach, any change in GPHE performance or amount of scale deposited is due to the change in the test parameter.

The study focuses on investigating the impact of three parameters on the onset of $CaCO_3$ scaling: the flowrate of the cold medium, the inlet temperature of the cold medium, and the duty exchanged by the T2B. Since this study focuses on the onset of scale, the time that it takes for the scale to be detrimental to GPHE performance determines which parameter has the greatest influence on the GPHE performance. Additionally, the weight of the scale deposited on the plates determines which parameter has the greatest influence on scaling tendency. Hence, by considering these two results from the 10 experiments, the parameter that most greatly influences the onset of scale in GPHEs can be determined.

Owing to the limitations of the boiler, the design of experiments had to be re-configured. As a result of this, the ratio between the maximum and minimum value of a parameter is no longer

constant. For the flowrate of the cold medium, the ratio between the maximum and minimum values used in the experiments is 1.75. In the case of the inlet temperature, this ratio is 1.65, while for the duty, it is 1.27. This makes it difficult to compare the results for the effect of variation of one parameter with another, since the step size, expressed as a percentage, was not held constant. However, in spite of a smaller variation in duty as compared to inlet temperature, the results for time for onset of scale are very similar. In the experiments studying the effect of inlet temperature variation, the maximum and minimum time for onset of scaling is 362 minutes and 294 minutes respectively. Whereas, in the experiments studying the effect of change in duty, the maximum and minimum time for onset of scaling is 358 minutes and 293 minutes respectively. Hence, in terms of time of onset of scale, a change in duty exchanged by the T2B has a bigger effect on $CaCO_3$ scaling than a change in inlet temperature of the cold medium. On analysing the results of the weight of the scale deposited on the plates, the maximum and minimum value for the experiments studying the effect of variation in inlet temperature is 0.79 grams and 0.36 grams respectively. For the experiments studying the effect of variation of duty, the maximum and minimum amount of scale deposited is 1.11 grams and 0.39 grams respectively. For a smaller change in the duty of the T2B as compared to the inlet temperature, a larger difference in the weight of the scale deposited was observed. Hence, in terms of the weight of the scale deposited on the plates, a change in duty has a greater influence on $CaCO_3$ scaling as compared to inlet temperature of the cold medium. Therefore, the duty exchanged by the T2B has a greater effect on the onset of $CaCO_3$ scaling, as compared to the inlet temperature of the cold medium.

On analysing the results for the effect of flowrate variation, a sharp decrease in time for onset of scaling and an exponential increase in weight of scale deposited on the plates is noticed when the flowrate is decreased from 250 kg/hr to 200 kg/hr, or when the shear stress on the plate is decreased from 50 Pa to 32 Pa. Hence, if the flowrate is below 250 kg/hr or the shear stress is below 50 Pa, flowrate of the cold medium is the most influential parameter in the context of $CaCO_3$ scaling. However, for a flowrate higher the 250 kg/hr, the effect of changing the flowrate of the cold medium on $CaCO_3$ scaling is similar to the effect of changing the inlet temperature. The changes in time for onset of scaling and weight of scale deposited are not dramatically different where one parameter can be classified as more influential than the other.

Hence, after analysing the data collected from the 10 experiments, it can be concluded that as long as the shear stress on the plate is above 50 Pa, the duty exchanged by the GPHE has a greater influence on the onset of $CaCO_3$ scaling of the GPHE, as compared to the flowrate and inlet temperature of the cold medium. However, below a shear stress value of 50 Pa, the effect of flowrate on $CaCO_3$ scaling is significantly larger than the effect of duty and inlet temperature.

5.4 Establishing an optimal performance region

The results from the 10 experiments can be used to determine an optimal performance region to minimise scale deposition on the plate for the current system. This can be accomplished by plotting the weight of the deposited scale against the three parameters (flowrate, inlet temperature, and duty) and determining the range of values for which the scale deposition on the T2B is minimal. As seen in figure 64, a 3-dimensional plot is created with the flowrate, inlet temperature and duty as the 3 axes. For each experimental case, a point is plotted on the graph corresponding to the value of the parameters for that case. Subsequently, the points are coloured based on the amount of scale deposited on the plate, with dark blue representing zero scale deposition and red indicating the maximum value of scale deposited in the 10 experiments. Below the base case flowrate of 250kg/hr, the weight of the scale deposited increases dramatically. This is seen by the red dot on the left end of the graph. Additionally, above the base case inlet temperature of 25°C and duty of 9.87kW, a large increase in the weight of the scale deposited is observed. This is observed by the dots in lighter shades of blue. Hence, the optimal performance region which minimises scale deposition on the plates is a region that encompasses flowrates above 250

kg/hr, inlet temperatures below 25 °C, and a duty of below 9.87 kW. This region is indicated in figure 64 by the shaded volume. Operating the current T2B in these conditions would result in less than 0.5 grams of scale deposited on the plates in a test run for 8 hours with 25°dH hard water.

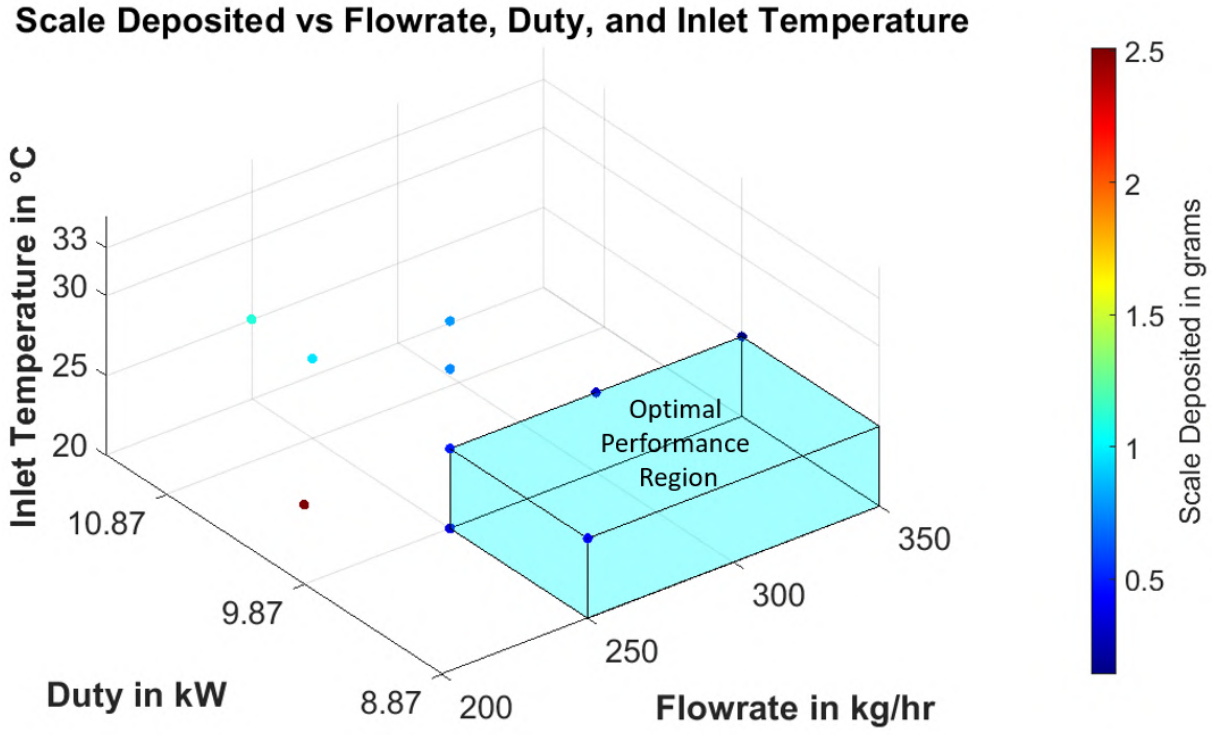

Figure 64: Optimal Performance Region for the current system

5.5 Predicting the scale deposited on the plates through regression analysis

The final step in analysing the results of the 10 experiments is determining a function that predicts the amount of scale deposited on the plates based on the flowrate and inlet temperature of the cold medium and the duty of the T2B. This is achieved by defining a non-dimensional duty(λ), as seen in equation 26. In this equation, Q refers to the duty exchanged by the T2B in watts, m refers to the mass flowrate of the cold medium in kg/hr and T_{in} refers to the inlet temperature of the cold medium in degrees celsius. T_{ref} is defined as a reference temperature and is selected as 100°C.

$$\lambda = \frac{Q}{m \cdot c_p \cdot (T_{\text{ref}} - T_{\text{in}})} \tag{26}$$

Once λ is defined, it can be calculated for all 10 experimental cases by substituting the respective values for all 3 parameters. The amount of scale deposited on the plate can then be plotted against the value of λ, as seen in figure 65. Finally, to predict the total weight of the scale deposited on the plates as a function of λ, a regression analysis was performed to determine the quantitative relationship between the two variables. A 5th-degree polynomial was fitted to the data, mentioned in equation 27. The fitted polynomial function is also plotted in figure 65. The R^2 value, also known as the coefficient of determination, is also mentioned in the figure. It quantifies the degree to which the model accurately reproduces observed outcomes, by evaluating the extent to which the model accounts for the variation in outcomes. It ranges from 0 to 1, where 1 indicates a perfect fit. Since the value of R^2 for this curve is 0.99, the fitted curve and observed data indicate a strong fit.

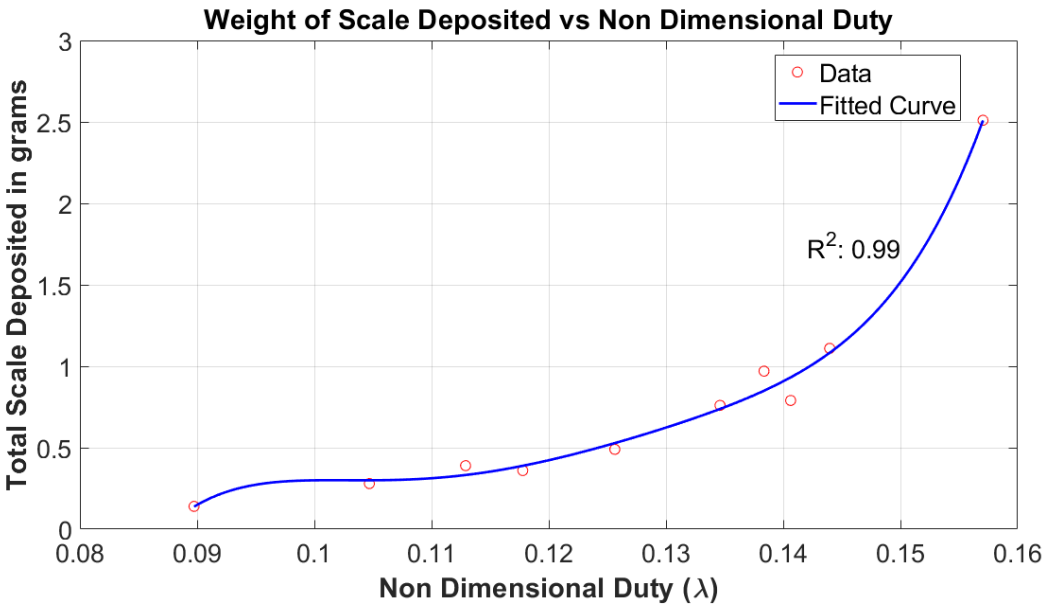

Figure 65: Weight of scale deposited vs non-dimensional duty

$$\text{Scale Deposited (g)} = 2.04\times10^{7}\cdot\lambda^{5} - 1.22\times10^{7}\cdot\lambda^{4} + 2.93\times10^{6}\cdot\lambda^{3} - 3.48\times10^{5}\cdot\lambda^{2} + 2.05\times10^{4}\cdot\lambda - 483.1 \quad (27)$$

By computing the value of λ for a specific combination of the three parameters, it becomes possible to predict the quantity of scale that will be deposited on the plate using equation 27. This enables the estimation of the scaling tendency of the plate under experimental conditions that were not directly tested but fall within the range of the values examined.

6 Recommendations for Future Research

In order to conduct future research investigating scaling on GPHEs using the same setup built in the TU Delft lab, some improvements can be made to enable more constant system conditions which results in more reliable data collection.

To address the limitation of the modulating heating cycle of the boiler and inconsistent heating cycles at higher flow rates, an improvement can be made by incorporating an insulated pressurized stainless steel tank between the boiler and the T2B. Additionally, a pump can be installed after the stainless steel tank. This modification will help mitigate the fluctuations in the supply temperature from the boiler by averaging out the temperature variations. The hot medium will be pumped from the tank to the T2B at a more constant temperature, ensuring more stable and reliable experimental conditions.

Another limitation of the current setup is the fluctuation in the supply temperature of the cooling water to the TL3B. This issue can be addressed by investing in an industrial recirculating chiller. This would offer more precise control of the cooling water supply temperature and allow for better control of the system conditions.

The inability to use cooling tower water for this study resulted in the need to artificially prepare hard water. As a result of this, a drop in the hardness value of the tank during an experimental setup was observed. This prevented the selection of hardness as a test parameter for this study. Hence, future research on this setup can be done using cooling tower water. This would eliminate the problems encountered with artificially prepared hard water, while also allowing for the selection of hardness as a test parameter.

This study can also be broadened by increasing the range of the values used for the test parameters. By performing more experiments at different flowrates, inlet temperatures and duties, more accurate trends in time for onset of scaling and weight of scale deposited on the plate can be obtained. This can be especially important for the flowrate of the cold medium, where an extreme change in scaling tendency was observed when the flowrate was dropped to 200 kg/hr. Performing more experiments at different initial conditions can also help better determine which parameters have the strongest and weakest influence on $CaCO_3$ scaling.

An extension of this study can be to investigate the effects of a parameter beyond the onset of scale condition. Since the scale will continue to deposit and the overall heat transfer coefficient will further reduce if the experiment duration is increased, investigating the rate and extent of change in these quantities after the onset of scale can provide useful insights into understanding and preventing scale formation. Finally, the same study can be repeated by using a different heat exchanger to determine if the results are generalizable to all GPHEs or are the results specific to the T2B.

7 Conclusion

Gasketed Plate Heat Exchangers (GPHEs) are compact, efficient, and versatile heat exchangers used in various industries. However, they are susceptible to fouling, particularly scaling caused by calcium carbonate ($CaCO_3$). To understand the impact of scaling on GPHE performance, experiments using an Alfa Laval GPHE were conducted. The experimental setup includes a cold loop with hard water and a hot loop with de-hardened water centred around the GPHE. Ten experiments were designed to study the effects of flowrate and inlet temperature of hard water and duty exchanged by the T2B. For each experiment, scaling was quantified by monitoring temperatures and calculating the overall heat transfer coefficient and fouling resistance. Additionally, each experimental case's onset of scaling is determined by comparing the overall heat transfer coefficient for the experiment with a reference value. In addition, the weight of the deposited is determined, and images of the scaled and cleaned plates are compared to better understand the effect of a parameter on scaling tendency.

The results from the 10 experiments indicate that all 3 selected parameters have a significant influence on scaling. For the experiments studying the effect of change in flowrate, it was observed that flowrate is directly proportional to GPHE performance and inversely proportional to scaling tendency. Increasing the flowrates led to a lower amount of scale deposited on the plates and led to an increase in the time for onset of scaling. This is primarily because of the higher shear stress on the wall due to the high flowrates, which hinders the ability of the $CaCO_3$ to adhere to the plate. Additionally, a dramatic increase in the amount of scale deposited and a decrease in time for the onset of scaling is deposited is observed when the flowrate is reduced below 250 kg/hr. This corresponds to a drop in the shear stress value of the plate below 50 Pa. Hence, to avoid scaling on the current system, the flowrates of the cold medium must be chosen such that the shear stress on the plate always exceeds 50Pa.

Upon studying the effect of inlet temperature and duty, the opposite trend was observed. The inlet temperature and duty were inversely proportional to the GPHE performance and directly proportional to the tendency of the plate to scale. Increasing the inlet temperature of the hard water and the duty exchanged by the T2B led to higher amounts of scale deposited and lowered the time for the onset of scaling. This is because an increase in either of these quantities increases the overall temperature of the hard water. Since $CaCO_3$ is an inverse soluble salt, its tendency to precipitate on the plate increases with an increase in temperature. Consequently, a greater deposition of scale was observed at the exit of the plate in all 10 experiments. This is because the hard water increases in temperature as it flows along the length of the plate, thereby increasing the tendency of the $CaCO_3$ to precipitate.

This study also aimed to determine which parameter has the greatest effect on scaling in GPHEs. By studying the results from the 10 experiments, it was observed that as long as the shear stress is above 50Pa, a change in duty exchanged by the T2B has a bigger impact on the weight of scale deposited and time for onset of scaling when compared to the inlet temperature and flowrate of the cold medium. However, for a shear stress value below 50Pa or flowrate below 250 kg/hr, the effect of change in flowrate is significantly larger than the effect of inlet temperature and duty.

To minimise the amount of scale deposited on the plate, an optimal performance region was determined and visualised in a 3-dimensional plot. It was determined that operating the T2B with a flowrate above 250 kg/hr, inlet temperature lower than 25°C and duty lower than 9.87kW results in minimising the amount of scale deposited on the plates. Since CAS cannot account for fouling on the GPHE, this graph can be referred to when designing the operating conditions for a similar system. Finally, a polynomial function was determined to predict the amount of scale deposited on the plates as a function of the test parameters by conducting regression analysis.

References

[1] Ahmed T. Al-Sammarraie and Kambiz Vafai. "Heat transfer augmentation through convergence angles in a pipe". In: *Numerical Heat Transfer, Part A: Applications* 72.3 (2017), pp. 197–214. DOI: 10.1080/10407782.2017.1372670. URL: https://doi.org/10.1080/10407782.2017.1372670.

[2] Sadik Kakaç and Hongtan Liu. *Heat Exchangers: Selection, Rating and Thermal Design*. CRC Press, 2002.

[3] Hassan Al-Haj Ibrahim. "Fouling in Heat Exchangers". In: *MATLAB*. Ed. by Vasilios N. Katsikis. Rijeka: IntechOpen, 2012. Chap. 3. DOI: 10.5772/46462. URL: https://doi.org/10.5772/46462.

[4] Wikipedia. *Plate heat exchanger*. https://en.wikipedia.org/wiki/Plate_heat_exchanger.

[5] Alfa Laval. *5 Reasons to use plate-and-frame heat exchangers instead of shell-and-tube*. https://www.alfalaval.com/microsites/gphe/tools/gphe-vs-shell-and-tube/.

[6] Alfa Laval. *Industrial gasketed plate heat exchangers*. https://www.alfalaval.com/microsites/gphe/types/industrial/.

[7] A. Cooper, J. W. Suitor, and J. D. Usher. "Cooling Water Fouling in Plate Heat Exchangers". In: *Heat Transfer Engineering* 1.3 (1980), pp. 50–55. DOI: 10.1080/01457638008939562.

[8] "Understanding exchanger fouling". In: *Filtration + Separation* 56.5 (2019), pp. 28–30. ISSN: 0015-1882. DOI: https://doi.org/10.1016/S0015-1882(20)30143-9. URL: https://www.sciencedirect.com/science/article/pii/S0015188220301439.

[9] T.R. Bott. *Fouling of Heat Exchangers*. Chemical Engineering Monographs. Elsevier Science, 1995. ISBN: 9780080531908. URL: https://books.google.nl/books?id=5px8GzscIRsC.

[10] Hans Müller-Steinhagen. "Cooling-Water Fouling in Heat Exchangers". In: ed. by James P. Hartnett et al. Vol. 33. Advances in Heat Transfer. Elsevier, 1999, pp. 415–496. DOI: https://doi.org/10.1016/S0065-2717(08)70307-1. URL: https://www.sciencedirect.com/science/article/pii/S0065271708703071.

[11] A. M. Pritchard. "The Economics of Fouling". In: *Fouling Science and Technology*. Ed. by L. F. Melo, T. R. Bott, and C. A. Bernardo. Dordrecht: Springer Netherlands, 1988, pp. 31–45. ISBN: 978-94-009-2813-8. DOI: 10.1007/978-94-009-2813-8_3. URL: https://doi.org/10.1007/978-94-009-2813-8_3.

[12] Verein Deutscher Ingenieure and VDI-Gesellschaft Verfahrenstechnik und Chemieingenieurwesen. *VDI Heat Atlas*. Heidelberg: Springer, 2010.

[13] Wikipedia. *Limescale*. https://en.wikipedia.org/wiki/Limescale.

[14] Wikipedia. *Fouling*. https://en.wikipedia.org/wiki/Fouling.

[15] Alfa Laval. *The theory behind heat transfer - Plate Heat Exchangers*. https://www.alfalaval.com/globalassets/documents/microsites/heating-and-cooling-hub/alfa_laval_heating_and_cooling_hub_the_theory_behind_heat_transfer.pdf.

[16] Jure Berce et al. "A Review of Crystallization Fouling in Heat Exchangers". In: *Processes* 9.8 (2021). ISSN: 2227-9717. DOI: 10.3390/pr9081356. URL: https://www.mdpi.com/2227-9717/9/8/1356.

[17] Xu Zhao and Xiao Dong Chen. "A Critical Review of Basic Crystallography to Salt Crystallization Fouling in Heat Exchangers". In: *Heat Transfer Engineering* 34.8-9 (2013), pp. 719–732. DOI: 10.1080/01457632.2012.739482. URL: https://doi.org/10.1080/01457632.2012.739482.

[18] R&D - Alfa Laval) Olga Santos (Materials Technology & Chemistry. *Fouling in GPHE (part 1) [webinar]*. Sept. 2019.

[19] Bipan Bansal, Xiao Dong Chen, and Hans Müller-Steinhagen. "Analysis of 'classical' deposition rate law for crystallisation fouling". In: *Chemical Engineering and Processing: Process Intensification* 47.8 (2008), pp. 1201–1210. ISSN: 0255-2701. DOI: https://doi.org/10.1016/j.cep.2007.03.016. URL: https://www.sciencedirect.com/science/article/pii/S0255270107001754.

[20] Wikipedia. *Hard Water*. https://en.wikipedia.org/wiki/Hard_water.

[21] Frantisek Kozisek. "Regulations for calcium, magnesium or hardness in drinking water in the European Union member states". In: *Regulatory Toxicology and Pharmacology* 112 (2020), p. 104589. ISSN: 0273-2300. DOI: https://doi.org/10.1016/j.yrtph.2020.104589. URL: https://www.sciencedirect.com/science/article/pii/S0273230020300155.

[22] Mart Beeftink et al. "Carbon footprint of drinking water softening as determined by life cycle assessment". In: *Journal of Cleaner Production* 278 (2021), p. 123925. ISSN: 0959-6526. DOI: https://doi.org/10.1016/j.jclepro.2020.123925. URL: https://www.sciencedirect.com/science/article/pii/S0959652620339706.

[23] Daniel A. Meier, Bingzhi Chen, and Craig Myers. "Chapter 11 - Cooling water systems: An overview". In: *Water-Formed Deposits*. Ed. by Zahid Amjad and Konstantinos D. Demadis. Elsevier, 2022, pp. 239–267. ISBN: 978-0-12-822896-8. DOI: https://doi.org/10.1016/B978-0-12-822896-8.00020-0. URL: https://www.sciencedirect.com/science/article/pii/B9780128228968000200.

[24] Nalco Chemical Company. *The NALCO Water Handbook*. McGraw-Hill Book Company, 2018. ISBN: 9781259860973.

[25] Kang Sub Song et al. "Composite fouling characteristics of CaCO3 and CaSO4 in plate heat exchangers at various operating and geometric conditions". In: *International Journal of Heat and Mass Transfer* 136 (2019), pp. 555–562. ISSN: 0017-9310. DOI: https://doi.org/10.1016/j.ijheatmasstransfer.2019.03.032. URL: https://www.sciencedirect.com/science/article/pii/S0017931018349676.

[26] Hans Müller-Steinhagen. "Cooling-Water Fouling in Heat Exchangers". In: ed. by James P. Hartnett et al. Vol. 33. Advances in Heat Transfer. Elsevier, 1999, pp. 415–496. DOI: https://doi.org/10.1016/S0065-2717(08)70307-1. URL: https://www.sciencedirect.com/science/article/pii/S0065271708703071.

[27] Jitka MacAdam and Simon A. Parsons. "Calcium carbonate scale formation and control". In: *Reviews in Environmental Science and Bio/Technology* 3 (2004), pp. 159–169. DOI: 10.1007/s11157-004-3849-1.

[28] Bipan Bansal, Hans Müller-Steinhagen, and Xiao Dong Chen. "Performance of plate heat exchangers during calcium sulphate fouling — investigation with an in-line filter". In: *Chemical Engineering and Processing: Process Intensification* 39.6 (2000), pp. 507–519. ISSN: 0255-2701. DOI: https://doi.org/10.1016/S0255-2701(00)00098-2. URL: https://www.sciencedirect.com/science/article/pii/S0255270100000982.

[29] Eungchan Lee et al. "Thermal resistance in corrugated plate heat exchangers under crystallization fouling of calcium sulfate (CaSO4)". In: *International Journal of Heat and Mass Transfer* 78 (2014), pp. 908–916. ISSN: 0017-9310. DOI: https://doi.org/10.1016/j.ijheatmasstransfer.2014.07.069. URL: https://www.sciencedirect.com/science/article/pii/S0017931014006589.

[30] Zhenhua QUAN, Yongchang CHEN, and Chongfang MA. "Experimental Study of Fouling on Heat Transfer Surface During Forced Convective Heat Transfer". In: *Chinese Journal of Chemical Engineering* 16.4 (2008), pp. 535–540. ISSN: 1004-9541. DOI: https://doi.org/10.1016/S1004-9541(08)60117-2. URL: https://www.sciencedirect.com/science/article/pii/S1004954108601172.

[31] T.M. Pääkkönen et al. "CFD modelling of CaCO3 crystallization fouling on heat transfer surfaces". In: *International Journal of Heat and Mass Transfer* 97 (2016), pp. 618–630. ISSN: 0017-9310. DOI: https://doi.org/10.1016/j.ijheatmasstransfer.2015.11.099. URL: https://www.sciencedirect.com/science/article/pii/S0017931016304409.

[32] T.M. Pääkkönen et al. "Crystallization fouling of CaCO3 – Analysis of experimental thermal resistance and its uncertainty". In: *International Journal of Heat and Mass Transfer* 55.23 (2012), pp. 6927–6937. ISSN: 0017-9310. DOI: https://doi.org/10.1016/j.ijheatmasstransfer.2012.07.006. URL: https://www.sciencedirect.com/science/article/pii/S0017931012005339.

[33] K.H. Teng et al. "Calcium carbonate fouling on double-pipe heat exchanger with different heat exchanging surfaces". In: *Powder Technology* 315 (2017), pp. 216–226. ISSN: 0032-5910. DOI: https://doi.org/10.1016/j.powtec.2017.03.057. URL: https://www.sciencedirect.com/science/article/pii/S0032591017302747.

[34] Wei Li et al. "Investigation of $CaCO_3$ fouling in plate heat exchangers". In: *Heat and Mass Transfer* 52.11 (Nov. 2016), pp. 2401–2414. DOI: 10.1007/s00231-016-1752-2.

[35] T. Kho et al. "Effect of Flow Distribution on Scale Formation in Plate and Frame Heat Exchangers". In: *Chemical Engineering Research and Design* 75.7 (1997). 5th UK National Heat Transfer Conference, pp. 635–640. ISSN: 0263-8762. DOI: https://doi.org/10.1205/026387697524245. URL: https://www.sciencedirect.com/science/article/pii/S0263876297715831.

[36] D.A. Al-Otaibi, M.S.J. Hashmi, and B.S. Yilbas. "Fouling resistance of brackish water: Comparision of fouling characteristics of coated carbon steel and titanium tubes". In: *Experimental Thermal and Fluid Science* 55 (2014), pp. 158–165. ISSN: 0894-1777. DOI: https://doi.org/10.1016/j.expthermflusci.2014.03.010. URL: https://www.sciencedirect.com/science/article/pii/S0894177714000818.

[37] T.M. Pääkkönen et al. "Modeling CaCO3 crystallization fouling on a heat exchanger surface – Definition of fouling layer properties and model parameters". In: *International Journal of Heat and Mass Transfer* 83 (2015), pp. 84–98. ISSN: 0017-9310. DOI: https://doi.org/10.1016/j.ijheatmasstransfer.2014.11.073. URL: https://www.sciencedirect.com/science/article/pii/S0017931014010692.

[38] B. Bansal and H. Mu¨ller-Steinhagen. "Crystallization Fouling in Plate Heat Exchangers". In: *Journal of Heat Transfer* 115.3 (Aug. 1993), pp. 584–591. ISSN: 0022-1481. DOI: 10.1115/1.2910728. URL: https://doi.org/10.1115/1.2910728.

[39] Jitka MacAdam and Simon Parsons. "Calcium carbonate scale formation and control". In: *Reviews in Environmental Science and Bio/Technology* 3 (June 2004), pp. 159–169. DOI: 10.1007/s11157-004-3849-1.

[40] B. Bansal and H. Müller-Steinhagen. "Pressure Drop in Plate Heat Exchangers during Crystallisation Fouling". In: *Proceedings of the Conference of the Institution of Professional Engineers* 2.2 (1996), pp. 302–307.

[41] W. Augustin and M. Bohnet. "Influence of the ratio of free hydrogen ions on crystallization fouling". In: *Chemical Engineering and Processing: Process Intensification* 34.2 (1995), pp. 79–85. ISSN: 0255-2701. DOI: https://doi.org/10.1016/0255-2701(94)03002-2. URL: https://www.sciencedirect.com/science/article/pii/0255270194030022.

[42] FP Carr and Frederick DK. *Kirk-Othmer Encyclopedia of Chemical Technology. Calcium Carbonate*. John Wiley & Sons, 2003.

[43] European Chemicals Agency (ECHA). *Calcium Carbonate*. `https://echa.europa.eu/registration-dossier/-/registered-dossier/16050/4/5`.

A Appendix I

All 10 experiments in the updated design of experiments are configured in CAS and are seen in figures 66 - 74.

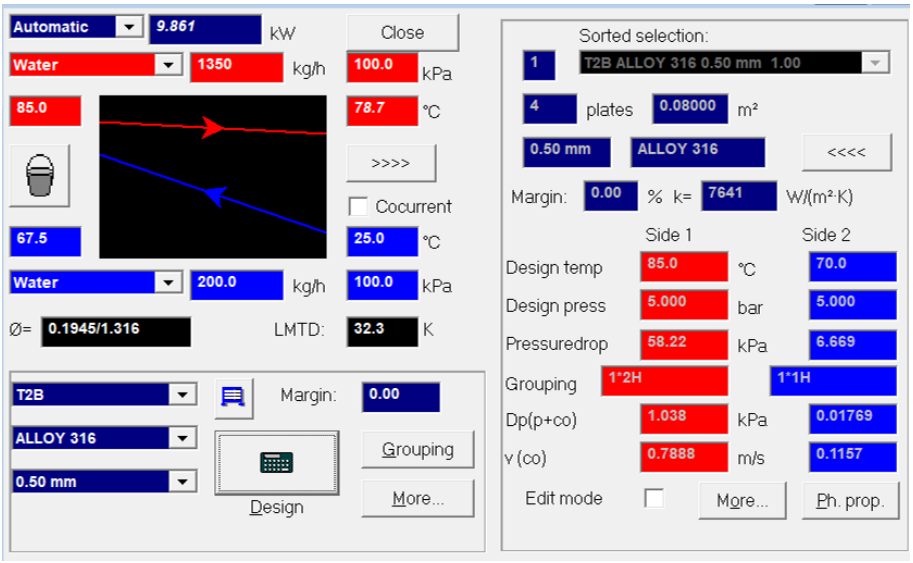

Figure 66: Configuration of Case 1 on CAS

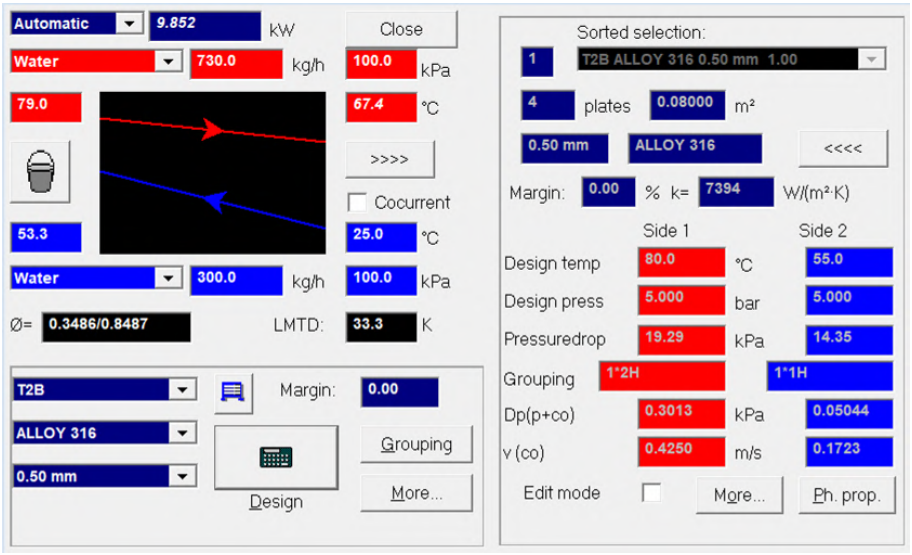

Figure 67: Configuration of Case 3 on CAS

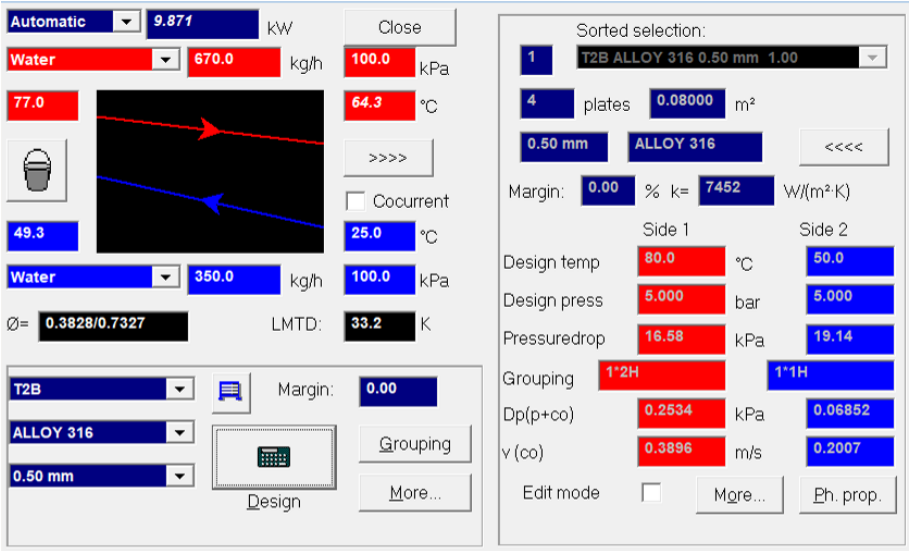

Figure 68: Configuration of Case 4 on CAS

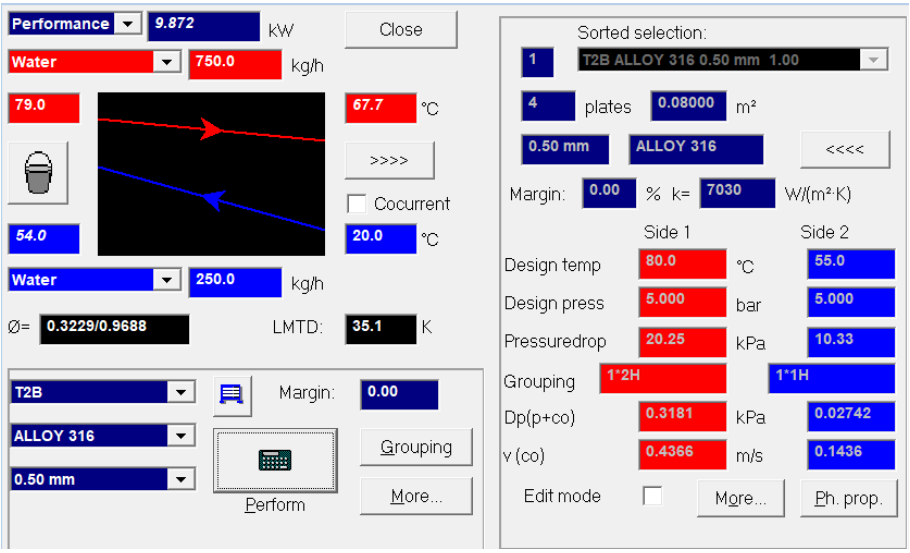

Figure 69: Configuration of Case 5 on CAS

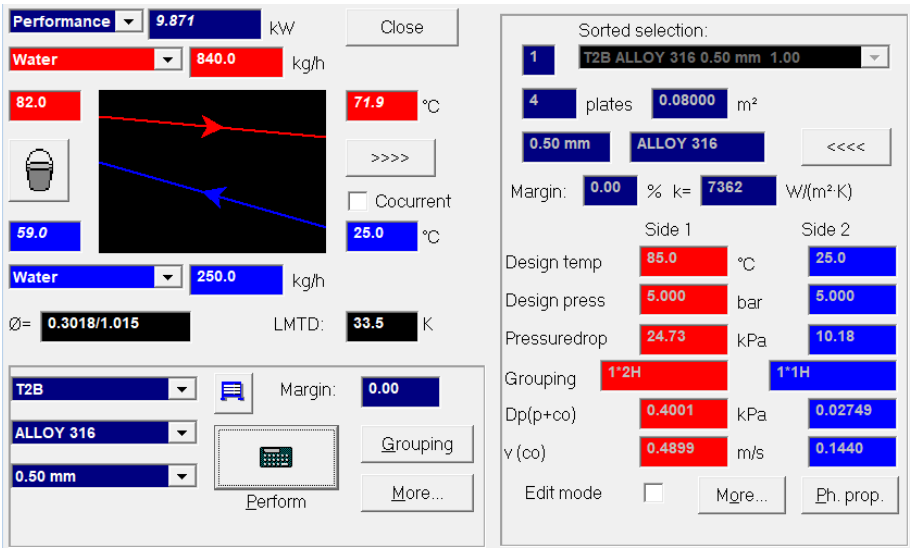

Figure 70: Configuration of Case 7 on CAS

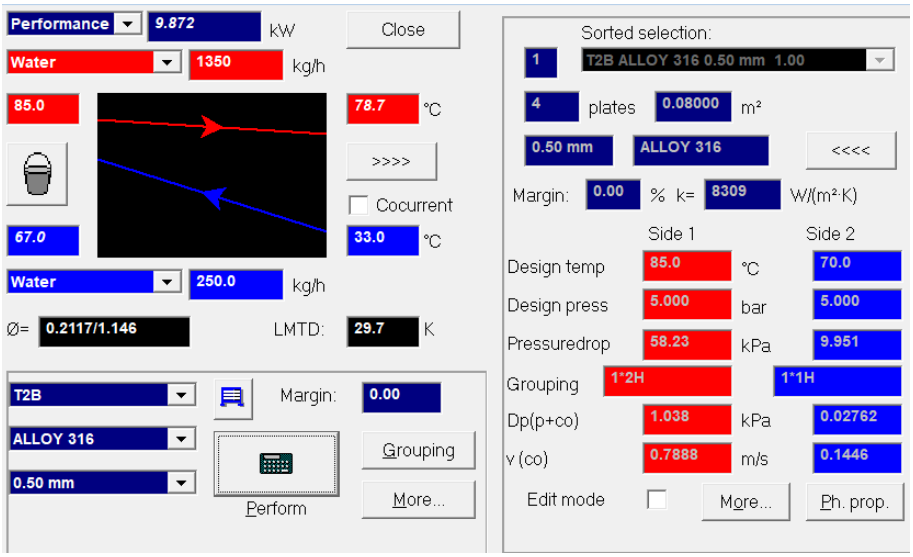

Figure 71: Configuration of Case 8 on CAS

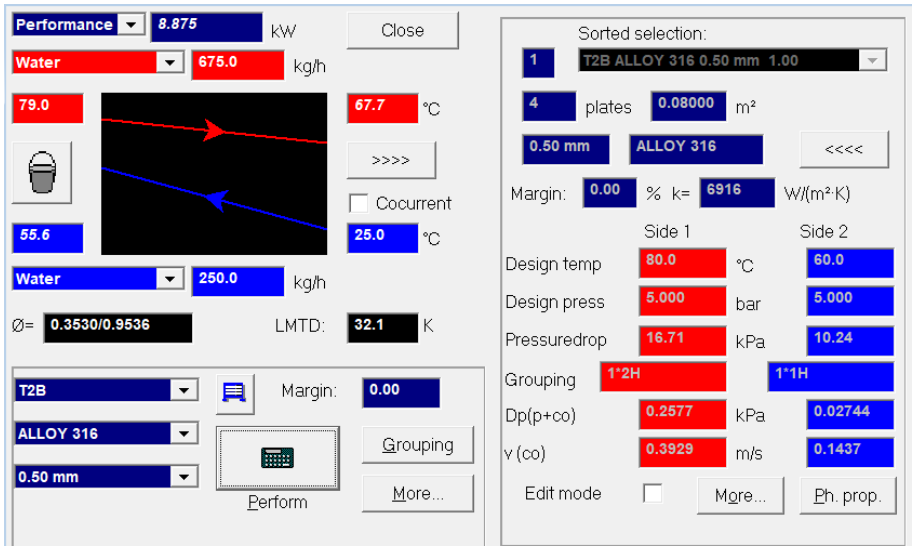

Figure 72: Configuration of Case 9 on CAS

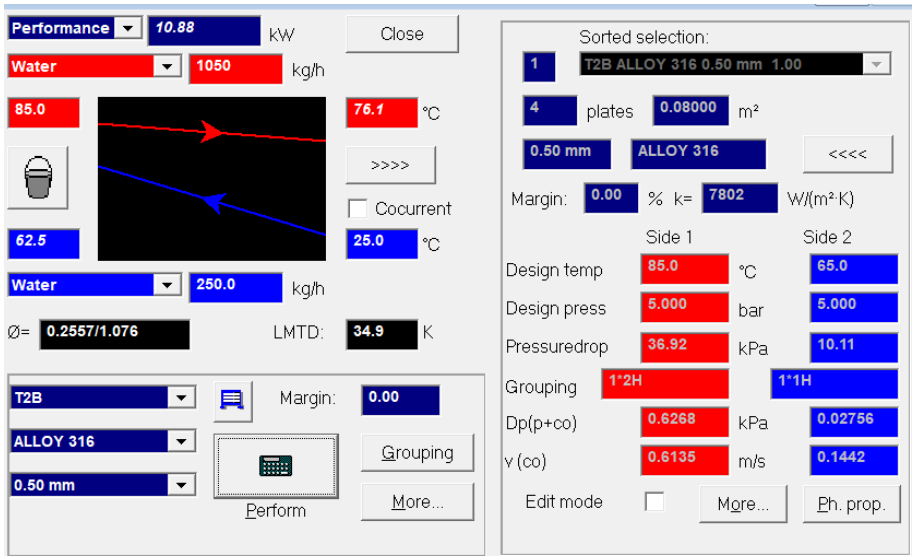

Figure 73: Configuration of Case 11 on CAS

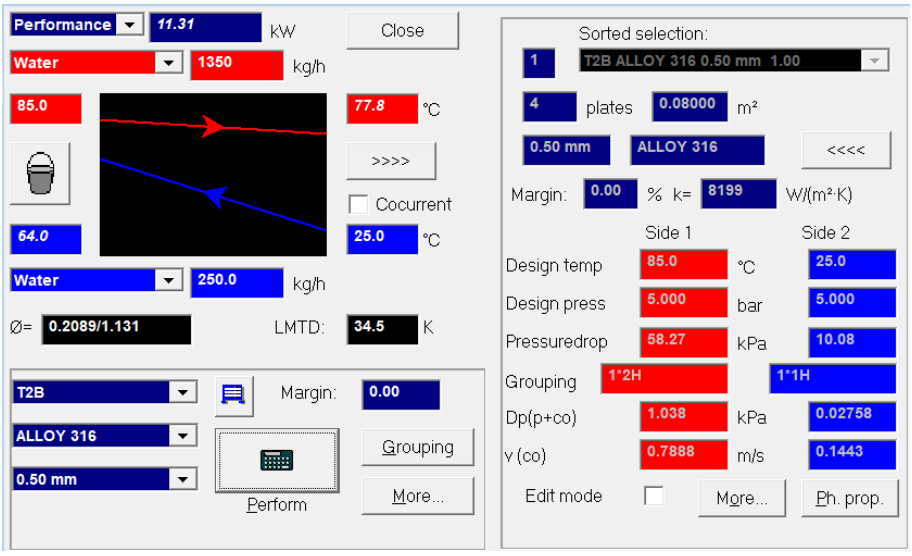

Figure 74: Configuration of Case 12 on CAS

B Appendix II

The Coriolis flowmeter in the cold loop and all 7 thermocouples in the setup were calibrated before conducting the experiments, as seen in figures 75 - 82.

The minimum and maximum flowrate of the cold medium is 200 kg/hr and 350kg/hr, respectively. The flowmeter indicates the flowrate in litres/second. Considering the density of water at 25 °C is 997 kg/m^3, the minimum and maximum flowrate of the cold medium is 0.055 l/s and 0.975 l/s, respectively. Hence, the flowmeter was calibrated in a similar range of flowrates, as seen in figure 75. The maximum difference in flowmeter reading and the measured flowrate is 1%. Hence, no fitting function or correction factor was applied to the readings from the flowmeter.

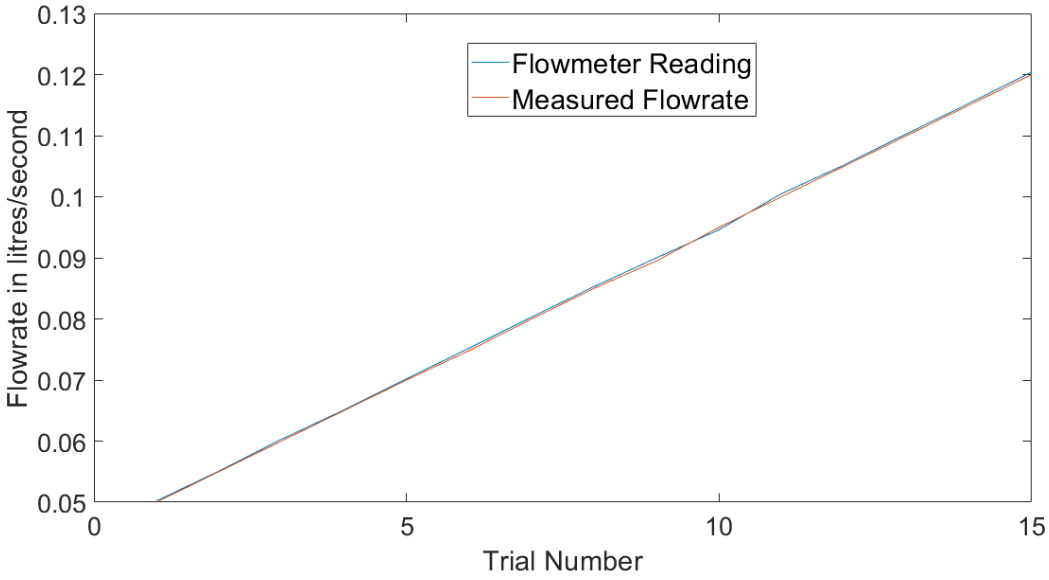

Figure 75: Calibration Curve for Coriolis flowmeter

Owing to the configuration of each case on CAS, approximate values of the maximum and minimum temperature each thermocouple needs to measure are known. Hence, the thermocouples

were calibrated in a similar range of temperatures. Thermocouples 1-6 measured approximately the same temperatures as the pre-calibrated thermocouple, as seen in figures 76 - 81. Hence, no fitting function or correction factor was applied to the data. However, thermocouple 7 consistently reported a temperature 1.5 °C higher than the pre-calibrated thermocouple, as seen in figure 82. Hence, within the DAQ software, an offset of -1.5 °C was applied to the reading.

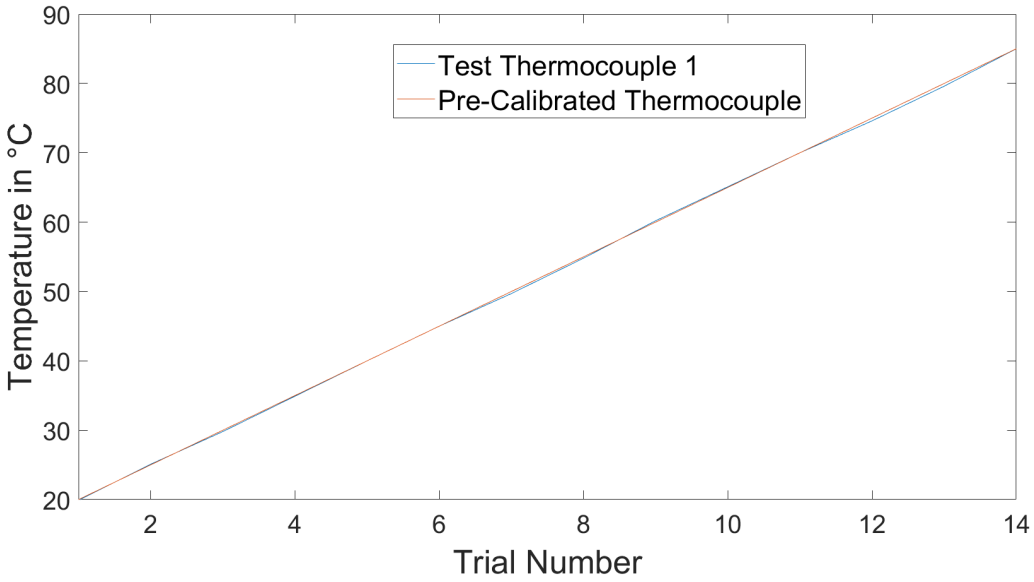

Figure 76: Calibration Curve for Thermocouple 1

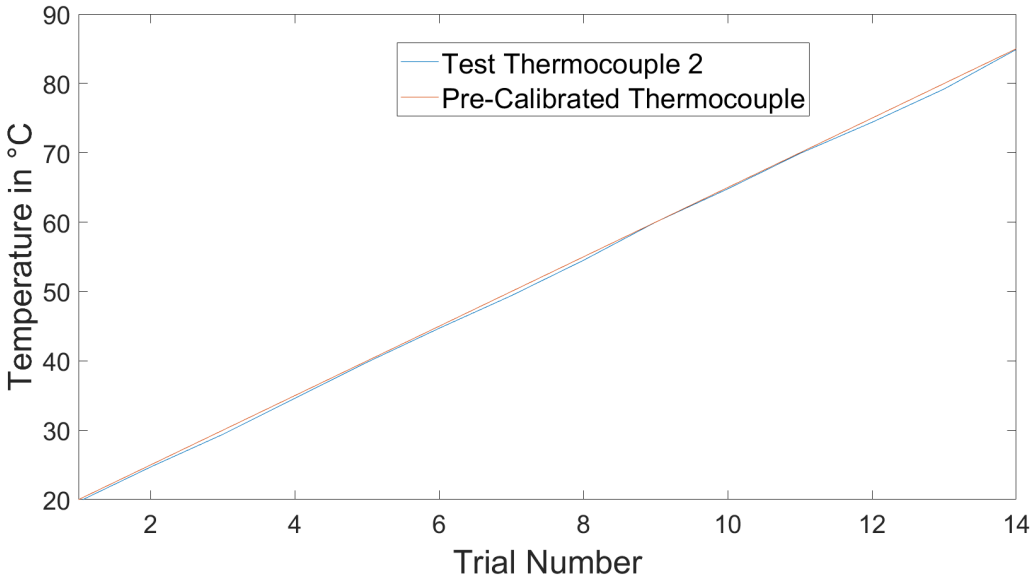

Figure 77: Calibration Curve for Thermocouple 2

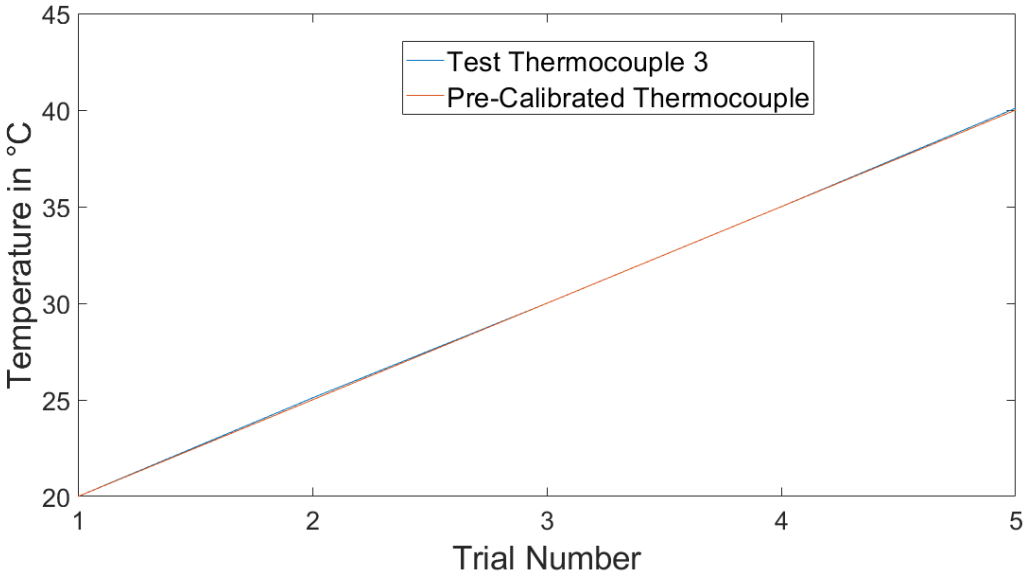

Figure 78: Calibration Curve for Thermocouple 3

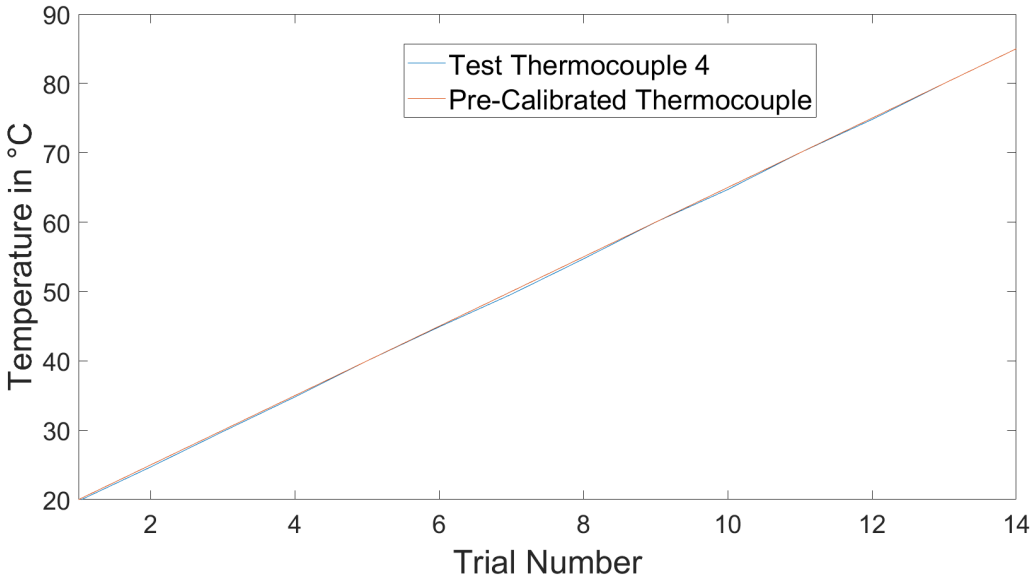

Figure 79: Calibration Curve for Thermocouple 4

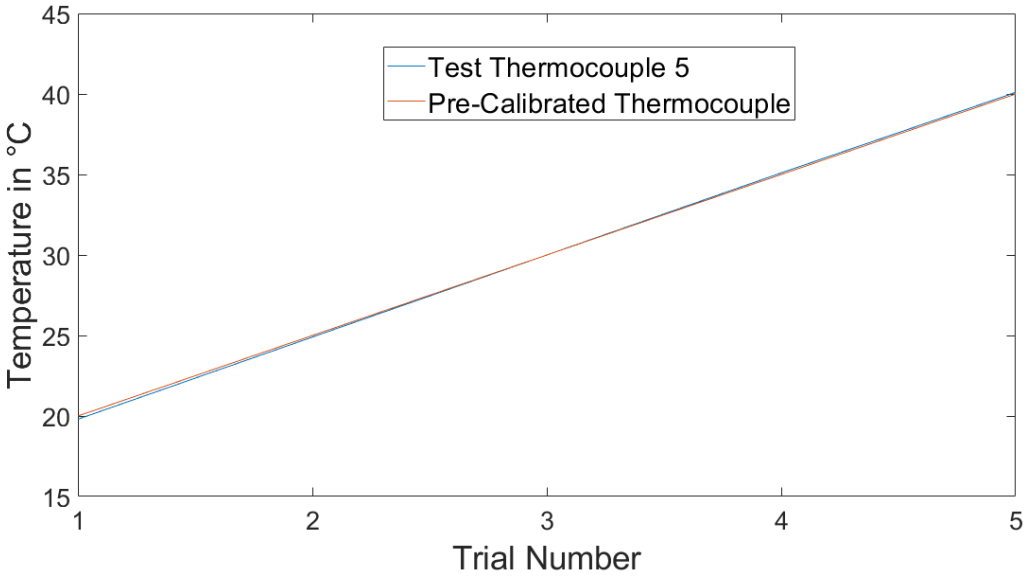

Figure 80: Calibration Curve for Thermocouple 5

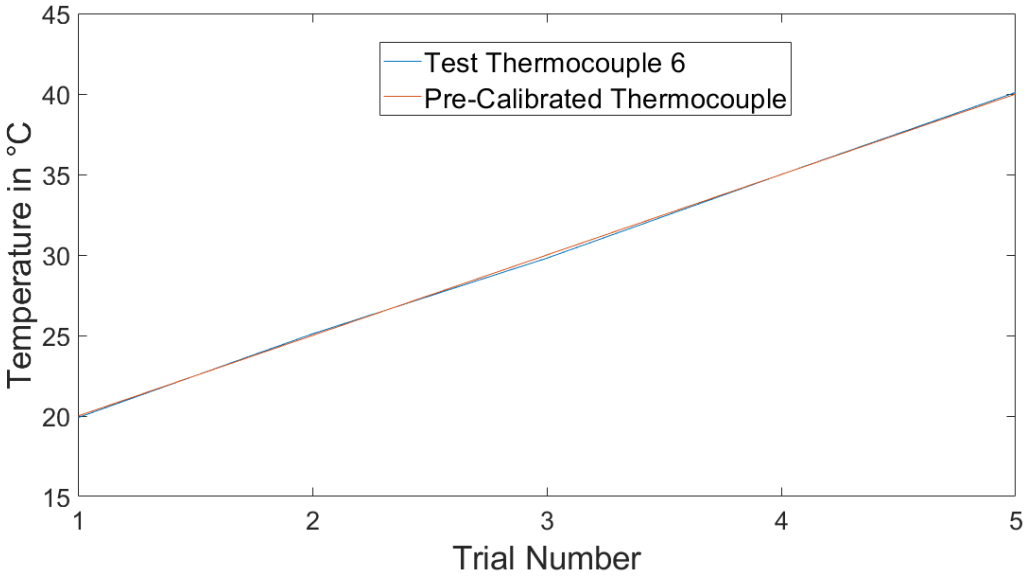

Figure 81: Calibration Curve for Thermocouple 6

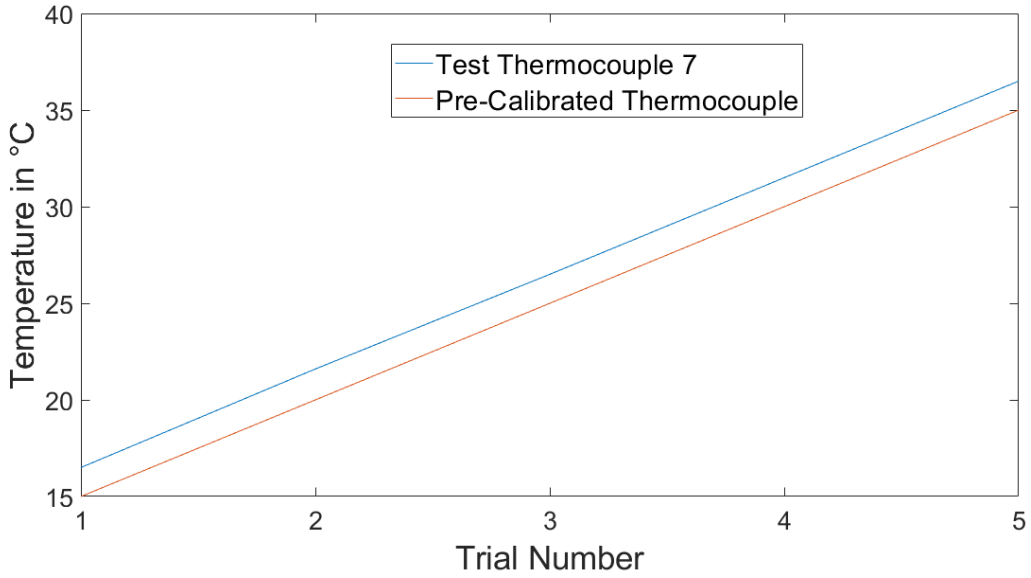

Figure 82: Calibration Curve for Thermocouple 7

C Appendix III

The plots for temperature averaged every 10 minutes (°C) vs time (minutes) for the two repetitions of the base case and for the additional 9 experiments performed with de-hardened water are seen in figures 83 - 93.

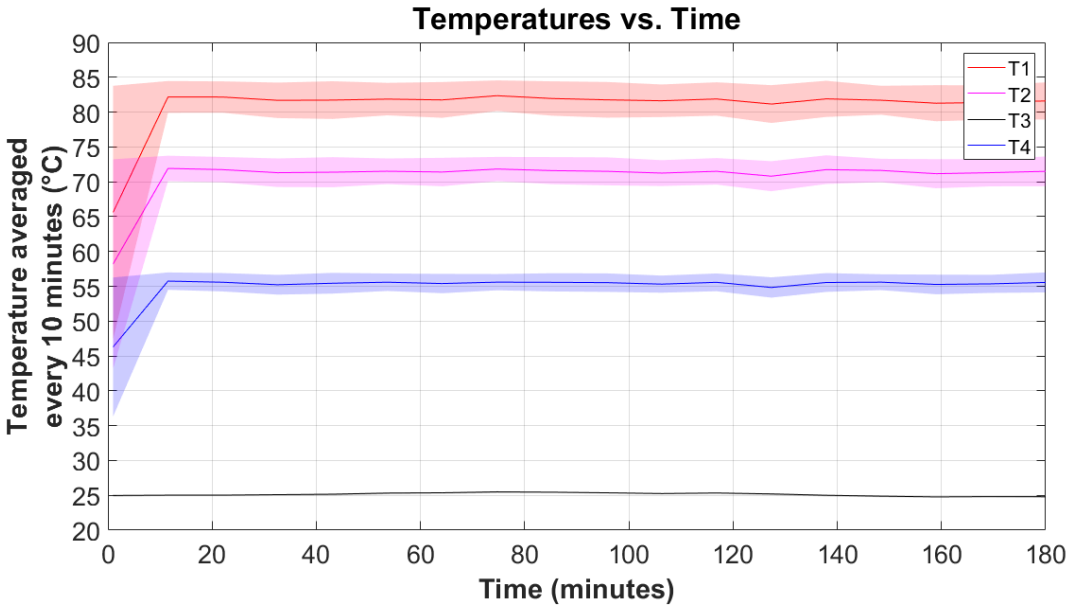

Figure 83: Temperature (°C) averaged every 10 minutes vs time (seconds) for the base case - repetition 1

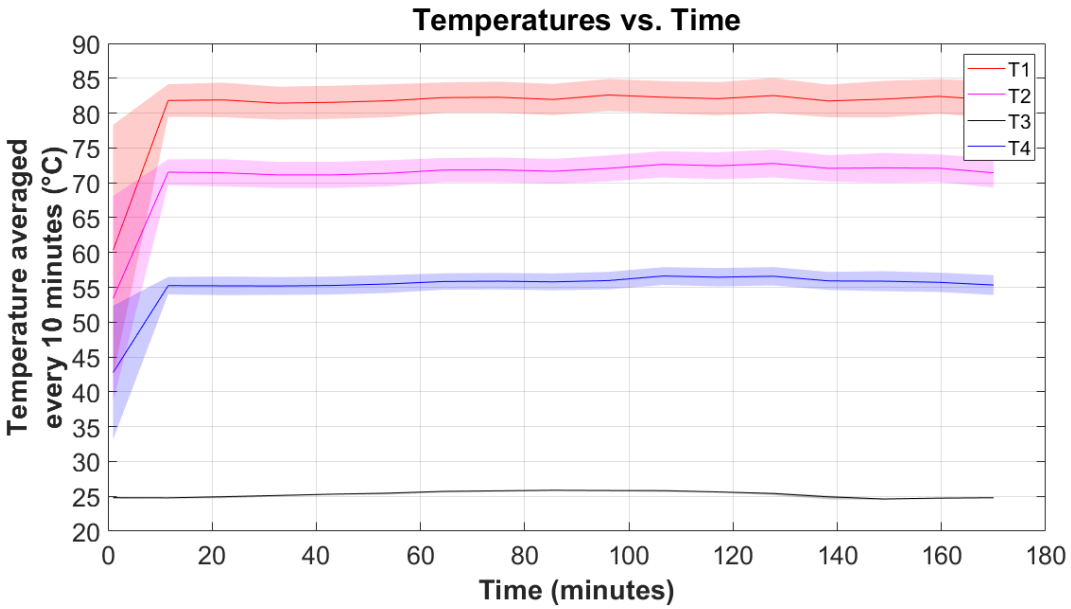

Figure 84: Temperature (°C) averaged every 10 minutes vs time (seconds) for the base case - repetition 2

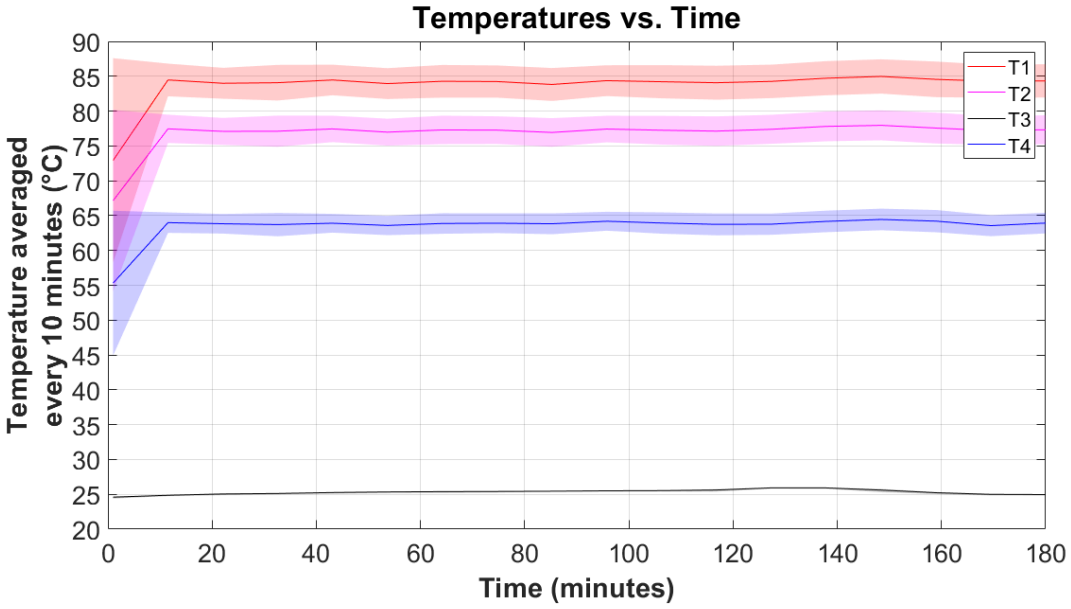

Figure 85: Temperature (°C) averaged every 10 minutes vs time (seconds) for case 1

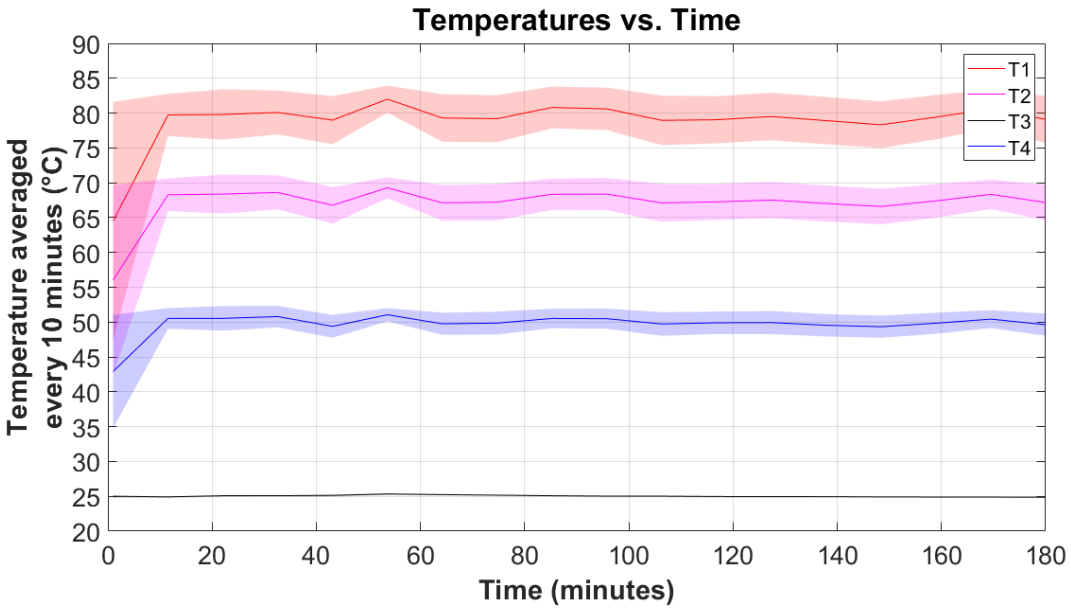

Figure 86: Temperature (°C) averaged every 10 minutes vs time (seconds) for case 3

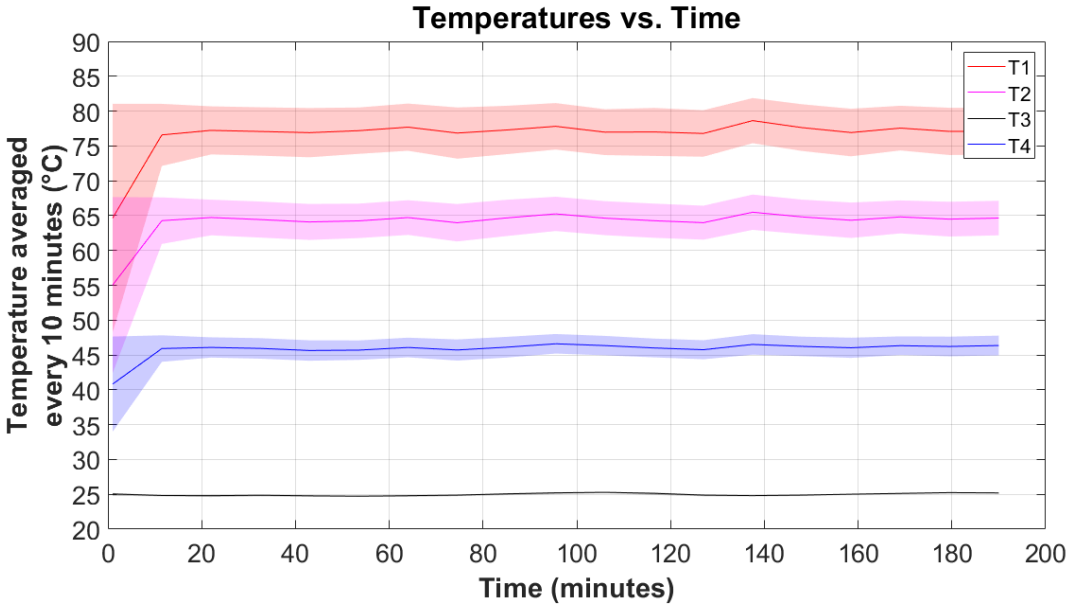

Figure 87: Temperature (°C) averaged every 10 minutes vs time (seconds) for case 4

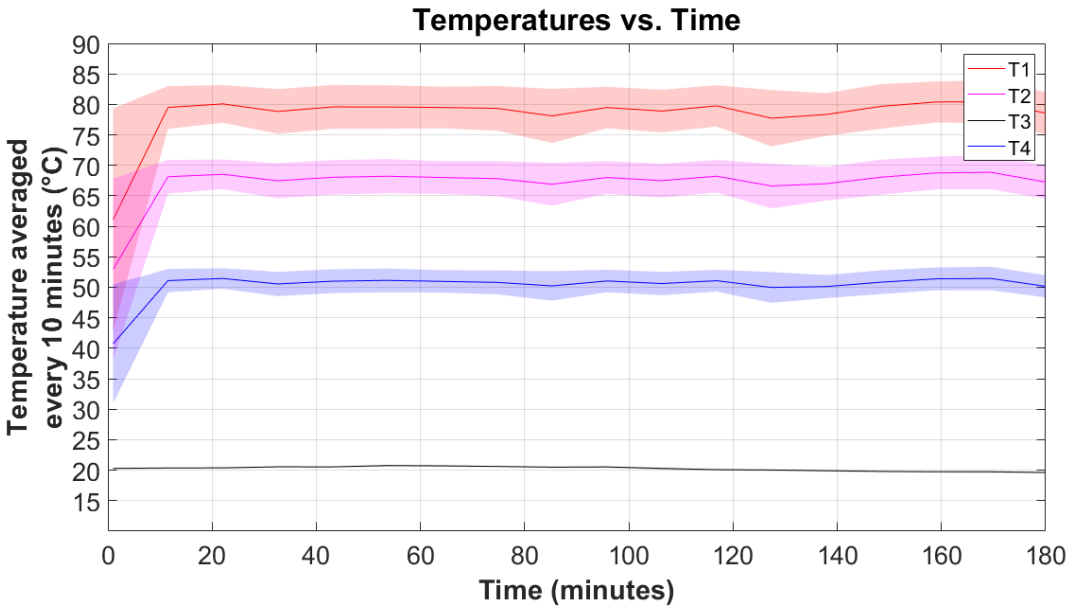

Figure 88: Temperature (°C) averaged every 10 minutes vs time (seconds) for case 5

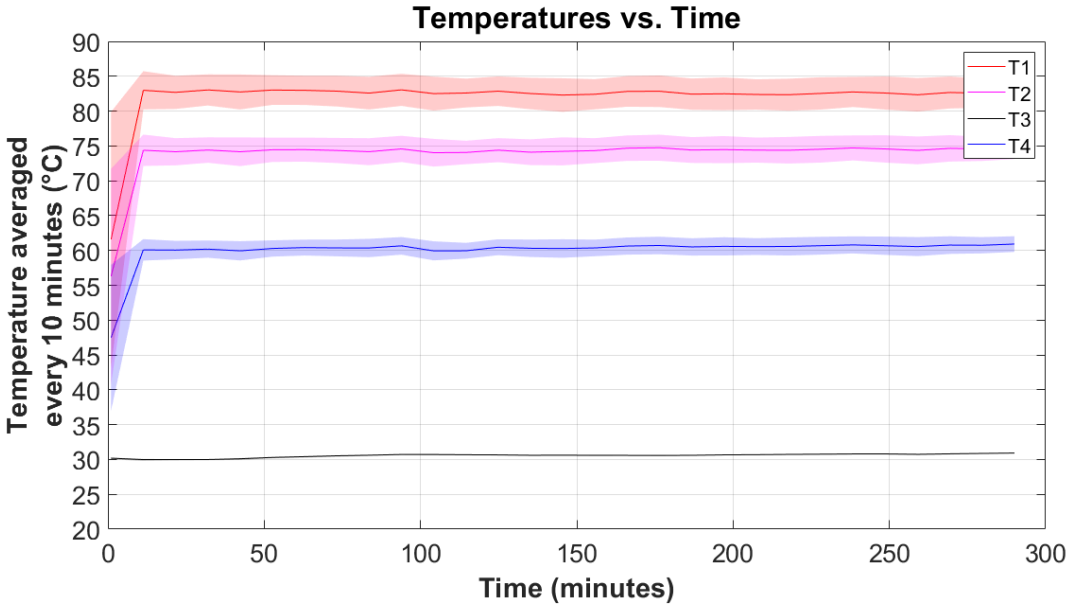

Figure 89: Temperature (°C) averaged every 10 minutes vs time (seconds) for case 7

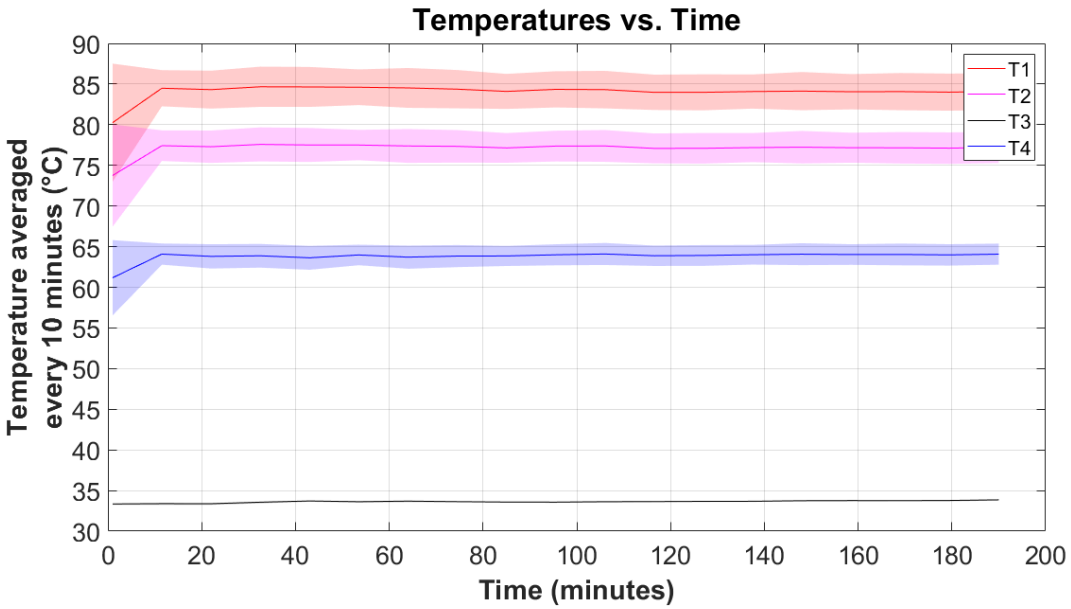

Figure 90: Temperature (°C) averaged every 10 minutes vs time (seconds) for case 8

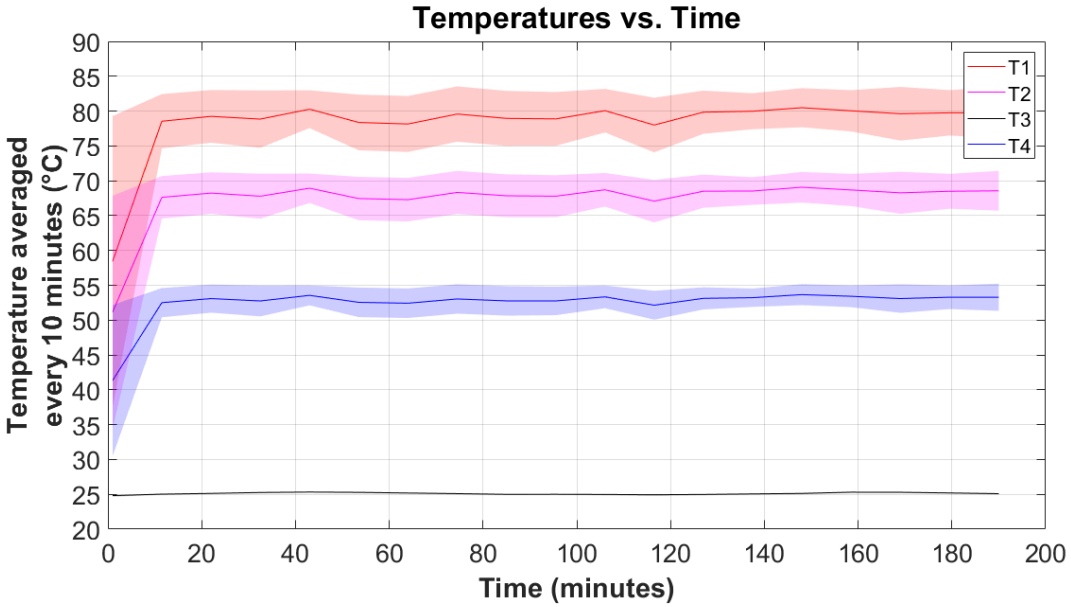

Figure 91: Temperature (°C) averaged every 10 minutes vs time (seconds) for case 9

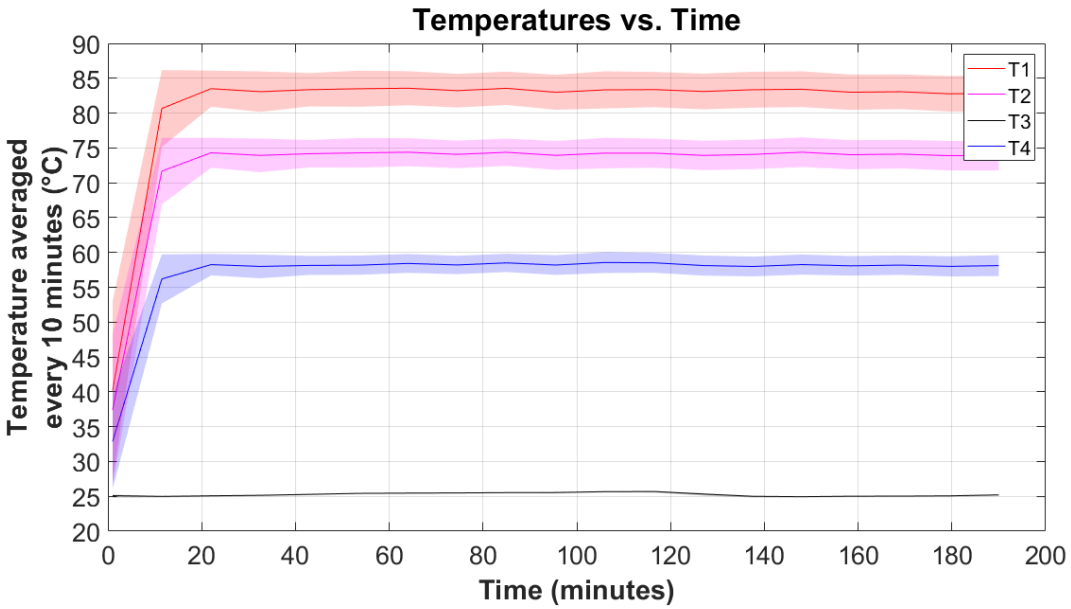

Figure 92: Temperature (°C) averaged every 10 minutes vs time (seconds) for case 11

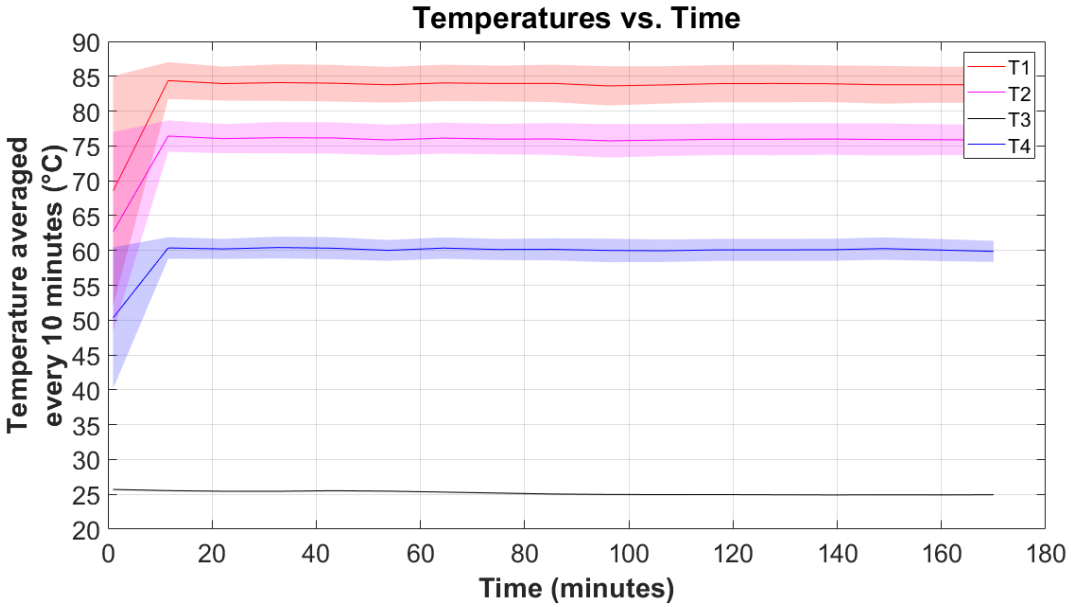

Figure 93: Temperature (°C) averaged every 10 minutes vs time (seconds) for case 12

D Appendix IV

The plots for temperature averaged every 10 minutes (°C), overall heat transfer coefficient (W/m^2K), and fouling resistance (m^2K/W), vs time (minutes) for the two repetitions of the base performed with hard water as the cooling medium are seen in figures 94 - 99.

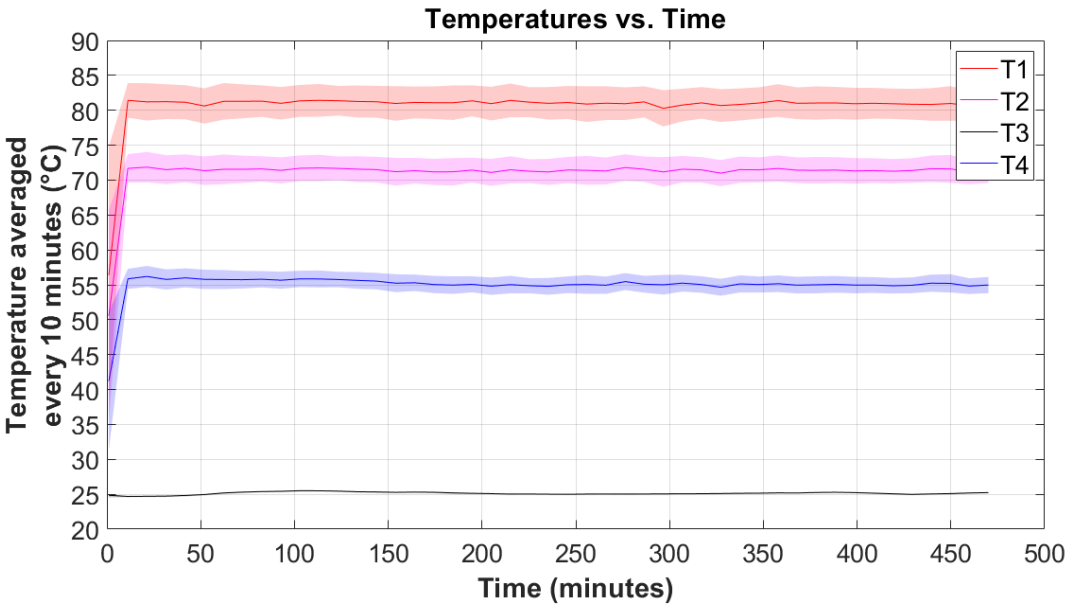

Figure 94: Temperature (°C) averaged every 10 minutes vs time (seconds) for the base case performed with hard water - repetition 2

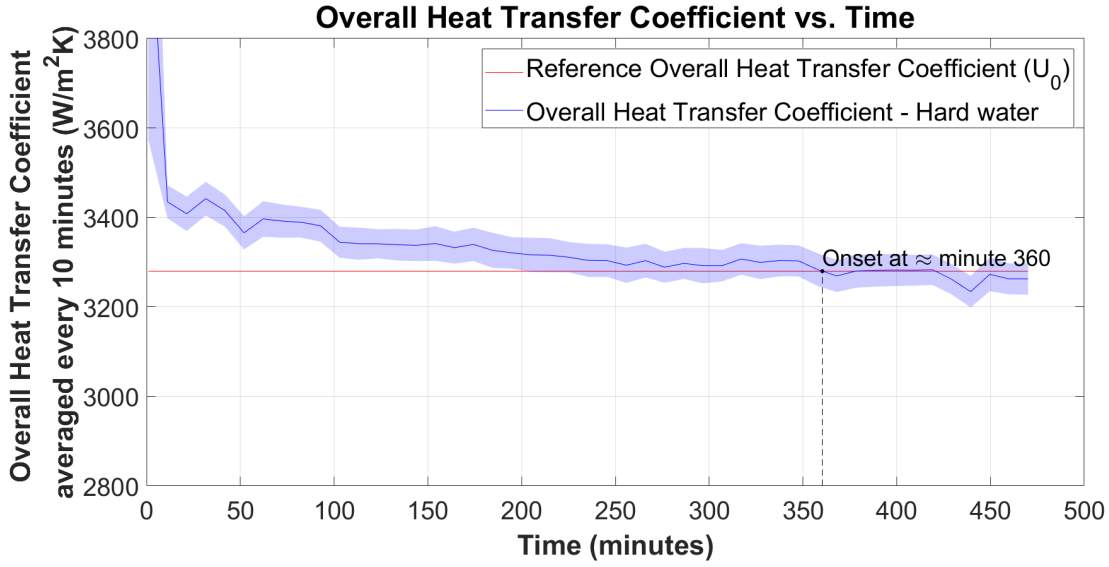

Figure 95: Overall heat transfer coefficient (W/m^2K) averaged every 10 minutes vs time (minutes) for the base case - repetition 2

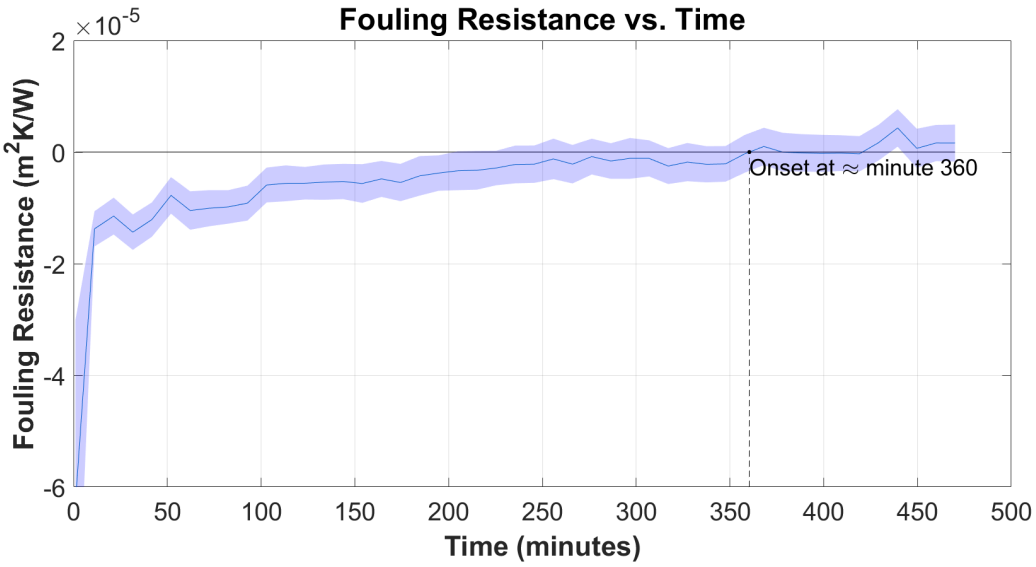

Figure 96: Fouling Resistance (m^2K/W) averaged every 10 minutes vs time (minutes) for the base case - repetition 2

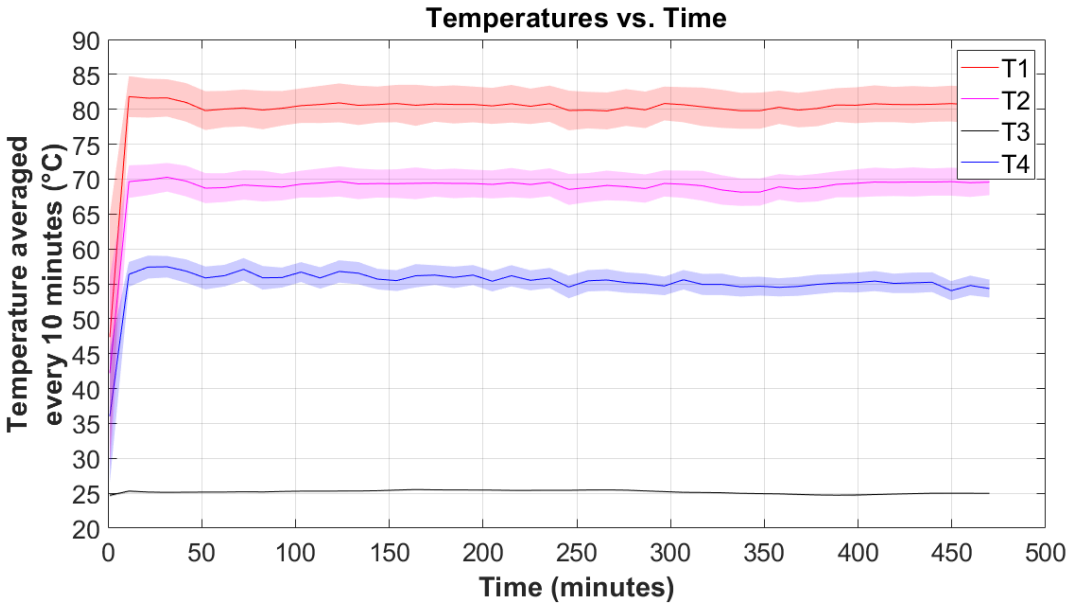

Figure 97: Temperature (°C) averaged every 10 minutes vs time (seconds) for the base case performed with hard water - repetition 3

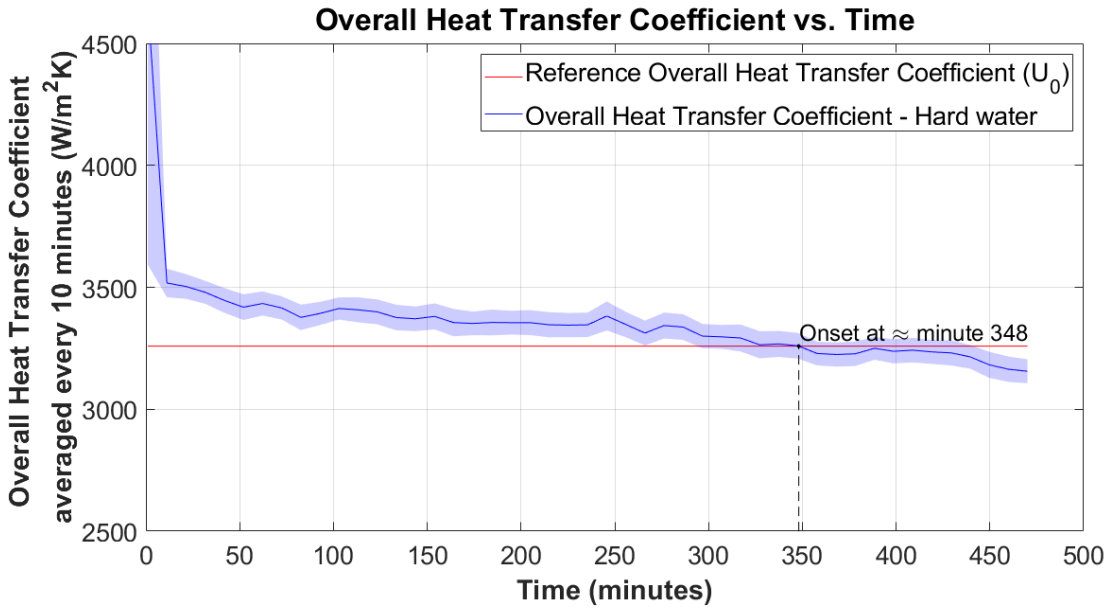

Figure 98: Overall heat transfer coefficient (W/m^2K) averaged every 10 minutes vs time (minutes) for the base case - repetition 3

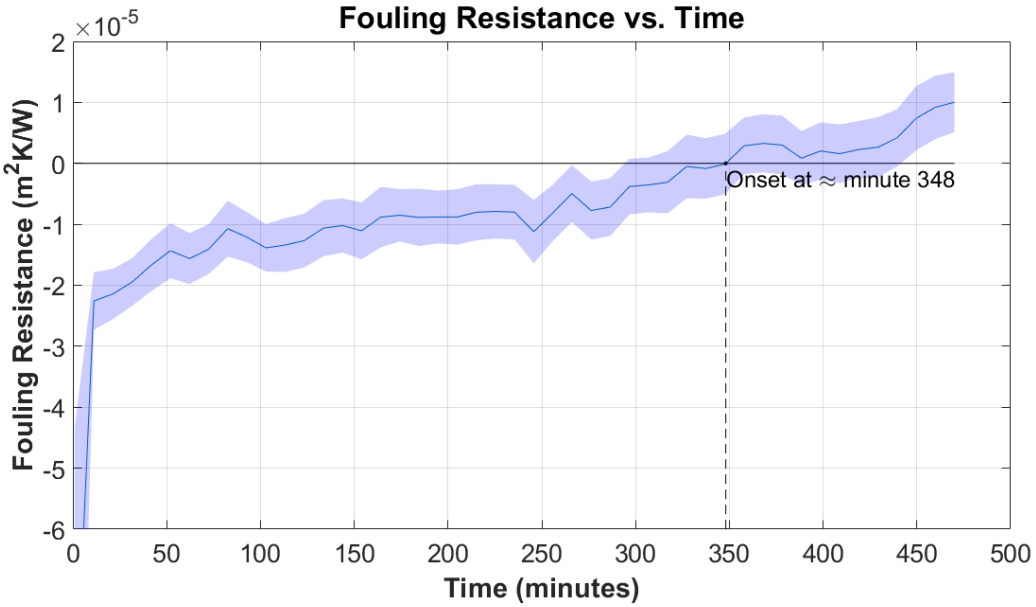

Figure 99: Fouling Resistance (m^2K/W) averaged every 10 minutes vs time (minutes) for the base case - repetition 3

The plots for temperature averaged every 10 minutes (°C) and fouling resistance (m^2K/W), vs time (minutes) for the remaining 9 experiments performed with hard water as the cooling medium are seen in figures 100 - 117.

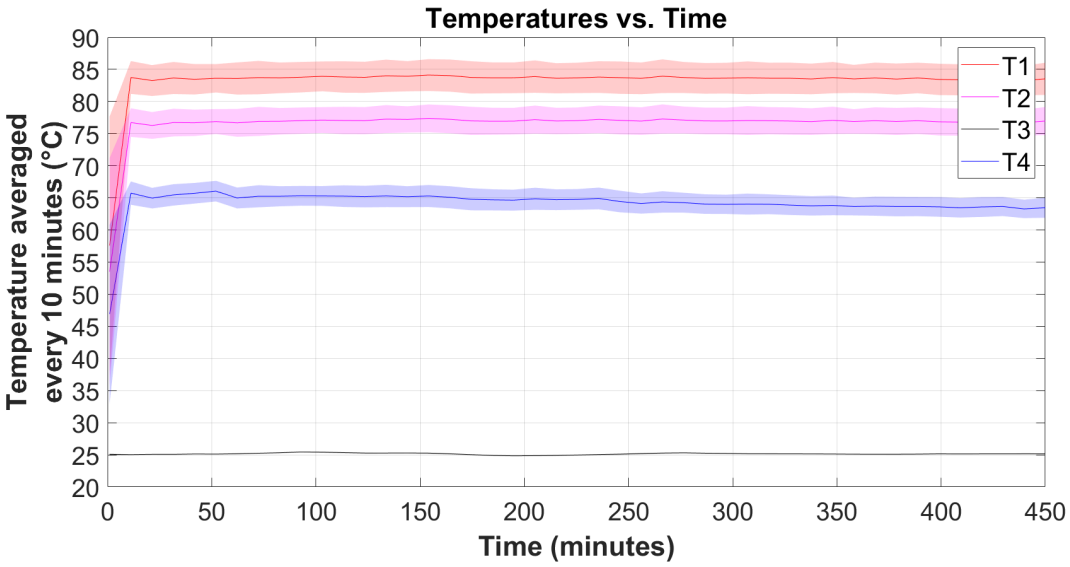

Figure 100: Temperature (°C) averaged every 10 minutes vs time (seconds) for case 1 performed with hard water

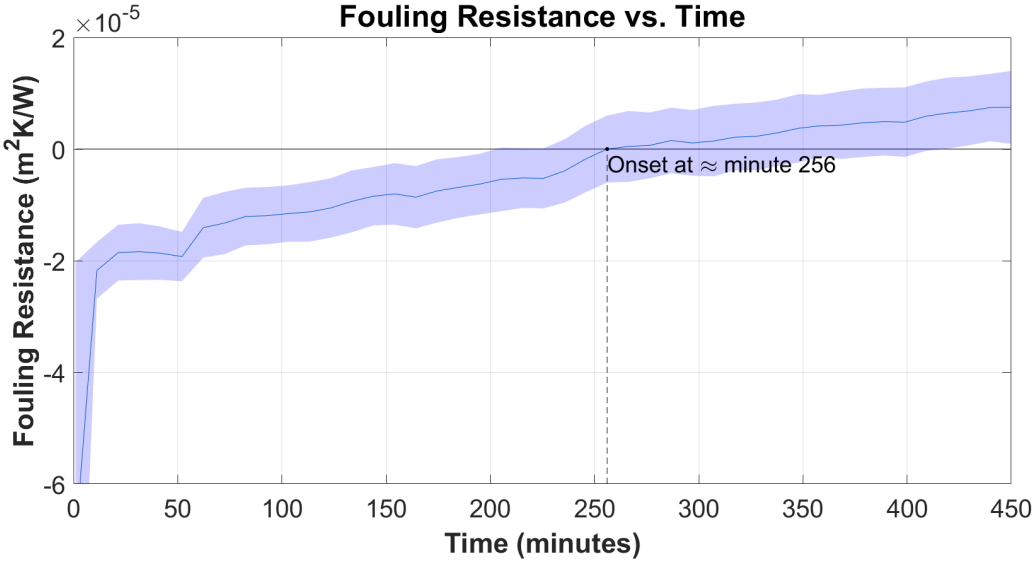

Figure 101: Fouling Resistance (m^2K/W) averaged every 10 minutes vs time (minutes) for case 1

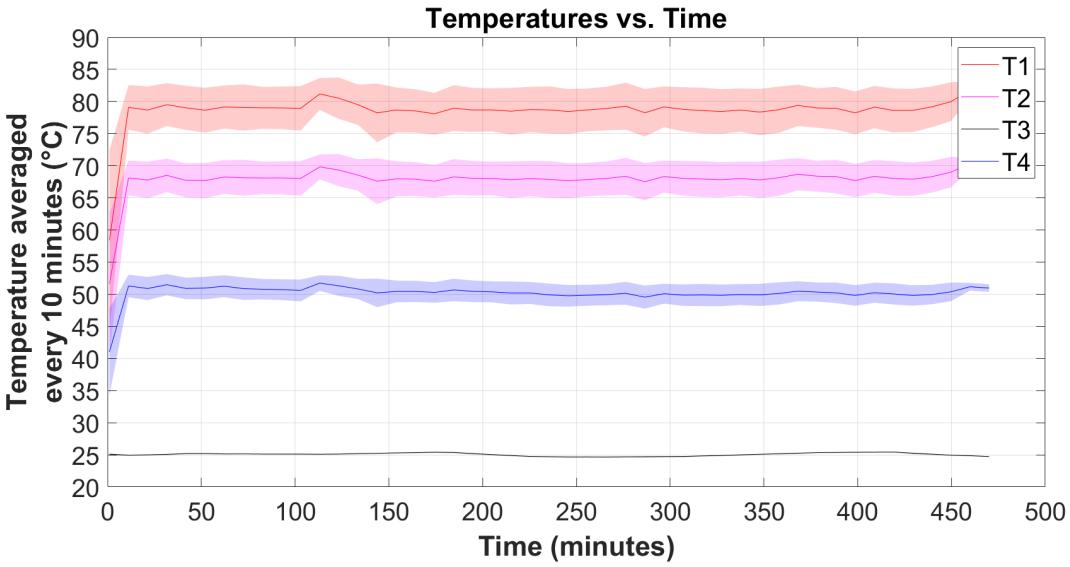

Figure 102: Temperature (°C) averaged every 10 minutes vs time (seconds) for case 3 performed with hard water

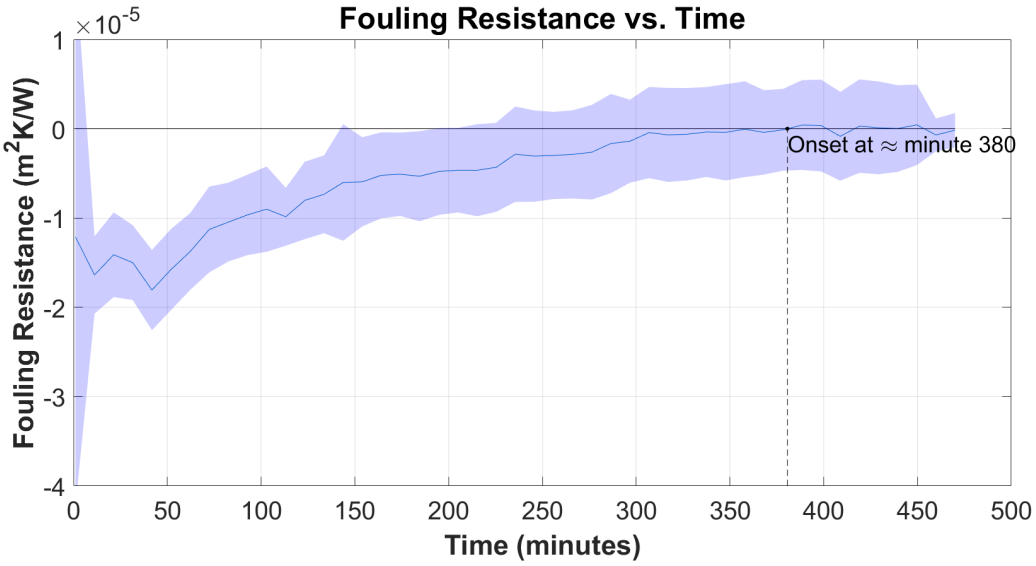

Figure 103: Fouling Resistance (m^2K/W) averaged every 10 minutes vs time (minutes) for case 3

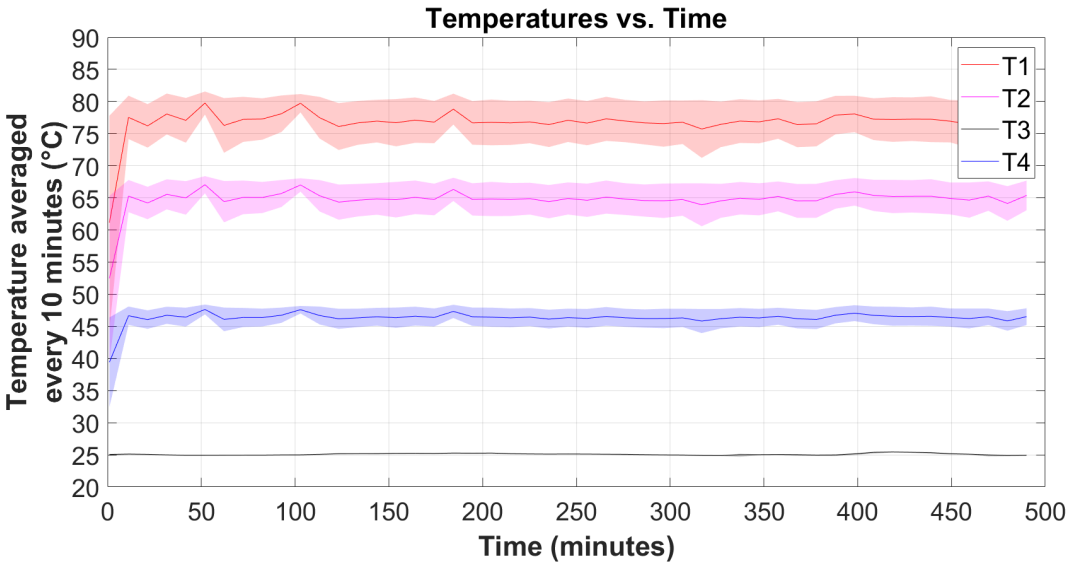

Figure 104: Temperature (°C) averaged every 10 minutes vs time (seconds) for case 4 performed with hard water

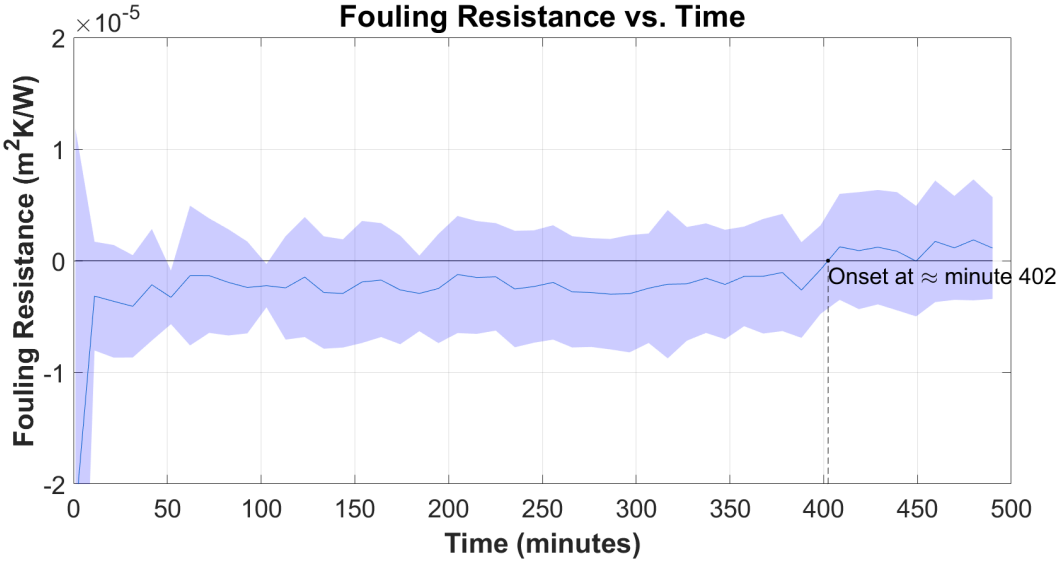

Figure 105: Fouling Resistance (m^2K/W) averaged every 10 minutes vs time (minutes) for case 4

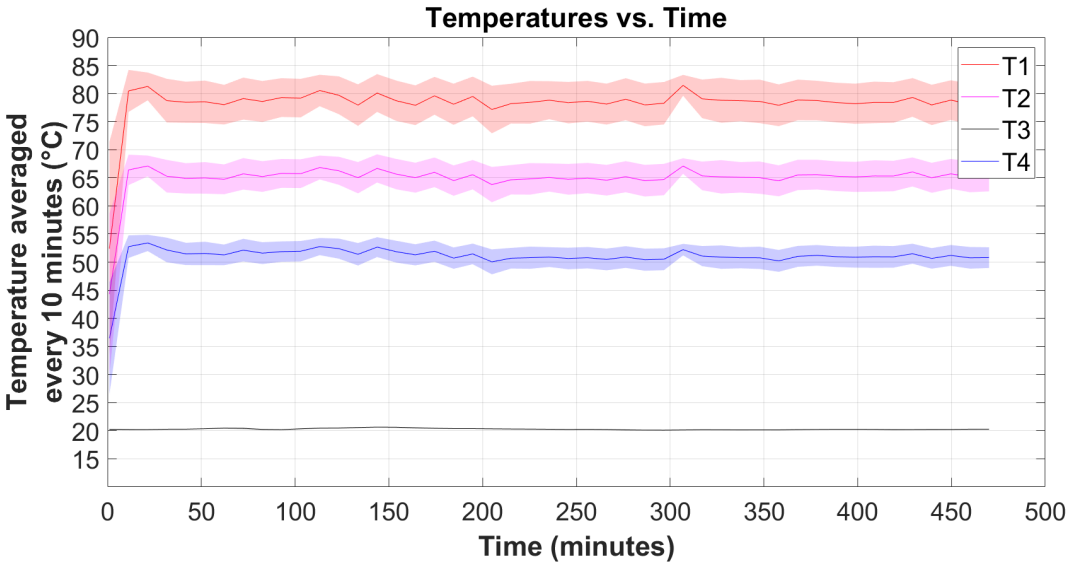

Figure 106: Temperature (°C) averaged every 10 minutes vs time (seconds) for case 5 performed with hard water

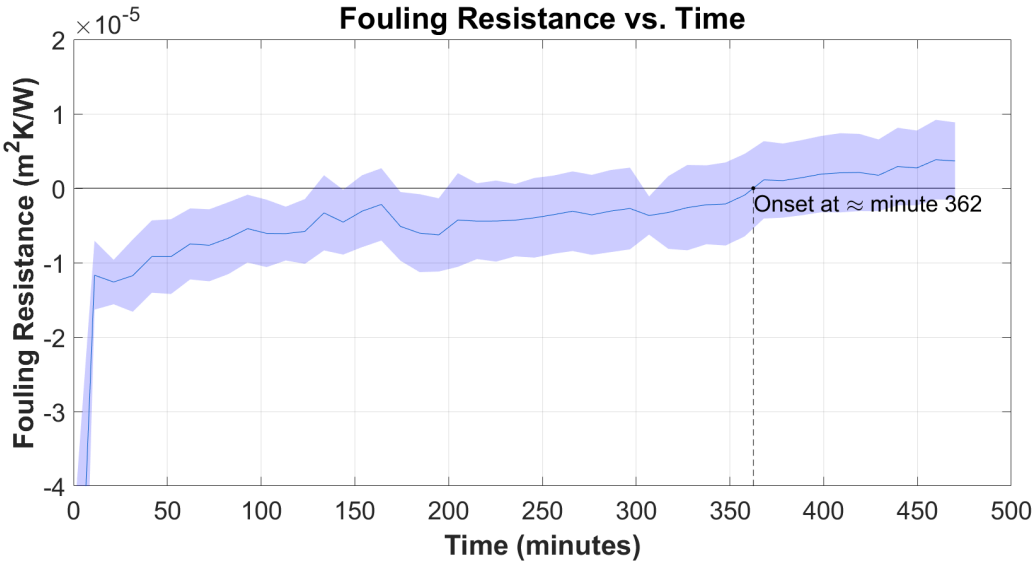

Figure 107: Fouling Resistance (m^2K/W) averaged every 10 minutes vs time (minutes) for case 5

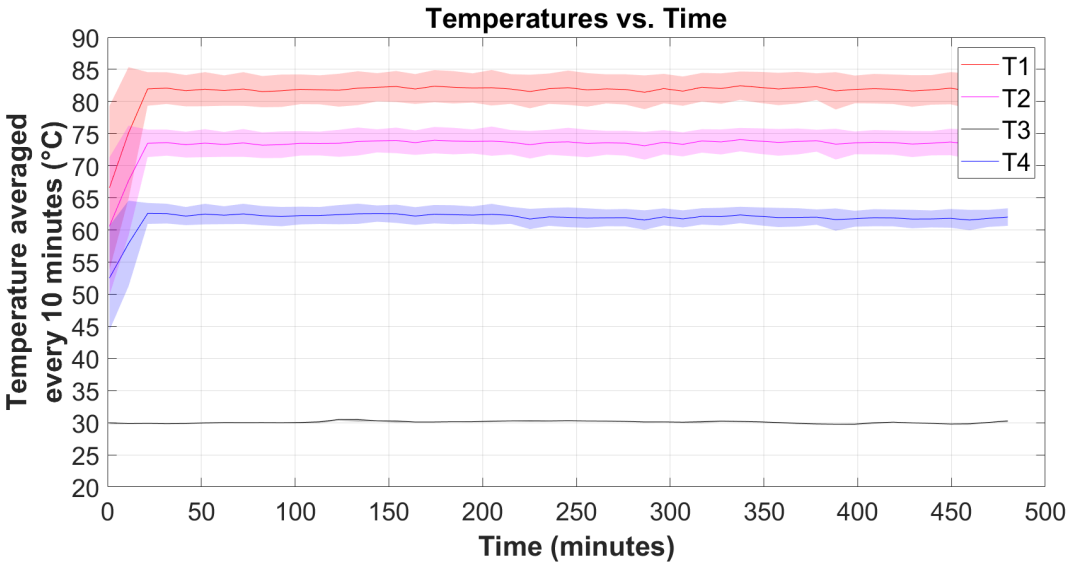

Figure 108: Temperature (°C) averaged every 10 minutes vs time (seconds) for case 7 performed with hard water

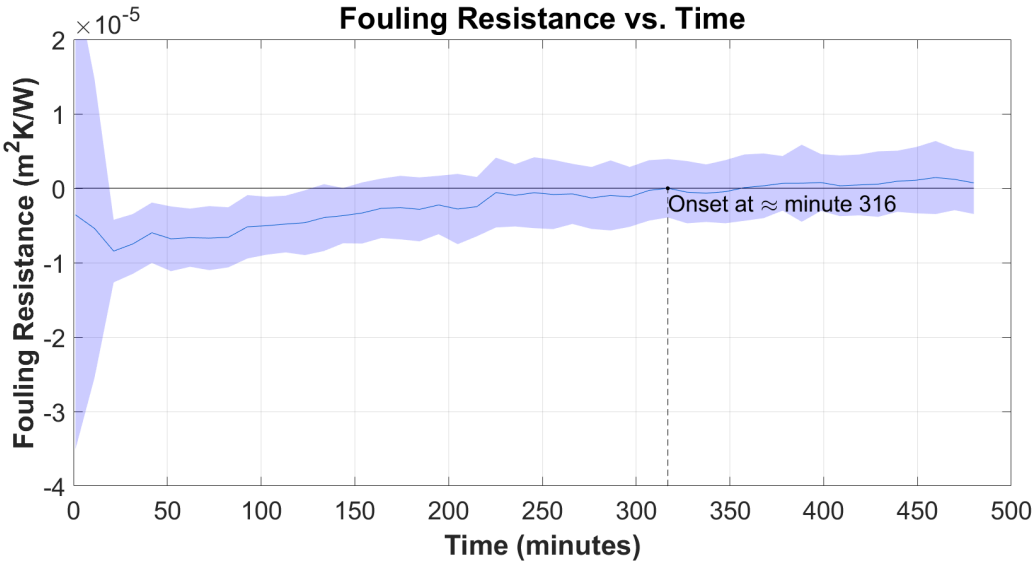

Figure 109: Fouling Resistance (m^2K/W) averaged every 10 minutes vs time (minutes) for case 7

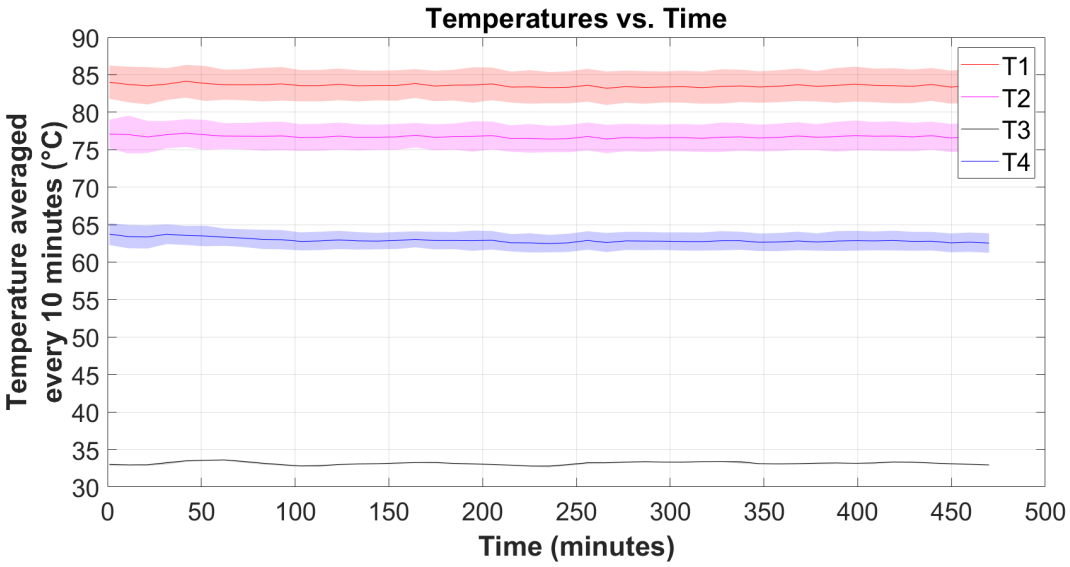

Figure 110: Temperature (°C) averaged every 10 minutes vs time (seconds) for case 8 performed with hard water

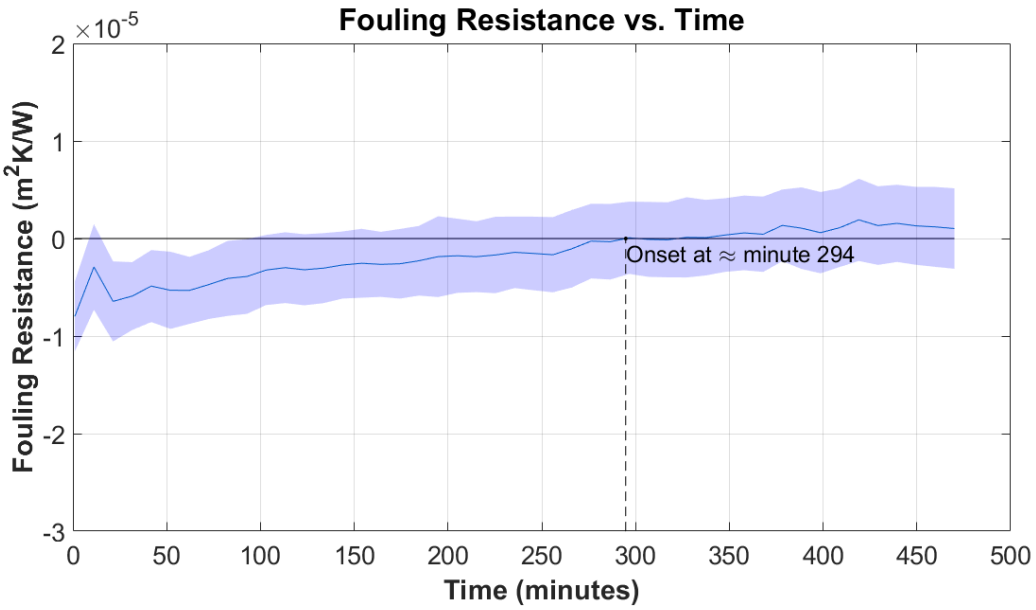

Figure 111: Fouling Resistance (m^2K/W) averaged every 10 minutes vs time (minutes) for case 8

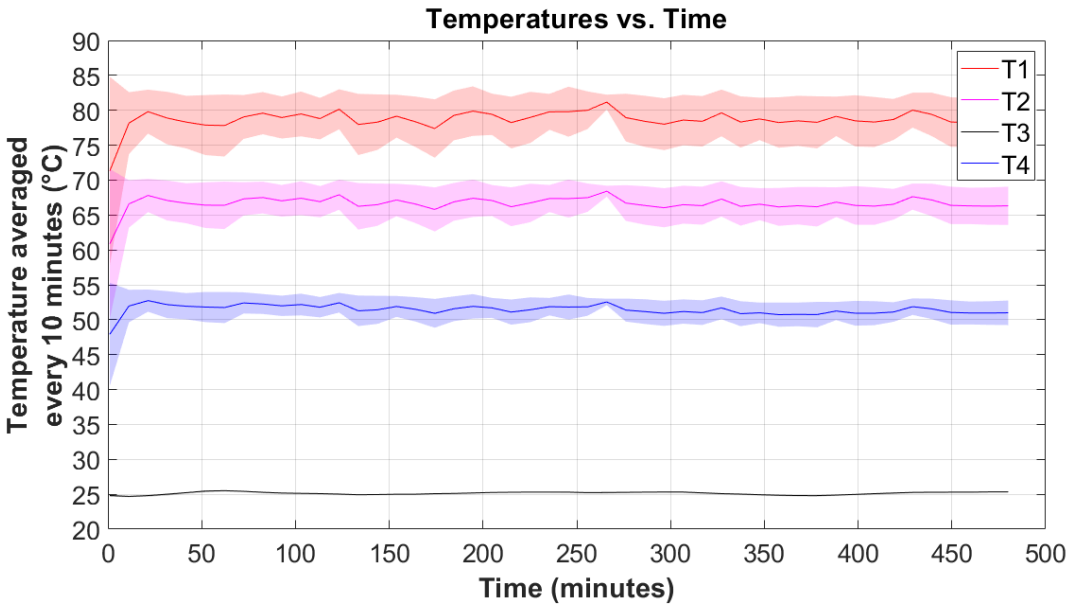

Figure 112: Temperature (°C) averaged every 10 minutes vs time (seconds) for case 9 performed with hard water

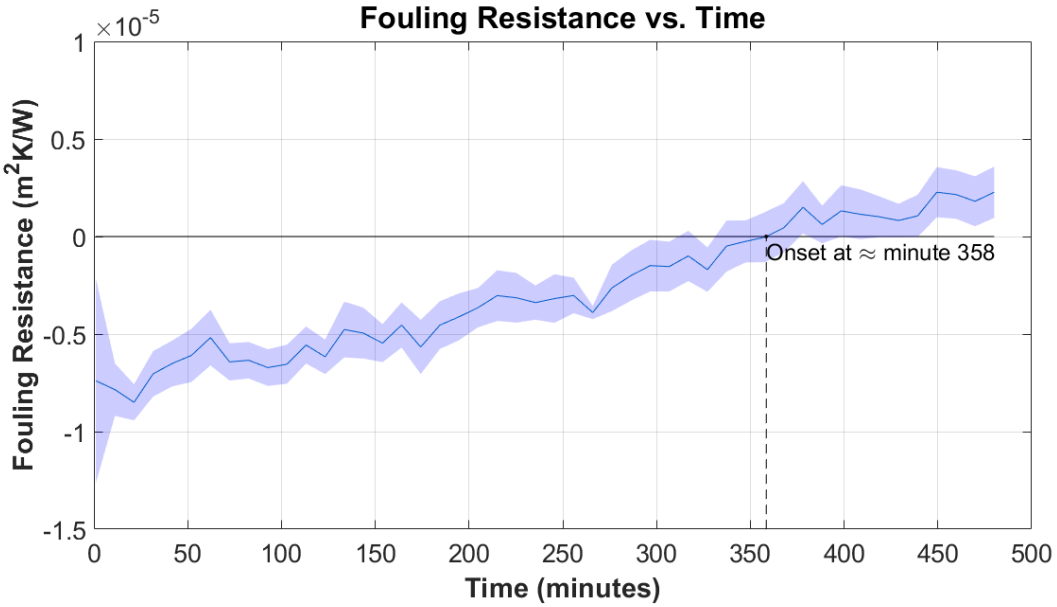

Figure 113: Fouling Resistance (m^2K/W) averaged every 10 minutes vs time (minutes) for case 9

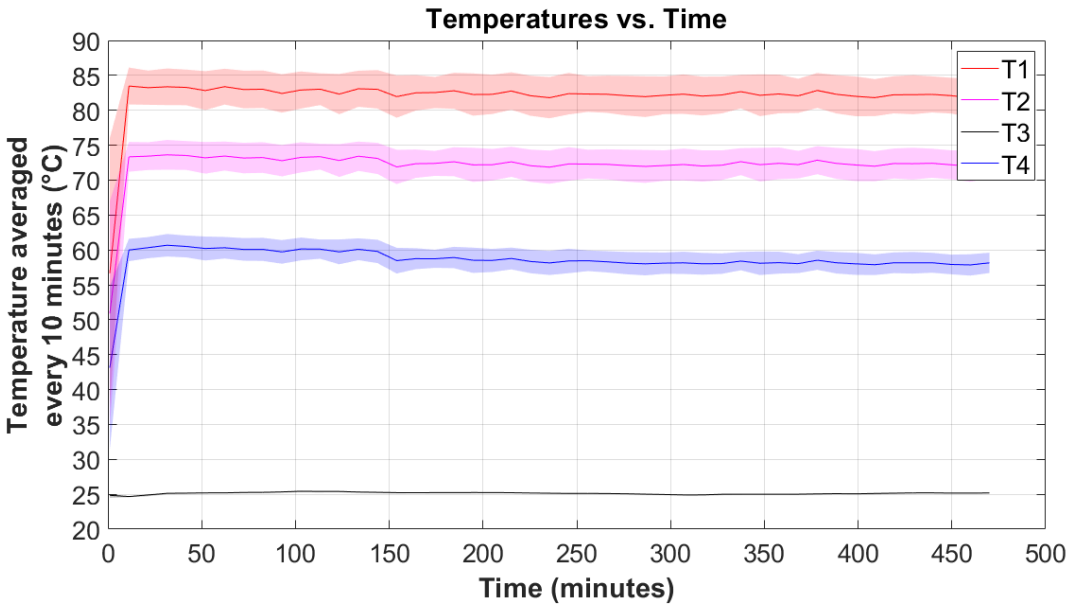

Figure 114: Temperature (°C) averaged every 10 minutes vs time (seconds) for case 11 performed with hard water

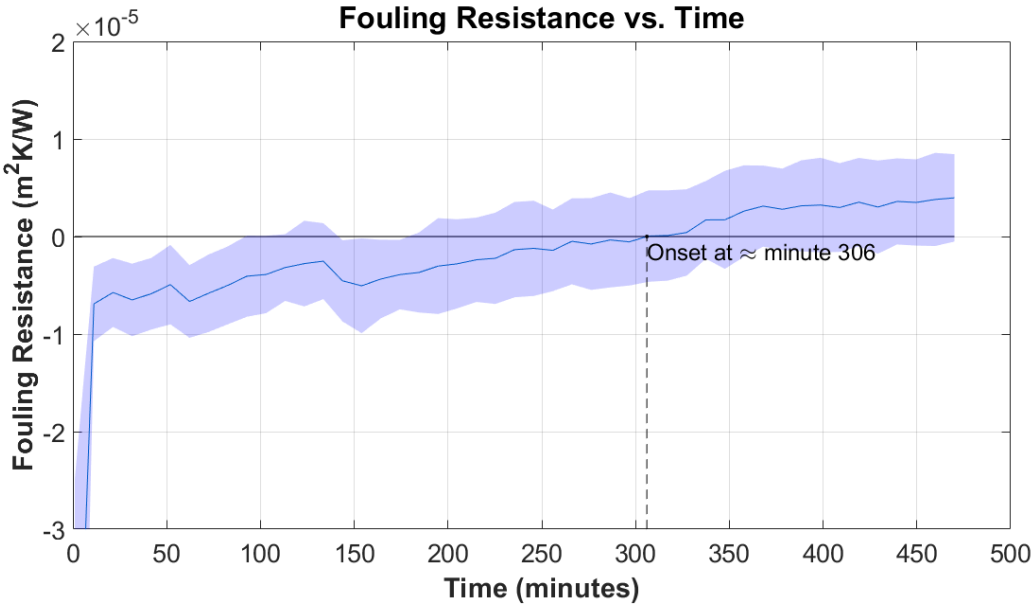

Figure 115: Fouling Resistance (m^2K/W) averaged every 10 minutes vs time (minutes) for case 11

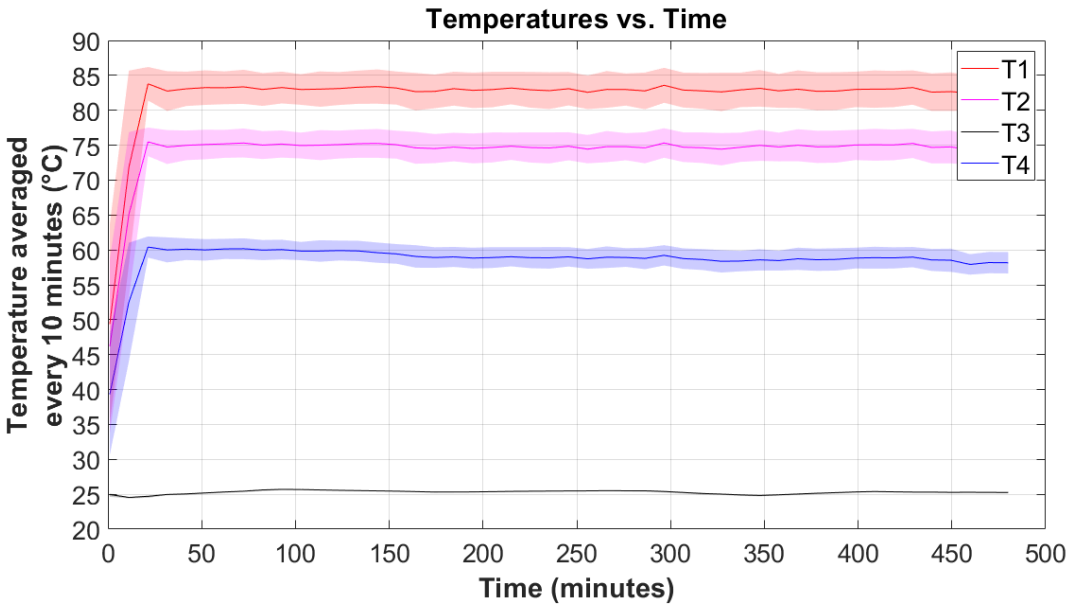

Figure 116: Temperature (°C) averaged every 10 minutes vs time (seconds) for case 12 performed with hard water

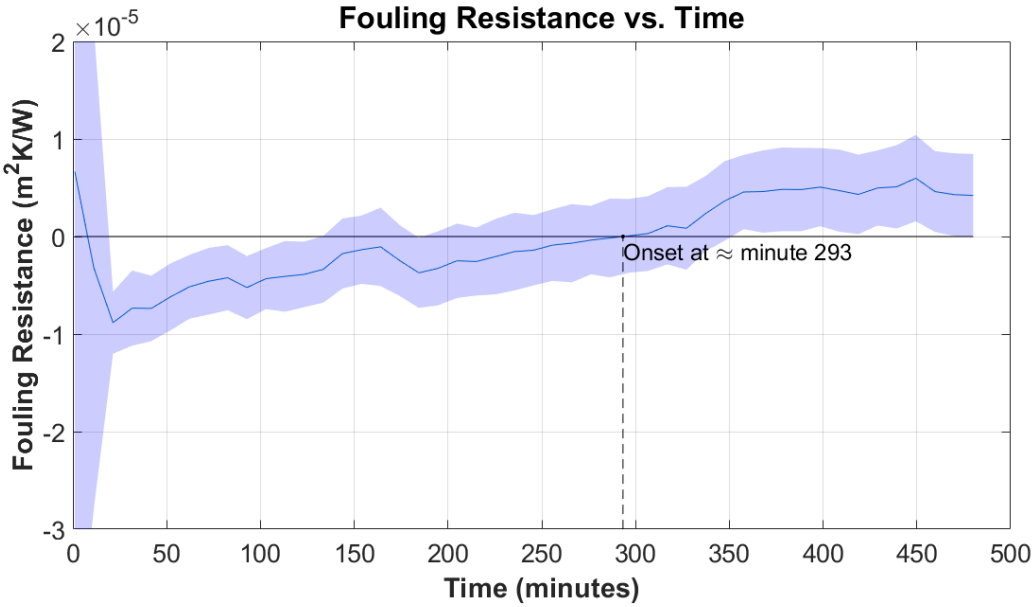

Figure 117: Fouling Resistance (m^2K/W) averaged every 10 minutes vs time (minutes) for case 12

E Appendix V

The Approved Saftey Report for conducting experiments in the TU Delft lab, is seen below.

Report number:
3699
Status:
Approved
User/author:
Nanda, Rahul (R.R.Nanda@student.tudelft.nl)

1. Specific data

Phone Number in case of Emergency:
+31 0613217072
Name of Experimental unit:
Scaling in Plate Heat Exchangers

Objective of the experimental unit:
Objective of experimental unit is to conducts tests to determine the effect of flowrate, temperature and hardness of working fluid on scaling tendency and performance of the plate heat exchanger
Enter the experimental approach:
Experiments will be run by varying different parameters and observing change in working fluid temperatures. Using these temperatures, fouling resistance will be obtained and subsequently compared for each experimental run .

First Flow Chart of the Process:
/uploads/3699-Setup_Diagram.png (https://labservant.tudelft.nl/index.php/file/get/uploads/3699-Setup_Diagram.png)
Second Flow Chart of the Process:
(https://labservant.tudelft.nl/index.php/file/get)
Third Flow Chart of the Process:
(https://labservant.tudelft.nl/index.php/file/get)
First Plan of the Laboratory:
(https://labservant.tudelft.nl/index.php/file/get)
Second Plan of the Laboratory:
(https://labservant.tudelft.nl/index.php/file/get)
Third Plan of the Laboratory:
(https://labservant.tudelft.nl/index.php/file/get)

Location of the experimental unit:
Process & Energy Lab

Area supervisor:
Brink, Michel van den
Committee for Safety, Health, Welfare and Environment:
3mE P&E
Head of section/group leader:
Boersma, Bendiks Jan
Head of department:
Poelma, Christian

2. Chemicals, gases, biologicals

Chemicals

CAS NR:
144-55-8

Name:
Sodium Bi Carbonate

Quantity:
10kg

Chemwatch hazard ratings

Sodium hydrogen carbonate, 5 kg ADR class:

Flammability

Toxicity

Body Contact

Reactivity

Chronic

Nanomaterial:
No
CMR agent:
No
Hazards and Precautions:

I work with this chemical in a fume hood:
No
Make an exposure analysis

CAS NR:
10043-52-4

Name:
Calcium Chloride

Quantity:

20kg

Chemwatch hazard ratings

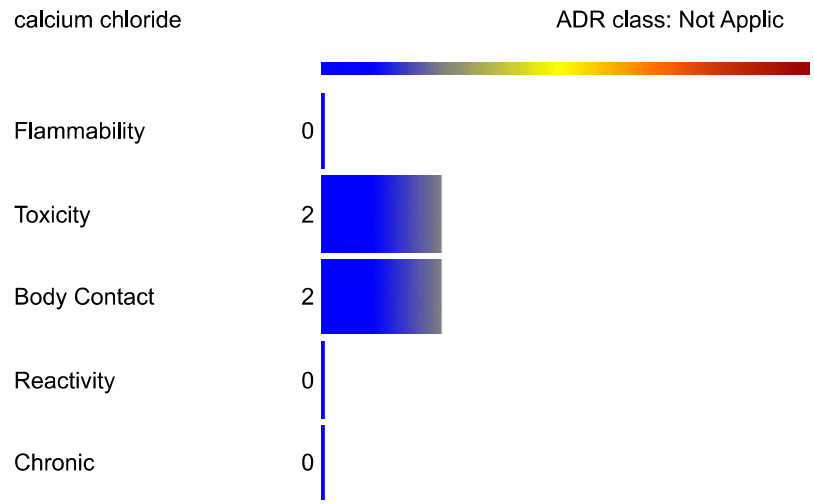

Nanomaterial:
No
CMR agent:
No
Hazards and Precautions:

I work with this chemical in a fume hood:
No
Make an exposure analysis

Biologicals

Miscellaneous

---

3 Equipment

Equipment

Number:

Name:
Electric Central Heating Boiler -
Description:
The Electric Central Heating Boiler (Masterwatt Calida Compact) has a 3 phase 400V connection with a maximum power consumption of 24kW. The device has it's own pump, flowmeter and temperature sensors. The purpose of the device is to produce hot water at a required temperature.

Health risks & safety measure(s)

Number:

Name:
Gasketed Plate Heat Exchangers
Description:
The setup consists of 2 gasketed plate heat exchangers (GPHE) from Alfa Laval. The smaller GPHE is the 'T2B' with 25 plates and is the unit on which scaling will be investigated. The larger GPHE is the 'TL3B' with 8 plates. The purpose of this is to cool the hot water using cooling water from the lab.

Health risks & safety measure(s)

Number:

Name:
Pump
Description:
The Ebara pump used in the setup has a nominal power of 1.2kW. The purpose is to pump the water from the tank into the GPHE. The pump is electrically connected using a residual current device to for automatic shut down in case of electrical faults.

Health risks & safety measure(s)

Number:

Name:
IBC Heating Jacket
Description:
A 2kW IBC heating jacket is wrapped around the 1000L tank to maintain a constant temperature of water in the tank. The electrical connection is made using a residual current device to for automatic shut down in case of electrical faults.

Health risks & safety measure(s)
Additional information

Miscellaneous:

---

4 Failures & exceptional conditions

Failure/condition

Failure/condition:
electricity: hazard of electrocution
Safety measure(s):
All electrical connection are made using a Residual Current Device for automatic shut down of electricity in case of an electrical fault.

Failure/condition:
work environment: pressurized equipment
Safety measure(s):
The hot loop consisting of copper pipes that connect the central heating boiler to the GPHE are pressurized at 1.5bar. The loop is fitted with pressure relief valve to prevent pressures higher than 3 bar in the system.

Miscellaneous:

5 Emergency Card

Description of emergency shutdown

Turn the lower knob on the central heating boiler clockwise to put it on the 'OFF' position. Unplug the residual current device to switch off electricity supply to all other components. Turn the valves of the cooling water supply such that the flow is blocked.

6 Ergonomics

Ergonomic risks:

Miscellaneous:

All controls of the setup are located in the basement of the P&E lab and are easily accessible. In order to switch on the supply of the cooling water from the lab to the setup, easily accessible valves are present on the ground floor of the P&E lab

7 Disposal and Waste

Used/produced chemicals

Sodium Bi Carbonate
Quantity:
10kg
Way of disposal:
Sodium Bi Carbonate will be dissolved in water to run experiments. After completion of experiments, the water with the dissolved sodium bi carbonate can be safely drained into the manhole in the P&E lab basement.
Estimated costs:
0

Calcium Chloride
Quantity:
20kg
Way of disposal:
Calcium chloride will be dissolved in water to run experiments. After completion of experiments, the water with the dissolved calcium chloride can be safely drained into the manhole in the P&E lab basement.
Estimated costs:
0

Used/produced biologicals

Used equipment

Electric Central Heating Boiler -
Way of disposal:
The boiler can be reused for future experiments
Estimated costs:
0

Gasketed Plate Heat Exchangers
Way of disposal:
The plate heat exchangers can be reused for future experiments
Estimated costs:

0

Pump
Way of disposal:
The pump can be reused for future experiments
Estimated costs:
0

IBC Heating Jacket
Way of disposal:
The IBC heating jacket can be reused for future experiments
Estimated costs:
0